CITRUS BIOTECHNOLOGY IN THE 21ST CENTURY

By

SHAUN PAUL JENSEN

A THESIS PRESENTED TO THE GRADUATE SCHOOL
OF THE UNIVERSITY OF FLORIDA IN PARTIAL FULFILLMENT
OF THE REQUIREMENTS FOR THE DEGREE OF
MASTER OF SCIENCE

UNIVERSITY OF FLORIDA

2017

To my wife, daughter, and mother

ACKNOWLEDGMENTS

I thank my wife for all the time, effort, and love she has spent in helping me get to this point in my career and education. I thank my parents for always being supportive of my decisions and my life goals. I thank my all my sisters for helping me learn valuable life skills without having to experience them. Truly, my whole family is wonderful.

TABLE OF CONTENTS

page

LIST OF TABLES

LIST OF FIGURES

LIST OF ABBREVIATIONS

2AEE	2-(2-aminoethoxy)ethanol
A	Alanine. An amino acid.
AAV	Adeno-associated virus
ACC	Asiatic citrus canker
ACP	Asian citrus psyllid, *Diaphorina citri*
CaMV 35S	Cauliflower mosaic virus. A viral constitutive promoter.
Cas9	CRISPR- associated system 9
Cas9m4	Cas9 with 4 point mutations
CBS	Citrus black spot
Cfu	Colony forming unit
Cl	Chloride
CLaf	"*Candidatus* Liberibacter africanus"
CLam	"*Candidatus* Liberibacter americanus"
CLas	"*Candidatus* Liberibacter asiaticus"
COP	Coat protein
CPP	Cell-penetrating peptide
CRISPR	Clustered regularly interspaced palindromic repeats
Csn	COP9 signalosome
D	Aspartic acide. An amino acid.
DIC	Differential interference contrast
DLS	Dynamic light scattering
DMac	N,N-dimethylacetamide
DMSO	Dimethyl sulfoxide
DNA	Deoxyribose nucleic acid

DSB	Double-stranded break
dsDNA	Double stranded DNA
EDTA	Ethylenediaminetetraacetic acid
F-Dex	FITC-Dextran.
FITC	Fluorescein isothiocyanate fluorescence setting
FMV	Figwort mosaic virus. A viral constitutive promoter.
FT	Flowering Locus T
GFP	Green fluorescent protein. A protein from Cnidarian species.
gRNA	Guide RNA
GUS	β-glucuronidase. A gene reporter system.
H	Histidine. An amino acid.
H_2O_2	Hydrogen peroxide
HLB	Huanglongbing. Also known as citrus greening.
HNH	Histidine- Asparagine-Histidine. A nuclease.
InDel	Insertion or deletion
IR	Infrared
JBS	Jena BioScience. A biotechnical company. The company uses this abbreviation for its proprietary peptides.
KRAB	Kruppel-associated box. A transcriptional repressor.
LB	Luria broth media
MCS	Multi-clonal site
MS	Murashige and Skoog. Refers to two researchers. Created an optimized plant growing salt mixture for use in tissue culture.
N	Asparagine. An amino acid.
NAA	Naphthaleneacetic acid
NaCl	Sodium Chloride

NCA	*N*-carboxyanhydride
NMR	Nuclear Magnetic Resonance
NPR	Non-expressor of pathogenesis-related
OD_{600}	Optical density at 600 nm. For measuring bacterial concentration.
PAM	Protospacer Adjacent Motif
PAMP	Pathogen activated molecular pattern.
PASP	Poly(aspartic acid)
PASPA	Polyaspartate
PBLA	$(Poly(\beta\text{-benzyl-L-aspartate})_{43})_3$
PBS	Phosphate buffer solution
PCR	Polymerase chain reaction
PHEA	Poly(hydroxyethylaspartimide)
PR	Pathogenesis related
PSI	Poly(succinimide)
PTD	Protein transduction domain
PTI	PAMP-triggered immunity
qRT-PCR	Quantitative real-time PCR
R	Arginine. An amino acid.
R9	Arginine-9
R9-FAM	Arginine-9-6-FAM fluorescein
RNA	Ribonucleic acid
RT	Room temperature, around 23-24 °C.
RuvC	Resolvosome-sensitive to UV subunit C. A nuclease.
RVD	repeat-variable di-residue
S	Serine. An amino acid.

SAR	Systemic acquired resistance
SDS	Sodium dodecyl sulfate
SEC	Size exclusion chromatography
sgRNA	Small guiding RNA
siRNA	Short interfering RNA
ssDNA	Single stranded DNA
T	Threonine. An amino acid.
TALEN	Transcription activator-like effector nuclease
TFL1	Terminal flower protein-1
tracrRNA	Trans-activating CRISPR RNA
v/v	Volume to volume ratio
VP16	A transcriptional activator from Herpes Simplex Viral Protein 16.
VP64	A transcriptional activator domain composed of four tandem repeats of VP16.
w/v	Weight to volume ratio
Xac	*Xanthomonas axonopodis* pv. *citri*
ZFN	Zinc finger nuclease
X-gal	5-bromo-4-chloro-3-indolyl-β-D-galactopyranoside. A compound used to stain for GUS in plants.
X-gluc	5-bromo-4-chloro-3-indolyl glucuronide. A compound used to stain for GUS in bacteria.

Abstract of Thesis Presented to the Graduate School
of the University of Florida in Partial Fulfillment of the
Requirements for the Degree of Master of Science

CITRUS BIOTECHNOLOGY IN THE 21ST CENTURY

By

Shaun Jensen

December 2017

Chair: Gloria A. Moore
Major: Plant Molecular and Cellular Biology

Citrus is one of the most economically significant agricultural crops. Over the past two decades, citrus has suffered substantial losses due to several citrus diseases. These losses have led the citrus industry to determine that it simply cannot wait for conventional methods to solve these issues, and instead want to try newer, alternative methods. This has led growers and organizations to increase funding of citrus genetic research.

This body of work plans to elucidate some of the new biotechnologies that have been used in various laboratories and resource centers abroad to help bring citrus from past techniques and into the 21st century and beyond, creating new opportunities to combat old problems.

First, the state of citrus as an industry and a fruit crop is discussed to address the economic importance of citrus and the problems associated with breeding and genetic transformation. In the following chapters, three potential biotechnological solutions are proposed to combat these difficulties associated with citrus propagation: cell-penetrating peptides for use as a molecular delivery system and potential transformation method,

nanoparticles as a targeted delivery system, and a modified CRISPR/Cas9 system to produce early flowering and reduce breeding and regeneration times.

CHAPTER 1
INTRODUCTION

Citrus on the Global Stage

The genus *Citrus* contains the most economically significant fruit tree crop species in the world. Citrus plants are classified in the subfamily Aurantioideae which belongs to the family Rutaceae (Penjor et al., 2013). Citrus consists of many species that are commercially produced in over 140 countries across the globe from Brazil and the United States to Southeast Asia and Australia. The consensus origin for the genus *Citrus* is in the equatorial regions of Southeast Asia, including parts of India, China, and Malaysia. In this region, three primary citrus varieties evolved through which all other citrus is hybridized: mandarins (*Citrus reticulata*), pummelos (*Citrus maxima*), and citrons (*Citrus medica*) (Nicolosi, 2007).

The most profitable cultivars include oranges (*Citrus x sinensis*), mandarins (*C. reticulata*), lemons (*Citrus x limon*), limes (*Citrus x aurantiifolia*), and grapefruits (*Citrus x paradisi*) (Liu et al, 2012). Citrus is utilized in a variety of ways: consumption of fresh fruit, imbibed as processed juice, its peels are used in the production of facial cleansers, and it even has some uses in the medical field, notably in the reduction of both stomach and breast cancer development (Gonzalez et al., 2013, Song et al., 2013).

In the 2013-2014 growing season, worldwide production of citrus exceeded 122 million tons (FAO, 2016). In the 2014-2015 citrus growing season, the United States alone produced 9.02 million tons of fruit worth 3.38 billion US Dollars, with the state of Florida responsible for 56% of total US production (USDA, 2016). Most of Florida's crop is used in processing, where 90% of all citrus gets processed into juice (USDA, 2016). For the state of Florida, the industry has much more significant impacts. It employs over

45,000 people is credited to generate over 8.6 billion dollars each year in economic impacts, and is responsible for the majority of its agriculture income in cash receipts at nearly 18% (USDA, 2016).

The production statistics of citrus are quite impressive. Despite the high numbers, they are only meant to illustrate that citrus has enormous impacts to agriculture in the United States, and more significantly Florida. Total citrus production for the United States is intrinsically tied to the production levels of Florida (USDA, 2016). While global total citrus production has mostly risen year over year at a rate of 1.6 million tons per year since the 2007-2008 growing season, the United States and Florida's production totals steadily declined since the 1997-1998 growing seasons at an approximate rate of 502,00 tons per year (FAO, 2016; USDA, 2016). The decline is due to a variety of factors, but is mostly due to citrus pathogenic diseases, such as citrus greening and citrus canker (APHIS, 2016), discussed in the section below.

Despite the never-ending threats that diseases place on citrus growers, demand and market value for citrus has steadily increased. This has led to multiple attempts to help stabilize the United States citrus industry and restore them to their historical highs from both the public and private sectors. This has led to enormous amounts of funding for citrus research, including genetic sequencing and producing new transgenic methods, and breeding back in traits from wild varieties of citrus or its relatives (Main et al., 2017, Febres et al., 2011, Velasquez et al., 2016).

In this work, three emerging biotechnologies, which have been heavily studied for their impacts in both plants and animals, have been re-focused towards their effects in citrus: cell-penetrating peptides (CPPs), nanoparticles, and a modified CRISPR/Cas9

promoter system. The following chapters will discuss these technologies at length. But first, in order to discuss these technologies, it is important to first understand the present state of citrus and the citrus industry, specifically, citrus characteristics, the major diseases affecting the industry, and the current biotechnologies already in use. These topics will be discussed with respect to global citrus production, but will place an emphasis on how these factors are important to the United States and especially to the state of Florida.

Citrus Characteristics

Citrus Plant Structure

The genus *Citrus* is characterized as a group of generally plant species that forms small shrubs to medium-height trees. There is an extreme amount of variation between citrus species and compared to its close relatives, such as trifoliate orange (*Poncirus trifoliata*) and eremocitrus (*Eremocitrus glauca*), but some general traits are associated with most varieties.

Citrus plants usually have a dense canopy of evergreen leaves. The seedlings will shoot up very quickly (approximately 6 weeks when the plant is about 6 inches tall above ground). The shoot trunk will lignify and harden usually after the first year. The branches tend to have many thorns, but this is generally associated with young plants. The leaves have a characteristically strong, waxy cuticle, making old leaves very hard to work with in the laboratory. Leaf structure ranges from trifoliate, palmately compound, and unifoliate. Some varieties will even have a wing petiole, especially grapefruit (*C. x paradisi*) (USDA, 2011).

Citrus Flowering: Timing, Morphology, and Juvenility

Citrus can flower throughout most of the year in the tropics, but it usually will flower in the late winter or early spring months in the subtropical regions, including Florida (Iglesias et al., 2007). Several researchers have shown that low temperatures may release bud dormancy and induce flowering (Southwick and Davenport, 1986; Tisserat et al., 1990; Iglesias et al., 2007).

Flowers are considered true flowers; they contain both the ovary and pollen-containing anthers, usually housed within five white petals. Most citrus varieties require a pollen source before the fruit will set and begins to mature, however some varieties are known to be parthenocarpic, where they can form a typical fruit in appearance, but generally make the fruit seedless (Iglesias et al., 2007).

During juvenility, citrus plants do not form flowers and plant metabolism is dedicated towards growth. Juvenility is defined as the time it takes a plant to flower from germination. As the plant matures, and becomes necessary for the plant to reproduce, only then do citrus produce their flowers. In citrus, juvenility can last for extremely long periods; some varieties do not flower for up to ten years before plants are able to produce flowers and bear edible fruit (Febres et al., 2007; Gmitter et al., 2007a). This makes breeding citrus much more difficult, discussed in detail below. Reduction in juvenility times is a positive trait wanted by both breeders and growers, and is the primary reason to the CRISPR/Cas9 work presented in Chapter 4. The molecular mechanisms of flowering and the role of the important flowering genes will be discussed further as well.

Citrus Fruits and Seed Development

Citrus fruits are a specialized form botanical berries, known as a hesperidium, which forms from a single ovary (Ladaniya, 2010). The fruit usually forms a globular shape and is green until ripening where it likely changes color to an orange or yellowish appearance, though this can vary greatly between different cultivars, such as the limes (*C. x aurantiifolia*). Fruit size ranges from the small citrus relatives known as kumquats (*Fortunella spp.*) (2.25 cm diameter) to the large pumelos (*Citrus grandis*) (over 20 cm in diameter).

Citrus fruit ripens very slowly, typically 6-8 months from pollination in mid-March to harvest in October for most varieties, but others like 'Valencia' sweet orange (*C. sinensis*) can take upwards of 12-14 months, where harvested fruit is picked alongside freshly pollinated flowers (Bain, 1958). In 1958, Joan Bain categorized fruit development into three distinct phases: cell division stage (Stage I), cell enlargement phase (Stage II), and the maturation period (Stage III). In brief, Stage I is where the fruit's cells rapidly divide and differentiate into either albedo or juice vesicle cells, Stage II is where the fruit grows to its final size, and Stage III is where the fruit matures, the flavedo changes color and the juice contains less acid (Bain, 1958).

As the fruit ripens, the ovary and the carpels, create the core of the fruit, from which the hair-like juice vesicle cells radiate. As the fruit ripens, these juice vesicles will fill causing the sacs to fill into the pulpy flesh that is consumed. The fruit is encased in a think peel known as the rind, which in itself is divided into the flavedo, or colored portion containing the oil glands which give off the characteristic citrus aroma, and the albedo, the white portion of the rind on which the juice vesicles terminate (Ladaniya, 2010).

Seed production begins immediately after pollination. The ovules present in the ovary begin to grow in size and mature around the newly created embryo. The seeds form along the fruit core and are known to increase in size nearly 13-fold (Koltunow et al., 1995). Citrus seeds, in general, have two seed coats, one extremely durable external coat that is usually cream-colored and one pliable and thin internal coat that is usually brown. Surrounding the entire embryo are two cotyledons that contain the carbohydrates needed by a freshly germinated sapling. Citrus cotyledons are discussed as possible tissues for transformation in the following chapter.

It is essential to understand the general characteristics of the genus *Citrus* and its closest relatives, in order to discuss the pathogenic problems associated with citrus. Without these basic concepts, the symptoms and severity of the diseases covered below could go unnoticed.

Primary Citrus Diseases

A multitude of challenges threaten the citrus industry and have caused total citrus production to decline dramatically over the past decade. Across the globe, each citrus producing nation has to respond to at least one disease that disrupts total output. Two of the most severe pathogens to invade Florida and other major citrus producing countries are Huanlongbing (HLB) and Asiatic citrus canker (ACC). Both diseases have had a devastating effect on the citrus industry over the past decade, significantly increasing the cost of production and maintenance of the groves. Not only has HLB and ACC produced devastating effects on commercial citrus production, but citrus black spot (CBS) and sweet orange scab have contributed to an Florida citrus industry plagued by one or more of these diseases in every acre (APHIS, 2016).

Citrus Greening/HLB

The worst disease for citrus is HLB, known colloquially as citrus greening. It has directly caused the death of millions of trees worldwide. The disease was first identified in China around the turn of the 20th century. Since then, especially from 2005, HLB has spread from China, to almost every major citrus producing region in the world.

Once a plants becomes infected with HLB, the plant will begin to suffer a multitude of systemic effects. The severity of the effects differ from species to species, but ultimately if a plant becomes infected, it will never recover and slowly die. HLB symptoms affect the whole plant: leaves can turn yellow or become mottled, fruit ripens unevenly causing lopsided fruit or turns green at the peduncular end, the juice becomes bitter, seeds can abort, and the whole tree suffers as if it had a nutrient deficiency (Bove, 2006).

The causal agent of HLB is a gram-negative, phloem-restricted bacteria known as "*Candidatus* Liberibacter." The term Candidatus is due to its inability to be cultured *in vitro*, despite the extent to which it has been studied. Liberibacter has a long latency period , whereby upon initial infection, the bacteria escapes detection by the plant's defense mechanisms and will not show symptoms for 6-12 months (Alvarez et al., 2016); the bacteria literally clog the phloem and siphon vital resources destined to go from the leaves to the roots, by the time the tree has finally begun to show symptoms. Liberibacter contains multiple strains: the *asiaticus* strain (CLas) is the primary agent in the United States and Asia, the *africanus* strain (CLaf) infects mostly African and Middle Eastern regions, and the *americanus* (Clam) strain infects Brazil and South America (Bove, 2014; Batool et al., 2007). CLas is more heat tolerant than its heat-sensitive relatives, CLaf and Clam, and this trait is considered a major reason as to how it has

become so widespread in Southeast Asia and in the state of Florida (Bove, 2014, Batool et al., 2007).

In nature, Liberibacter is only known to be spread by an insect vector. CLas and CLam are transmitted via the Asian citrus psyllid (ACP) (*Diaphorina citri*), while CLaf is transmitted by the African citrus psyllid (*Trioza erytreae*). These small, flying insects have a range of miles but can be blown or carried on the backs of citrus trucks over even longer distances. They feed on the fresh, young leaves of citrus trees, extracting the phloem sap with their proboscises. Once in contact with the phloem, the insect has a very high chance of infecting the plant if it carries the pathogen or becoming a carrier itself from an already infected tree. This problem can be exacerbated by the fact that female psyllids can lay thousands of eggs during a lifetime (Bove, 2014, Batool et al., 2007). Of note, CLas can also be graft transmissible, which aids researchers in developing tools to combat this deadly disease (Bove, 2014; McClean and Oberholzer, 1965).

Due to its rapid spread and long-lasting impact on trees, HLB is the most damaging disease to have ever affected the industry. By 2012, HLB was responsible for the loss of over 215 million boxes of citrus, 4.5 billion US Dollars in value, and 2,700 directly employed jobs for the state of Florida alone in between the 2006-2007 and 2010 -2011 growing seasons (Hodges and Spreen, 2012). As of 2016, Florida has lost nearly 40 percent of total planted citrus acreage and 49 percent of total production from their historical highs, most of which was directly or indirectly caused by HLB (Alvarez, et al., 2016).

Citrus Canker

ACC is caused by the bacteria *Xanthomonas axonopodis* pv. *citri* (Xac). Once the Xac infects a tree, the plant to forms many pustules and lesions on the leaves and fruit. These lesions contain more of the bacteria and will release more of the pathogen when damaged through mechanical or natural means, especially through high winds and large amounts of rain, which are a common occurrence in Florida afternoons (Gottwald et al., 2002). Hurricanes and other tropical weather systems can play a major role in how well Xac can spread. Indeed, in the 2004 and 2005 hurricane seasons, citrus canker spread further than could ever happen in a typical thunderstorm (Gottwald and Irey, 2007).

Citrus canker is second only to HLB in the amount of crop losses for citrus. Even though ACC usually affects the fruit with lesions unappealing to a potential consumer, in the short term the fruit can still be processed into juice. In the long-term however, ACC will cause a slow decline in total fruit production and will eventually kill the infected plant (Apis.usda.gov, 2016). Florida first identified the disease in 1995. Due to the severity of the disease, a statewide eradication program was enforced. However, after a decade, the program was terminated as the disease had spread so much that eradication was no longer possible (APHIS, 2016).

Citrus Black Spot and Sweet Orange Scab

Citrus black spot is caused by a fungal pathogen known as *Guignardia citricarpa*. CBS causes eponymous black spots on the fruit that significantly affects yield, especially in sweet orange varieties. CBS can infect all commercial citrus species and cultivars commonly grown in Florida. Lemons and late maturing types of sweet oranges, such as ‘Valencia’, are highly susceptible to black spot (Dewdney, et al. 2010; Dewdney

et al., 2017). It is found nearly worldwide, including Asia, Australia and the Unites States. I was first reported in south Florida in 2010 (APHIS, 2016).

CBS causes the fruit crop to drop early, lead drop, and will cause the tree to produce significantly less fruit (Dewdney et al., 2017). The fruit and leaf drop contribute tremendously to how *G. citricarpa* spreads, with the conidia spores maturing in the dead leaves and spreading to other plants through wind and rain. Much like HLB, CBS also has a long latency period and visual symptoms will not appear on the fruit for several months (Dewdney et al., 2017; APHIS, 2016).

Sweet orange scab (SOS), similar to CBS, is characterized by large lesions on the fruit rinds, leaves and twigs. It is caused by the fungal pathogen *Elsinoe australis* (Chung, 2011; Dewdney, 2017). SOS generally will cause problems long term effects in addition to its visible symptoms, such as tree stunting and early fruit drop. SOS does not damage the fruit itself or the juice, so those fruits that were destined to be processed, would still be salvageable if they had SOS symptoms. The disease cannot be neglected though, as over multiple growing seasons, the tree will produce significantly less fruit (APHIS, 2016).

Taken together, the fungal pathogens ACC and SOS, do not account for the total losses inflicted by HLB or citrus canker in the United States of Florida, but as a whole these two diseases are still critical to control for citrus growers. In fact, the European Commission has placed a ban on fruit coming in from South Africa, Brazil and Uruguay due to CBS (EC-HFS, 2016), and the United States has placed every citrus producing state in quarantine for SOS, except California, which has only quarantined a few regions (APHIS, 2016).

Addressing these major citrus diseases individually might overstate their significance in biotechnology applications, but due to HLB and other citrus pathogens, significant amounts of new funding opportunities have opened up for citrus research. In trying to find solutions to these pathogens, more and more questions arise, that open the door for researchers to find the solutions.

Citrus Technologies: A Response to Citrus Diseases and Industry Concerns

The citrus industry is affected by each of the previously mentioned diseases every growing season, but they are only a sample of the total amount of pathogens affecting citrus worldwide. They have had a devastating economic impact by reducing the number of fruit-producing trees, reducing the span of tree productivity and increasing the cost of managing the groves. Because of them, states and countries that produce citrus have responded to them with quarantines, regulations, or eradications.

Regulation is essential, but the main focus of the majority of producers is to generate lines of plants with traits that are resistant to one or more of these pathogens. Critical to this point is understanding the immune response in different citrus genotypes. By comparing citrus to the plant model system *Arabidopsis thaliana* researchers have been able to propose multiple gene models for plant resistance and how the response might differ between susceptible and resistant cultivars.

Initially studied in *Arabidopsis*, the Non-expressor of pathogenesis-related (NPR) family of genes has been implicated as key components of systemic acquired resistance (SAR) and basal levels of cellular defense. NPR-1 in particular is necessary for the establishment of SAR and inducing the expression of pathogenesis related (PR) proteins that ultimately eliminate the infection and render the plant resistant to invading pathogens (Cao et al. 1997). NPR1 is a transcriptional activator of PR genes, notably

PR1. *Arabidopsis* NPR3 and NPR4 are also transcriptional co-activators but they seem to suppress PR1 gene expression and are also associated with the salicylic acid (SA) signal transduction (Zhang et al., 2006; Fu et al., 2012; Moreau et al., 2012).

Using the *Arabidopsis thaliana* model of defense, it is clear that the four main pathogens can usually infect the plant due to some malfunction from the normal defense pathway. This means that a resistance gene(s) will not be present in commercial varieties and a resistance gene is unlikely to evolve into these cultivars since citrus is usually graft-propagated, like the centuries old varieties like navel and 'Valencia' sweet oranges. Therefore, the characterization of a natural resistance gene(s) for conventional breeding will have to be discovered in wild citrus types.

Conventional Breeding of Genetic Improvement in Citrus

Conventional breeding is one useful technology that has been in practice for quite some time, and has recently been given new life, due to the multitude of genetic data and other citrus research over the past two decades. Now, conventional breeding it can be fully integrated into a genetic improvement program (Gmitter et al., 2007b). This process is characterized by breeding citrus varieties with distinct genes or genetic markers linked with traits that help produce a more desirable harvest. This process can take many years.

Due to the many factors associated in growing citrus, including soil types, citrus diseases, and nematodes, different techniques are used for conventional breeding in developing both scions (the canopy and fruit producing part of the plant) and rootstocks (the root system and base of trunk). For fruit producing scions, traits which favor juice, smaller rind thickness, or seedlessness are highly sought after. In contrast, roostock cultivars are selected for their temperature tolerance, resistance to root pathogens, and

for resistance to flooding or salinity (Gmitter et al., 2007b). Breeding new traits into each require different strategies, but the end result is the same: after several years of testing the fruit for a new traits, it is subjected to a new set of evaluations and repetitions across a large region, and then it is subjected to commercial evaluation (Gmitter et al., 2007b).

The process is vigorous and tedious but dependable, however, it is requires a significant amount of time, often decades. Another faster method is widely used by citrus researchers: genetic transformation. Currently, the citrus industry understands that traditional, conventional breeding may not be as efficient in controlling these pathogens (Gmitter et al., 2007a). According to the National Research Council, genetic transformation of a disease resistance trait may be the only way to fully exterminate the spread of the most damaging pathogens (NRC, 2010).

Citrus Transformation

In this method, a single resistance gene from another species, genus, or family or even kingdom could be found and inserted into commercial citrus varieties in as little as one generation, with the trait being homozygous in only two generations. Seen as a quicker solution in producing resistant citrus plants, it is easy to overlook the problems associated with genetic transformation in citrus.

Introducing the exogenous DNA into a citrus genome is extremely difficult and tedious. In *Arabidopsis thaliana*, most transformation is done using the ‘floral dip’ method (Clough and Bent, 1998; Bent, 2006). A bacteria with the gene of interest in *Agrobacterium tumefaciens* is cultured and then the flowers are dipped into the culture media, where 1% of the thousands of seeds should contain the gene of interest (Bent, 2006). Citrus cannot be transformed so easily however. Due to its waxy cuticles, woody stems, and different genetics, citrus requires different strategies.

Three different methods have been performed in citrus: protoplast transformation, particle bombardment of DNA directly into the genome and *Agrobacterium*-mediated plasmid transfer (Febres et al., 2011). Usually the citrus tissue chosen for transformation is epicotyl segments but other tissues have become available more recently, including cotyledons, leaves, and even mature plants (Oliveira et al., 2015). Subsequently, extensive tissue culture is required for the regeneration of the tissue into whole plants with all three methods.

Protoplast transformation is the preferred method on varieties which are dependent upon graft propagating. Generation and culture of citrus using protoplasts is a daunting task, as citrus tends to form very small quantities of embryogenic callus, especially in commercial varieties (Guo et al., 2005). In one source using ‘Valencia’ sweet orange only a single transformation event occurred (Guo and Grosser, 2005). This method is therefore used minimally and in a few labs dedicated to the live culture of citrus protoplasts (Febres et al., 2011).

Particle bombardment of DNA coated projectiles directly into the tissue is another method that has been used in citrus transformation experiments (Yao et al., 1996). This method is preferred due to the use of mature tissue, as well as a lack of generating protoplasts, however it has a major setback in citrus, due to the low frequency of transformed callus. Therefore, this method is not used for most transformation experiments in citrus. This type of transformation is fascinating because it does not require the use of bacteria or its DNA sequences. It is something we would like to incorporate into this project.

Agrobacterium-mediated transformation is the most widely adopted method, since the regeneration frequency is greatest, producing transgenic plants at a recovery rate up to 45% in select cultivars (Febres et al., 2011). In *Agrobacterium*-mediated transformation, a plasmid containing a gene of interest, as well as antibiotic selection and reporter genes, are set in between a set of T-borders: the DNA sequences that are required for proper integration of the transgene. The plasmid cloned from *Escherichia coli* is transferred into a uniquely disarmed, non-pathogenic *Agrobacterium* strain, usually from *Agrobacterium tumefaciens*. The bacteria is placed in contact with plant tissue (the explant) during the transformation on co-cultivation media with the explant. Next, the bacteria will invade into wounded plant cells on the tissue and insert the vector on to the genome, using the plant's own DNA repair mechanisms (Ziemienowicz, 2008). After antibiotic selection for the explants with the resistance genes, shoots will form from the callus creating transformed plants.

There are several drawbacks to the use of *Agrobacterium* as a way to create disease resistant plants. One reason is that in most commercial varieties, optimized protocols can only achieve 5-10% transformation efficiency (Moore et al., 1992). Compared, to the mere 1% in *Arabidopsis*, citrus transformation rates appear high, but it requires more hours of work and more resources, including media preparation, antibiotics, citrus seed germination, sterile working conditions, and many weeks until you can even test the plants.

Another significant drawback is in the regulation of transgenic crops. Given that the trait would likely come from another plant species, like Spinach (*Spinacia oleracea*) (Stover et al., 2013), this method requires foreign DNA material that is highly regulated.

In order to construct a plant optimized-plasmid, several selection markers are required, primarily anti-biotic genes that are not native to plants or *Agrobacterium*, and require border sequences known as T-DNA in order to insert into host genomes (Ziemienowicz, 2008). Therefore successful creation of a transgenic plant, several hurdles would come from the United States Food and Drug Administration, the United States Department of Agriculture, and other global regulating organizations, which would severely limit their commercial introduction.

New and Prospective Citrus Biotechnologies

In the literature, other technologies have been addressed in citrus, including genetic mapping (Curtolo et al., 2017; Cuenca et al., 2016), sequencing and genome databases (Main et al., 2017), and most interestingly, CRISPR/Cas9 systems (Ledford, 2017; Jia and Wang, 2014). CRISPR/Cas9 is a genome-altering tool that is discussed further in Chapter 4 of this work. Each of these technologies, as well as citrus transformation, have unlocked powerful new information at a much faster pace. Problems faced by the citrus industry, can be researched further in the laboratory, solutions can be found and then applied in the field in very little time compared to just twenty years ago.

The purpose of this work hopes to elaborate upon new technologies adapted for citrus that have developed in Dr. Gloria Moore's laboratory at the University of Florida in Gainesville, Florida. Specifically, in order to decrease the amount of time it would take to breed desirable traits, through the use of an alternative transformation method, which could eliminate the need for transgenic regulations, and by decreasing the maturation rate and increasing flowering.

CHAPTER 2
CELL-PENETRATING PEPTIDES: A MOLECULAR DELIVERY SYSTEM IN CITRUS

CPP Literature Review

Characteristics of Cell-Penetrating Peptides

Cell-penetrating peptides (CPPs) are a class of peptides which consist of short chains of amino acids and have a net positive charge. CPPs have been observed to translocate across most organic membranes carrying with them other molecules, highlighting their function as a cellular delivery mechanism. CPP function was first identified in two independent studies, in which researchers discovered the protein transduction domain (PTD) during tissue culture experiments using the HIV-1 Tat protein. Each laboratory concluded that the Tat protein contained two domains: a cysteine-rich region, which homo-dimerizes to other Tat proteins, and a positively charged domain, named the PTD, rich with lysine and arginine (Frankel and Pabo 1988; Green and Loewenstein, 1988).

The PTD performs the both of the function as it binds to other molecules and can translocate across cell membranes carrying these other molecules, known herein as cargoes, which include nucleic acids and proteins. The PTD is so versatile that when isolated, it still retains its duality, delivering the cargo before it ultimately degrades (El-Sayed *et al.*, 2009). These short, isolated peptide fragments were later renamed cell-penetrating peptides, in honor of their function, translocating into cells and delivering specific molecules to their targets.

CPPs must always include the minimum requirements for membrane translocation and cargo binding by maximizing each amino acid residue, and is thus usually manufactured to incorporate an arginine arm. The arginine arm is a short

segment of the CPP which contains several arginine residues. The presence of the arginine arm has been observed to translocate at much higher rates than other CPPs lacking such a motif (Nakase et al., 2007; Ma et al., 2011; Walrant et al., 2012). Though the net charge in the amino acids arginine and lysine is identical, arginine is the preferred residue when synthesizing CPPs because arginine has two polar head groups compared to only one in lysine. This makes arginine a much more viable molecular component, which is much more likely to interact favorably with surface molecules of the opposite charge than is a lysine equivalent peptide (Fretz *et al*. 2006). Due to the importance of the arginine arm, the work presented in this chapter focuses heavily on the use of arginine-rich CPPs.

Cell-penetrating peptide types

Since the discovery and isolation of the CPP Tat, a number of other CPPs have been identified or synthesized. Conveniently, many of these are readily available for scientific use (Thoren et al., 2000; Vives et al., 2003; Langel, 2007). CPPs typically carry their cargo either covalently or non-covalently, and CPPs can be categorized accordingly (Langel, 2007, Eiriksdottir et al., 2010). However, this approach to differentiation not suitable when only use non-covalently attached cargoes are utilized. This has led some researchers to categorize CPPs into four different groups: naturally-derived, synthetic, chimeric and proprietary (Table 2-1).

Naturally-derived CPPs occur in a variety of organisms and have been isolated from a variety of sources, including viruses, bacteria and even from the common fruit fly, (*D. melanogaster*), from which Penetratin is derived (Thoren et al., 2000; Dom et al., 2003). Synthetic pepides include those that have been fabricated entirely in a laboratory setting and are created to maximize the effects of certain experiments. The CPP known

as Arginine 9 (R9), for instance was created specifically as a way to optimize the Tat protein and has gone on to be used in siRNA delivery, among other functions (Wender et al., 2000; Bartz et al., 2011). Chimeric have a synthetic localizing signal placed on a terminal end of a naturally-derived peptide. These include the simple HIV-Tat and the more complex MPG-α and MPG-β (Morris et al., 1997). Proprietary mixtures of CPPs can also be purchased for research use; in this case the exact types and concentrations of CPPs used are not divulged, which include “JBS-Nucleoducin” from Jena BioScience (Jena, Germany).

In 2010, Eiriksdottir et al. postulated another classification method based on how the CPPs interact with the cellular membrane and how they are internalized. They postulate three distinct groups of CPPs: helical, sheet, and disordered. Helical CPPs form alpha-helices in the presence of phospholipids and the cell through either electrostatic or hydrophobic interactions, such as MPG-α. Sheet CPPs in contrast for beta-sheets in the presence of phospholipids and only use electrostatic interactions, like Penetratin. The disordered group is characterized by the lack of any conformation changes and keeps its random state even in the presence of phospholipids. Examples from the disordered group include both Tat and R9 (Eiriksdottir et al., 2010). No matter which method of categorization used, CPPs have been used in a variety of ways since they were discovery.

Cell-penetrating peptide uses

Currently, CPPs are revolutionizing the pharmaceutical and medical industries where they are being investigated as vehicles for the delivery of therapeutic compounds and other cargoes into the blood-brain barrier. CPPs are thought to be beneficial in cancer research as macromolecular treatment delivery systems specifically targeted to

cancer cells (Wadia and Dowdy, 2005; Faingold *et al.,* 2012). These applications of specifically targeting certain cells has led scientists to believe that CPPs can also work in plants, where they have entered protoplasts (Chugh and Eudes, 2007), but were thought to be unable to penetrate the cell wall, preventing access to the cell membrane. Surprisingly, recent evidence indicated CPPs also function in plant cells to ferry cargoes across cell membranes despite the presence of an acidic cell wall (Chen *et al*., 2007; Chugh and Eudes, 2008a, Chugh and Eudes, 2008b). This offers a number of novel and creative possibilities regarding the improvement of plants that we would like to exploit in citrus.

Translocation Mechanisms of Cell-Penetrating Peptides

Most research, contributes to the utility and wide application of CPP and cargoes in plants and animals. However, despite the vast amount of research using CPPs, the exact mechanisms by which CPPs molecularly translocate across cellular membranes remains unclear (Langel, 2007; Eiriksdottir et al., 2010). In order to completely understand all of the potential applications of CPPs, the physiological mechanism for CPPs should be examined. Currently, three different supposed translocation mechanisms exist: direct penetration, macropinocytosis, and receptor-mediated endocytosis. Each mechanism is supported by detailed evidence, but are not mutually exclusive (Futaki et al., 2007; Langel, 2007; Nakase et al., 2007; Mishra et al., 2011).

Direct translocation

Direct translocation is the most energetically conservative mechanism of the potential mechanisms. It requires only the passive rearrangement of the inner and outer lipid membranes as the positively charged PTD electrostatically interacts with the negative polar head groups of the inner cell membrane. When endocytosis processes

are halted at 4oC, CPPs still function and their translocation can increase. Results are similar during extended periods at low temperatures. This data indicates that the direct penetration model may be viable with the Tat PTD or similar CPP (Nakase et al., 2004). The direct penetration model may explain some CPP translocation, but it is not likely the primary mechanism for molecular cargo exceeding 2,000 Daltons. This would be due to a steric hindrance at the lipid bi-layer with larger cargoes (Nakase et al., 2008).

Macropinocytosis

Macropinocytosis is a cellular process that requires the complete rearrangement of the cytoskeleton in which the cell physically engulfs the peptide/cargo complex in the presence of dynamin and actin (Fretz et al. 2006; Mishra et al., 2011). Initiation of macropinocytosis requires large quantities of ATP and is highly dependent upon cell membrane structures. The CPPs are known to bind to proteoglycans, most notably the negatively charged heparan sulfates (HS) embedded in the cell membrane (Tyagi et al., 2001; Wadia, Stan, Dowdy 2004). When a CPP binds to a HS, the initiation of actin filaments manipulates the cytoskeleton to engulf the CPP and its cargo (Vives et al., 2003; Nakase et al., 2007). This method of uptake forms a lipid endosome, which absorbs the whole complex in its own lipid bi-layer. Current literature states that once the complex has been engulfed, the cargo still may not be actively present in the cells due to inadequate vesicle release post-uptake (El-Sayed et al., 2009; Ma et al., 2011). Further research is needed to elucidate how these vesicles are lysed and their contents made available to the cell.

Receptor-mediated endocytosis

Receptor-mediated endocytosis is a process in which the CPP and cargo complex interacts with a membrane-bound receptor that elicits a downstream cell

response. This response signals the subsequent uptake of the CPP and its cargo via formation of an endosome (Richard et al., 2003; Futaki et al., 2007). This mechanism is similar to macropinocytosis, except that it does not require as much energy input and does not require the rearrangement of cytoskeleton elements. Endocytosis is more sensitive to exogenous CPP application than other CPP translocation types (Wadia and Dowdy, 2005). Current literature states that endocytosis is the most probable pathway for overall enzymatic efficiency and has the most variability (i.e. clathrin-dependent vs. clathrin-independent) (Richard et al., 2003; El-Sayed et al., 2009; Ma et al., 2011). This pathway has been shown to improve efficiency in the presence of endosome digesting compounds similar to those of viruses (Wadia et al., 2004). Receptor-mediated endocytosis is difficult to study because there are currently no known CPP receptors that elicit the signal. One group contends that endocytosis is not the preferred method in CPPs because of their capability to function at 4oC, when endocytosis is stopped (Chugh and Eudes, 2009).

Each translocation mechanism is supported by detailed evidence. Therefore, we support the hypothesis of other authors that uptake of CPPs across the plasma membrane are not mutually exclusive and are highly dependent upon many factors, including atmospheric or solution temperature, concentration of CPPs, fluidity of the membranes, and cargo used (Fretz et al., 2007; Nakase et al., 2008).

Cargoes of Cell-Penetrating Peptides for Use in Plants

In contrast to the disputed translocation mechanisms, CPP cargoes are well-characterized and are currently being rapidly applied in a wide range of biotechnology applications. Cargoes in the generic sense are simply molecules that covalently or non-covalently bind to the CPPs at the PTD, and are translocated across the plasma

membrane along with the peptide. In this context, cargoes include nucleic acids, ranging from plasmid DNA, RNA, and siRNA, complete proteins, organic molecules, and even other peptides (Langel, 2007). Cargoes were originally thought to require a covalent bond before the CPP would be able to translocate into live cells, but new insights indicate that instead of a strong sharing of electrons, only the weak electrostatic forces of positively charged amino acids are enough to bind to negatively charged molecular cargo, such as that found on the sugar-phosphate backbone of DNA or in proteins with a high density of negatively charged amino acids, like glutamic acid. Though most of CPP research focuses on animals, this weaker binding has been shown to be effective in delivering cargo in both plants and animals (Langel, 2007; Chen et al., 2007; Chugh and Eudes, 2008).

In plants, Chen et al. (2007) have shown that plasmid DNA can be translocated into mung bean (*Vigna radiata*) root tips and onion (*Allium cepa*) epidermal cells. They used a plant optimized plasmid containing the sequence for green fluorescent protein (GFP), a protein isolated from *Cnidarian* species, and glows a very bright green when excited and examined using the appropriate light filters. Not only was translocation of the plasmid achieved, they were also able to see the protein expressed in the nuclei of the plant cells. This means that the plasmid was delivered into the nucleus of the plants, transcribed into messenger RNA (mRNA), exported out of the nucleus, where ribosomes translated the sequence into a protein that was then shuttled back into the nuclei, where Chen et al. (2007) were able to visualize the protein. This is an enormous feat for just plasmid and CPPs. Subsequently, Chugh and Eudes (2008) used immature

wheat (*Triticum aestivum cv.*) embryos in conjunction with CPPs and plasmid DNA, which also resulted in protein expression. (Chen et al. 2007, Chugh and Eudes, 2008).

We have conducted our own experiments with citrus tissue treated with CPPs bound with various cargoes. Our purpose was to determine which CPPs allowed import of protein cargo and with what efficiencies. The cargoes utilized were plasmid DNA or full-length proteins of GFP and β-glucoronidase (GUS). In all cases, it was apparent that the proteins were taken up, although various CPPs were more or less efficient. Protein or fluorescence was visualized within the plant cells, but not in control samples when CPPs or protein were omitted.

Materials and Methods

Materials

Cell-penetrating peptides

The CPPs used in this study are presented in Table 2-1.For protein and plasmid DNA delivery in mung bean and citrus, each peptide was used, For *in planta* trafficking experiments, we only used R9 and a fluorescence-labeled R9- 6-FAM fluorescein (R9-F) (Anaspec, Fremont, CA).

Genetic material and sequence data

Plasmid DNA used in this section were reporter plasmids, pCAMBIA-2201 (Figure 2-1A) and plasmid pCAMBIA-2202-sGFPS65T (Figure 2-1B) (Cambia Labs, Canberra, Australia). Both plasmids contain a multi-clonal site (MCS). The MCS allows the plasmid to easily contain a gene of interest. The plasmid pCAMBIA-2201 contains the GUS reporter gene and a kanamycin resistance gene, while the pCAMBIA-2202-sGFPS65T contains the GFP reporter gene and a chloramphenicol resistance gene.

Sequence data was obtained from the source and uploaded into a genetic sequence program known as Vector NTI (Thermo Fisher Scientific, Waltham, MA).

Citrus cultivars and other plant tissue used

The citrus types and cultivars used were ‘Pineapple’ sweet orange (*C. sinensis* Osb.), ‘Duncan’ grapefruit (*C. paradisi*Macf.) and ‘Carrizo’ citrange (*C. sinensis x Poncirus trifoliata* (L.) Raf.). These cultivars were specifically chosen for commercial or laboratory uses. Sweet orange cultivars have enormous market value and is the leading citrus crop in North America and other Western countries (Bond and Roose, 1998). ‘Duncan’ grapefruit has great potential for regeneration when used in tissue culture experiments and as such has a large transformation yield. ‘Carrizo’ citrange is used extensively as a rootstock for its cold hardiness and tolerance of abiotic factors when compared to other citrus.

From these cultivars, multiple plant tissue types were used and was dependent on the experiment. To investigate the potential use of CPPs in systemic transport of molecules and to optimize the best conditions and tissues to use in our transformation experiments, citrus epicotyl segments were primarily used. In the citrus transient expression optimization experiments, epicotyl segments and young leaves were used. Uptake activity and systemic transport in multiple citrus species using fluorescent CPP tracking assays. Understanding the systemic nature is useful for delivering cargoes into mature tissues *in vivo*, and could even be used to inoculate plants with bactericides. We wanted to determine their transport capabilities using two tissue types: intact seedlings and mature plants.

Mature plants have not historically been used in plant tissue culture because of their distinct lack of sterility. We are interested in creating an all new method of

transformation, therefore we do not have to limit ourselves to traditional tissue culture transformation methods. Initially, we are interested in whether or not CPPs can be transported systemically *in planta*. But, we are interested in delivering specific proteins directly into the plant. For this experiment, we used 15 three year old 'Pineapple' sweet orange (*Citrus x sinensis*) plants. The plants were trimmed and allowed to grow new flushes of about 20-30 cm.

Once flushed, new leaves were infiltrated with PBS, containing a final concentration of 1 mM *R9-F*. The concentration of peptide was adjusted as needed depending upon initial findings. Our experiments used two target points of entry into the recently flushed plant: one in the younger, upper leaves and the other in the slightly older, lower leaves. Systemic movement of the R9-F peptide in plants was determined by examining select leaves. Initially, the injected and adjacent leaves were removed and immediately examined for fluorescence. If these results indicated that CPPs can move beyond the injection site, we began to look beyond the adjacent leaves including the opposite end from inoculation point, and include longer time intervals. We expected that at least one cultivar should have provided enough evidence to indicate that CPPs can move throughout whole plants. This would have far reaching effects that could ultimately eliminate the need for tissue culture in gene transfer experiments.

Methods

Large scale purification of plasmid DNA

Amplification of plasmids: Autoclaved 500 ml Luria broth media (LB) in a 2L flask, cooled LB overnight. The *E.coli* mutant containing the reporter plasmids, pCAMBIA-2201-GUS or pCAMBIA-2202-GFP- S65T (Figure 2-1) was cultured in 10 mL of LB in 150 mL culture tubes with 10 µL 50mg/mL kanamycin or 100mg/mL

chloramphenicol, respectively, and shaken in a bacterial incubator at 37 °C at 225 rpms overnight. At OD_{600} of 0.6, the 10 mL culture was added to pre-warmed (37 °C) LB, which was shaken for 2.5 hours at 37 °C until the OD_{600} reached 0.4. Added 250 µL of appropriate antibiotic at the same concentrations, and shaken at the same conditions overnight (12-16 hours).

Lysis of Bacteria and Recovery of Plasmid DNA: Separated the liquid culture into plastic centrifuge bottles. Harvested the bacteria through centrifugation at 4000 rpm in a pre-cooled centrifuge (4 °C) for 15'. Bacteria collected at the bottom. Poured off the supernatant and resuspended bacteria in 100 mL of ice cold buffer (0.1M NaCl, 10mM Tris Cl [pH 8.0], and 1mM EDTA [pH 8.0]). Collected the pellets once more via centrifugation described previously. Bacteria resuspended into a lysozyme buffer (50 nM glucose, 25 nM Tris Cl [8.0] and 10 mM EDTA [8.0]). Added 1 mL lysozyme (10 mg/mL), 20 mL of a basic detergent solution (0.2 N NaOH and 1% (v/v) SDS) and 10 µL of 100 mg/mL of RNaseA then incubated at room temperature for 10 minutes. To neutralize the alkalai solution, 15 mL of ice-cold a weak acid solution (5M potassium acetate, 11.5% (v/v) glacial acetic acid) was added and the mixture was shaken vigorously by hand and stored on ice for 10 minutes. Bacteria was recovered via centrifugation as described. Supernatant now contained the plasmid DNA. Decanted supernatant through four layers of cheesecloth. DNA washed with a 0.6 ratio (v/v) with isopropanol, mixed and incubated at room temperature for 10 minutes. DNA was recovered by centrifugation at 5000 rpms for 15 minutes in a room temperature centrifuge. Supernatant removed, and the DNA pellet dried inverted at room temperature for 10 minutes. DNA was dissolved into 10-15 mL of an elution buffer.

Purification of Plasmid DNA: To purify the DNA for laboratory use, the dissolved DNA was divided into multiple PCR purification columns. DNA was further purified according to the “Re-purification of plasmid DNA prepared by methods other than QIAGEN tips” Protocol (QIAGEN, Hilden, Germany). Plasmid DNA was run on a 0.8% (w/v) agarose gel at 100V for 30 minutes to view the purification and verify the proper size (Figure 2-2A). To verify that the extractions contained the appropriate plasmid, restriction enzyme digestion was performed to linearize using the restriction nuclease EcoRI at 37 °C for 4 hours. Linear plasmid DNA was verified on a 0.8% (w/v) agarose gel (Figure 2-2B). DNA concentration and purity were measured using a spectrophotometer.

CPP protein delivery in citrus

In order to deliver protein in citrus plants, samples of epicotyls or cotyledons were used. Samples were mixed in increasing concentrations of GUS protein from 1:1, 1:2, and 1:3, CPP to protein to determine the most efficient. To determine which CPPs were the best at delivering protein in citrus, 5 different CPPs (Chariot, JBS_Nucleoducin, MPG-α, MPG-β and R9 were tested in a 1:1 mixture.

For both experiments, the CPP was combined with the GUS protein in solution and incubated for 1 hour at 37 °C and then administered to the plant tissue.

CPP transient expression method in citrus

For transient expression experiments, 4-5 week old citrus seedlings, cut into 2cm segments or citrus cotyledons were used. Optimization of this process was completed in small experiments, usually modifying the procedure by adding or removing a reagent pre- or post-treatment. Standard tubes and large plates were used.

Etiolated grapefruit epicotyl segments were imbibed in a phosphate buffer solution for 1 hour. A GUS reporter plasmid, pCAMBIA-2201, was purified using plasmid maxi-prep. 10 µg of plasmid was suspended with 10 µg of the CPP, Arginine 9 (R9) into 12 mL of phosphate buffer solution and incubated at 37 °C for 30 minutes. Before introducing the epicotyl segments into solution, a lipid transfection agent, Escort, was added to the CPP-plasmid complex solution in differing concentrations and incubated for another 10 minutes at 37 °C. The segments were then incubated in the CPP-plasmid-Escort solution overnight (16 hours) at 37 °C. The segments were removed from solution and soaked in trypsin for 5 minutes, and then soaked in deionized water three times for 1 minute each. The samples were then suspended in X-gluc overnight (16 hours) and the resulting GUS score was recorded per segment.

CPP transformation protocol

Cell-penetrating peptide transformation procedure was tested for citrus. Etiolated citrus segments were co-cultivated with the CPP, Arginine 9 (R9), and pCAMBIA-2201 in liquid medium overnight (16 hours) at 25 °C. The segments were then removed from co-cultivation medium and transferred to solid medium containing the antibiotic kanamycin as a selection agent to apply pressure to uptake of the plasmid's T-borders. After 4-5 weeks, surviving segments turned green and some produced several new shoots. Shoots were excised and placed on auxin-containing (indole-acetic acid) rooting medium.

Once the roots were established, about 4 weeks later, the regenerated plants were placed in soil and set in a growth chamber with 12 hours of light per day. When the plants had enough leaf material to survive harvesting, a reporter screen for either GUS or GFP was performed, followed by PCR confirmation.

CPP tracking in citrus

To begin tracking the R9-F in citrus seedlings, all three cultivars were germinated and grown in darkness on MS solid medium at 27^{o}C. They were removed from solid medium and placed in a plant preservation medium containing a CPP with a fluorescent tag, R9-F for up to 48 hours. The medium includes a final concentration of 1 or 5 mM purified R9-F. Negative controls are 1 or 5 mM of a non-translocatable fluorescent polysaccharide, FITC-Dextran (F-Dex). Prior to examination, the seedling segments were removed from culture and washed to remove excess medium. A subsequent trypsin wash removed exogenous fluorescence by cleaving any peptide fragments apart on the outside of the seedlings. Rinsing the plant segment removes the excess trypsin, and the plants can be scored for fluorescence.

Samples of seedlings from each treatment and genotype are evaluated for relative fluorescence levels starting two weeks after planting and for a total of five weeks using the light parameters for FAM of Abs/Em = 494/521 nm. We expect to visualize R9-F in most samples taken throughout the entire plant as they grow. In this design, there should be no significant difference between relative fluorescence in both FAM concentrations when compared to controls, which indicates that R9 are moving systemically throughout the citrus plants. In our early experiments testing this method we have seen that R9 can be transported in the epicotyls all the up way to the leaves.

Development of a relative GUS scale

In order to determine its effectiveness at our transient expression method, we developed a relative GUS scale that we could use to compare treatments (Figure 2-3). The scale was rated from 0 to 5, where 0 was no expression, 1 was approximately 1-20%, 2 approximately 26-50%, 3 approximately 51-75%, 4 76-99%, and 5 was full

expression of every visible piece of tissue.The percentages were based on blue expression per area.

Results and Discussion

One of our main goals already under investigation is the transient expression of DNA using CPPs as the carrier agent. We hypothesize that a CPP transient expression assay could be used in combination with tissue culture in order to create a stable transformation protocol. Alternatively, CPPs could also be used to effectively deliver therapeutic treatments into field trees. In our preliminary studies using mung bean (*V. radiata*) and sweet orange (*C. sinensis*), CPPs proved capable of delivering protein and plasmid DNA cargo in epicotyls and cotyledons. Our data is presented below.

Protein Delivery

In order to determine if we could transiently express a plasmid (pCAMBIA-2201, containing a GUS gene, in plants we decided to use mung bean, where researchers have already proven them to work (Chen et al., 2007). First we isolated large amounts of plasmid DNA from *E. coli* and managed to recover and purify over 10 mg of plasmid to a concentration of 1µg/µL. Gel electrophoresis and restriction digestion confirmed the proper plasmid (Figure 2-2). A nanospectrophotomer was used to confirm the concentration (data not shown). Tissue used were mung seeds germinated in the dark on moist germination paper. 10µg plasmid cargo and 10µg CPP were mixed for 30 mins at 37^{o}C. Our experiments confirmed a previous report that a 1:1 ratio of CPP to DNA is the most optimal (Figure 2-4) (Chen et al., 2007). Five-day-old etiolated seedlings were incubated for 1 hour with the CPP:complex solution at 37^{o}C. Seedlings were washed with a trypsin solution and rinsed with deionized water three times as indicated in the methods. After rinsing, the seedlings were stained for GUS overnight and were examined for the blue reporter color after 8 hours. Our results in mung bean indicated that the CPP JBS_Nucleoducin performed the best in the assay, while R9 was a close

second and contained less variance (Figure 2-5).Systemic Tracking of CPPs Understanding the systemic nature is useful for delivering cargoes into mature tissues in vivo, and could even be used to inoculate plants with bactericides. We wanted to determine their transport capabilities using two tissue types: intact seedlings and mature plants.

Systemic Tracking of CPPs

Understanding the systemic nature is useful for delivering cargoes into mature tissues in vivo, and could even be used to inoculate plants with bactericides. We wanted to determine their transport capabilities using two tissue types: intact seedlings and mature plants.

For in planta trafficking experiments, we used fluorescent-labeled R9- 6-FAM fluorescein (R9-F) to investigate how far the CPP with a fluorescent label could travel and compared it to FITC-Dextran, a fluorescent labled polysaccharide. The plant was placed in solution (described in Methods) (Figure 2-6A). After treatment, the plant was dissected and examined for fluorescence (Figure 2-6B-E). The data indicate that R9-F is actually able to travel into the roots and through the vasculature (Figure 2-6B, C) all the way up into the leaves (Figure 2-6D, E).

For the next tracking experiment both R9 and R9-F were used and complexed with GUS enzyme to determine the relative efficiency at transporting cargo and being systemic in the plant. Our data indicate, R9-F and R9 perform similarly in sweet orange cotyledon reporter assays when β-glucuronidase (GUS) protein is used as a cargo. Only R9-F indicates fluorescence activity, but both are capable of delivering the GUS protein cargo (Figure 2-7).

CPP-mediated Transient Expression of Plasmid DNA

The protein delivery results, prompted the next plasmid experiments. Since protein was so efficiently delivered, plasmid DNA would be more difficult to optimize, but could potentially be just as repeatable. The first step to this goal would be to discover which CPP actually could deliver the plasmid in citrus efficiently.

As described in Methods, five-week-old etiolated grapefruit (*C. paradisi*) segments were excised into 2 cm hypocotyl segments. 10µg pCAMBIA-2201 plasmid cargo and 10µg JBS-Nucleoducin, R9, or MPG-α were mixed for 30 mins at 37ºC. Explants were incubated for 4 hours with the complex mixture at 37ºC. Seedlings were washed with a trypsin solution and rinsed with deionized water. The seedlings were stained for GUS overnight and were examined for the reporter color. The data indicate that *R9* was expressed the most the most consistently (Figure 2-8). This result led to the optimization of transient expression and transformation based solely around the R9 CPP.

However, this method was only successful on about 20% of total citrus explants across all the treatments, and only about 60% of explants treated under R9, prompting an optimization to the procedure. Since CPPs can uptake via endocytosis, we decided increasing vesicle formation could improve our transient expression method. Therefore, we investigated the use of a lipid transfection reagent, Escort (Sigma Aldrich, St. Louis, MO), in order to accomplish this. This chemical has been implicated in delivering molecular cargoes, into cells *in vitro* (Tabatt et al., 2004)

Five-week-old *C. x paradisi* explants were treated with 10µg pCAMBIA-2201 plasmid cargo and 10µg of *R9*, along with different amounts (10, 20, 30, 40 µg) of Escort for 12 hours. Segments were moved and cultivated on non-selection media for 5

days, then washed with trypsin, rinsed, and stained and examined for the reporter color. Escort clearly showed an enhanced effect when 10 or 20 µg was used (Figure 2-9), while a decreased effect was seen in the 30 and 40 µg treatments. The most effective treatment was 20 µg Escort, but since it was negligible to the 10 µg treatment and it used half as much, 10 µg was used in transformation experiments. At 10 µg of Escort, 100% of explants expressed the GUS reporter. While the results seem to contrast with one another that the more Escort added, the worse it performs at delivering the plasmid cargo, but the likely reason is that the addition of Escort improves vesicle formation, but is limited by plant's ability to release the vesicles. . This procedure ideally works on all citrus, but we acknowledge that certain cultivars will require further optimization, since we have only qualified use in grapefruit, sweet orange, and citrange. CPP-Mediated Transformation in Citrus

The completion of this experiment and its data brought us one step closer to completing our transformation goal, as we used what we have learned toward our project purpose. Next, we wanted to determine if we can reduce the amount of bacterial DNA by replacing plasmid T-borders for P-borders and removing the selection markers. Our goal with this method is to be able to express a minimal gene PCR products, which includes only a promoter, gene and terminator, *in planta.*

In order to increase efficiency upon *Agrobacterium*-mediated transformation in citrus and eliminate the need for bacterial sequences, we used CPPs as carriers of genes and develop a new transformation method. We accomplished this task by combining our CPP transient expression data with "conventional" regeneration methods to recover transgenic plants via tissue culture to improve such methods. The percent of

explants producing shoots, total shoots produced, and average number of shoots produced per responding explant, reporter positives, and PCR positives were scored. We hypothesized that at least one cultivar would provide a clear protocol for stable integration of foreign genes when using CPPs as the delivery vector given the optimal conditions.

Previous plant studies indicate that the combination of CPPs and conventional tissue culture methods could provide a new avenue for plant transformation (Ziemienowicz et al., 2012). The seedlings were *in vitro* germinated on Murashige and Skoog (MS) solid medium at 27^{o}C in the dark for three to five weeks. This makes the tissue much more nubile and lighter. These seedlings were cut into five to six 1-2 cm epicotyl sections. For cotyledon experiments, seed coats were removed aseptically and the two halves recovered.

This work relies heavily on the use “conventional” regeneration techniques as demonstrated in combination with this technique in order to regenerate transformed plants.The segments or cotyledons were imbibed in a phosphate-buffered saline solution with 5% DMSO or a 1:20 toluene/ethanol (v/v) treatment to increase permeability. Meanwhile, 50 µg of the CPP was be mixed in 1 mL of phosphate buffer with 50µg plasmid. The mixture, incubated at 37^{o}C for one hour, was next placed in contact with the citrus explants to a final concentration of 10 µg of CPP and plasmid DNA per 1 mL of solution overnight (16 hours)(Figure 2-10A). Next the plants were placed on co-cultivation media for 5 days and then switched to shooting media (Figure 2-10B). Once the segments shooted or died, the shoots were carefully removed from the segments and placed directly into rooting media (Figure 2-10C). Once the root

system was established the plantlets were placed into soil and allowed to grow covered in a 12 hour day growth chamber (Figure 2-10D).

The total number of segments and shoots used in the experiment is presented in Table 2-2. Using this method, under the treatment using the plasmid pCAMBIA-2202-GFP- SGFPS65T and R9*,* shoots were regenerated that (Figure 2-10B) passed the first round of reporter analysis with the visualization of the GFP protein (Figure 2-11A, B), and some explants likewise produced visualization of GFP (Figure 2-11C) (Table 2-2).We have not yet obtained any GUS positive shoots with the pCAMBIA-2201 plasmid. When shoots might have had a blue color for GUS positive shoots, they were quickly identified them as PCR negative using our designed primers for our constructs (Table 2-3). As previously described, producing transgenic plants is a very involved and time consuming process and recovering positive PCR shoots was a major goal of this research however we were only ever able to transiently express plasmid in the plant samples, and were never able to stably transform citrus.

Cell-Penetrating Peptide Conclusions

The work presented in this chapter cab have great impact for the scientific community at large. CPPs are able to efficiently bind to and traffic protein into citrus cells. This can have farther reaching affects now that purified protein with respect to the new methods of delivering gene editing proteins directly into the plant. CPPs additionally can deliver

DNA plasmid into citrus cells, albeit a little inefficiently the optimization of plasmid delivery indicated that when paired with a lipid transfection agent transfection efficiency is much higher. By taking this method further we were able to show that although we

can deliver plasmid DNA directly, we were unable to get stable DNA integration or successful transformation.

In conclusion, CPPs offer a system for the quick delivery of proteins and the expression of genes without using bacteria. Such techniques are useful for choosing the best genes that should be used in conventional breeding programs but also could become a tool for the delivery of disease therapies to trees that are already planted in the field.

Tables

Table 2-1. Cell-penetrating peptides and their properties

CPP	Charge	Type	Sequence
R9	+9	Synthetic	RRRRRRRRR
R9-TAT	+9	Synthetic	GRRRRRRRRRPPQ
R9-F	+9	Chimeric	RRRRRRRRR-FAM
TAT	+8	Naturally-derived	GRKKRRQRRRPPQ
Penetratin	+7	Naturally-derived	RQIRIWFQNRRMRWRR
Chariot	+6	Synthetic	KETWWETWWTEWSQPKKKRKV
MPG-α	+5	Chimeric	Ac-GALFLAFLAAALSLMGLWSQPKKKRKV-NH-(CH2)2-SH
MPG-β	+5	Chimeric	Ac-GALFLGFLGAAGSTMGAWSQPKKKRKV-NH-(CH2)2-SH
JBS-Nucleoducin	?	Proprietary	Not published

Table 2-2. CPP-mediated transformation results

Cultivar	#Segments	#Shoots	% Shoot/Segments	Reporter Positive Shoots	% Positive Shoots/Segment	PCR Positive Shoots
Grapefruit	778	118	15.17	22	2.83	0
Sweet Orange	587	30	5.11	4	.68	0
Carrizo	684	95	13.89	14	2.05	0
Totals	2049	243	11.86	40	1.95	0

Table 2-3. Primers used in this chapter.

Primer #	Primer ID	Location on Template	DNA Sequence
SJ1	35S-P FW	35S Promoter	catggagtcaaagattcaaatagag
SJ2	Nos-T RV	NosT	tcccgatctagtaacatagatgac
SJ3	i35S-P FW	35S Promoter	ttcatttcatttggagagaacacg
SJ4	iGUS RV	GUS intron	catcgaaacgcagcacgatac
SJ5	35S-P2 FW	35S Promoter	gaagttcatttcatttggagagaacacg
SJ6	GUS-In RV	GUS intron	accgcatcgaaacgcagcacgatac

Figures

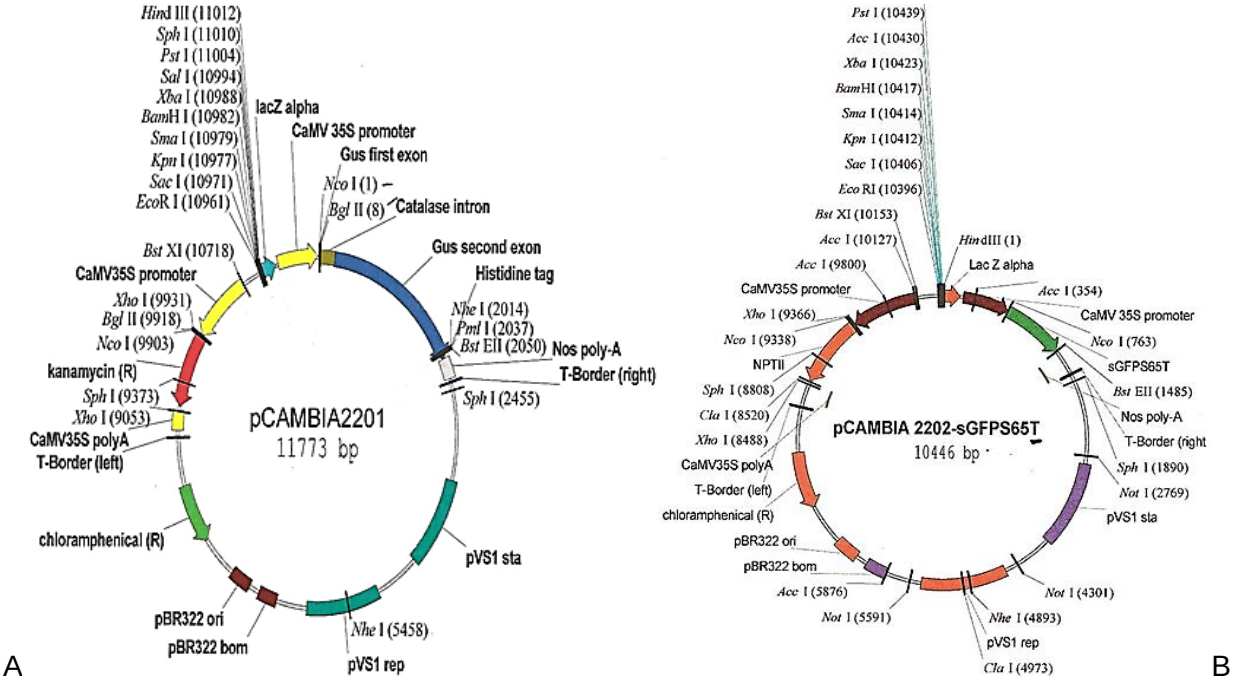

Figure 2-1. Visual representation of the plasmids used in the study. Sequences were uploaded from the source, CAMBIA labs, and uploaded into Vector NTI software. The features were either added manually or present upon retrieval. A) The plasmid pCAMBIA-2201. This plasmid contains the GUS reporter gene and two antibiotic resistance genes for chloramphenicol and kanamycin. B) The plasmid pCAMBIA-2202-SGFPS65T. The plasmid contains a gene for green fluorescent protein (GFP), and contains chloramphenicol and neomycin resistance genes.

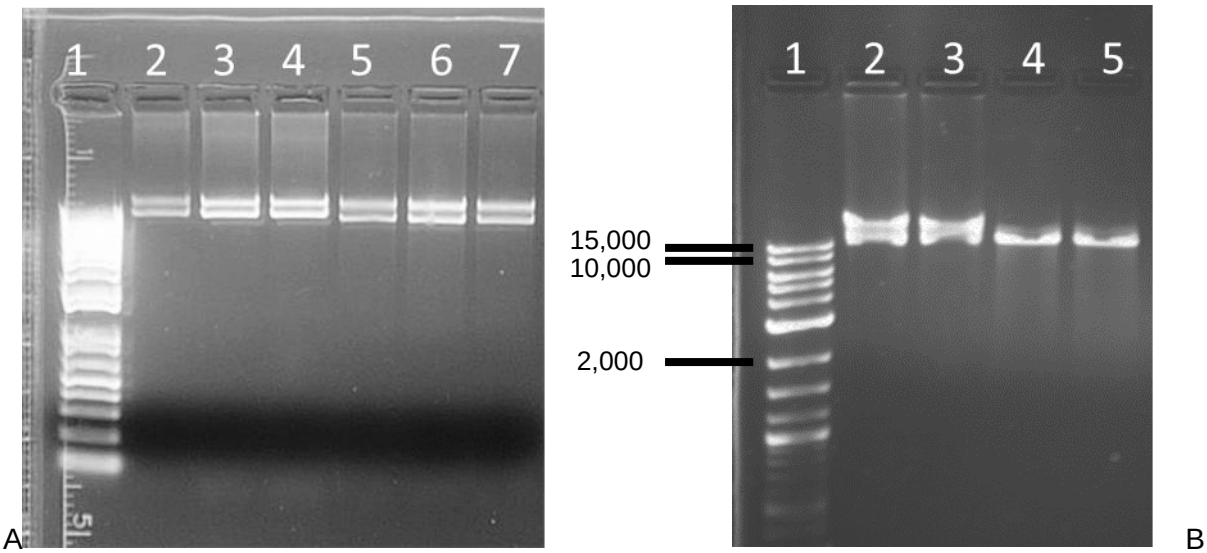

Figure 2-2. Preparation and confirmation of plasmid DNA. A) Prepared, circular/supercoiled plasmid DNA in three replicates (as pictured) from one 500 mL culture. 0.01 µg DNA in each well. Preparations were made of each plasmid 3 different times. Lane 1: 1 kb plus Ladder Lanes 2-4: pCAMBIA-2201(11,773 kb) Lanes 5-7: pCAMBIA-2202-GFP-S65T(10,446 kb). B) To further confirm the plasmid were suitable for experimentation, a restriction digestion was performed using EcoRI on pCAMBIA-2201. 1 µg of DNA was used in the digestion assay and the reaction was performed as per the manufacturer's instructions (New England BioLabs). Restriction digestion confirmation was performed in two replicates (as pictured) for both plasmids for each DNA preparation (3 times each). Lane 1: 1 kb plus Ladder Lanes 2-3: pCAMBIA-2201, undigested Lanes 5-7: pCAMBIA-2201, digested with EcoRI. Each large-scale DNA preparation yielded approximately 12 mL of plasmid at a concentration of 1 µg/µL (Total 12mg).

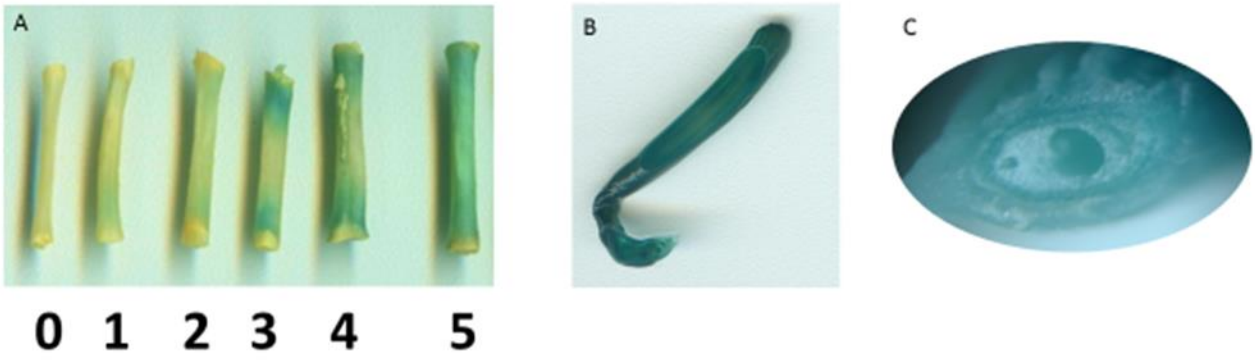

Figure 2-3. Relative quantification scale of GUS expression. To determine transfection efficacy of cell penetrating peptides (CPPs) using DNA or protein required the use of a relative quantification scale. After treatment with a GUS plasmid (pCAMBIA-2201) or isolated GUS protein, and subsequent staining with X-gluc, plant material was scored using a scale from 0 to 5, where 0=0% (no blue color), 1: >1%-25%, 2: 26-50%, 3: 51-75%, 4: 76%-99%, 5: 100% (entirely blue). A) Representative citrus from 'Duncan' grapefruit (*C. paradisi*) samples, with the scale presented below indicating their relative GUS levels. B) A representative sample with the score "5" for mung bean (*V. radiata*). C) A cross section from grapefruit, which was scored "5", indicating that the GUS stain is able to be expressed in the center of the plant segment.

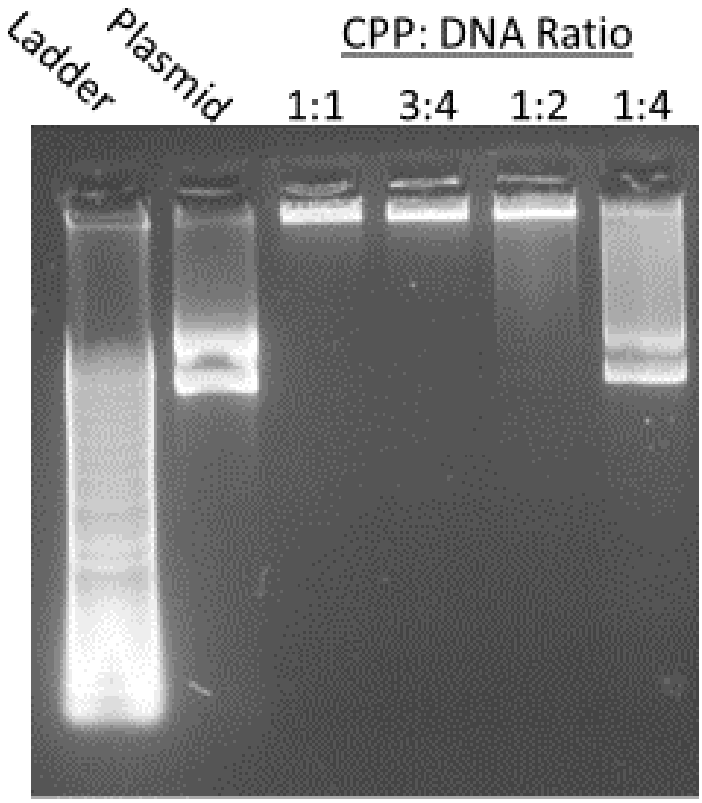

Figure 2-4. Cell-penetrating peptides (CPPs) complex with DNA plasmid cargo. Plasmid DNA, pCAMBIA-2201, was incubated for 1 hour at 37 °C with the given ratios of the CPP, Arginine 9 (R9). The solutions were run in a 0.8% agarose gel at 100 V for 30 minutes. The amount of DNA used was constant (0.1 µg). Lane 1: 1 kb ladder; Lane 2: plasmid only (0.1 µg DNA, 0 µg CPP); Lane 3: 1:1 ratio CPP to plasmid (0.1 µg CPP, 0.1 µg DNA); Lane 4: 3:4 ratio (0.075 µg CPP, 0.1 µg DNA); Lane 5: 1:2 ratio (0.05 µg CPP, 0.1 µg DNA); Lane 6: 1:4 ratio (0.25 µg CPP, 0.1 µg).This experiment was repeated three times.

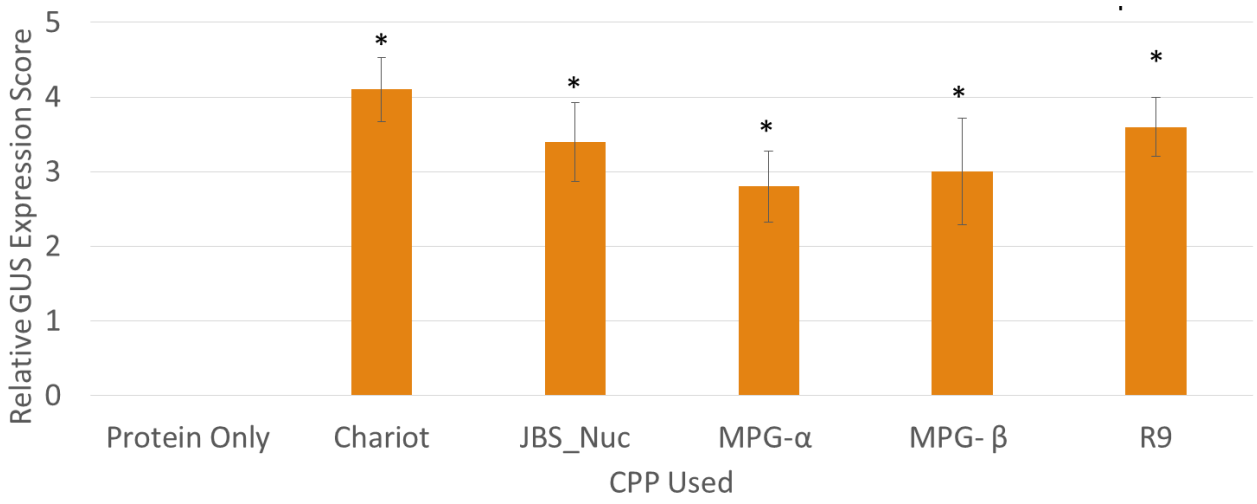

Figure 2-5. Comparison of five different CPPs in delivering purified GUS enzyme. Five different CPPs, Chariot, JBS_Nucleoducin, MPG-α, MPG-β, amd R9, were investigated for their efficiency in delivering GUS protein. The values are averages of 10 different segments, from 3 independent assays of 3 segments in the first two assays, and 4 in the third. Error bars represent the standard error from the mean. All values had an extremely low p-value and are considered significant.

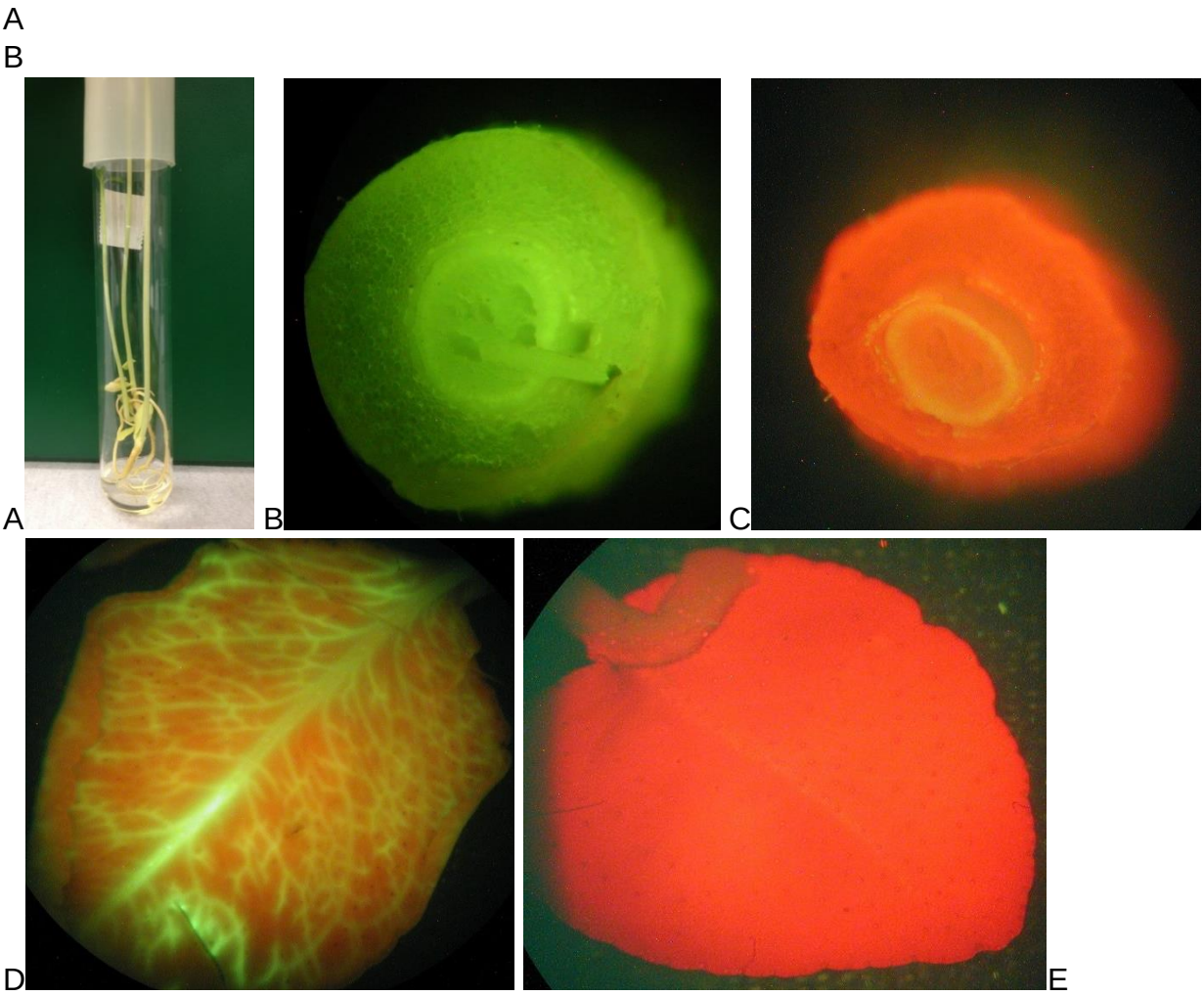

Figure 2-6. Systemic transport of the cell-penetrating peptide. Arginine 9- Fluorescein (*R9-F*), in 'Carrizo' citrange. 'Carrizo' citrange (*Citrus sinensis x Poncirus trifoliata*) were propagated on MS germination medium for five weeks in the dark. Seedlings were removed from the solid medium and placed in an *R9-F* containing a fluorescent CPP, R9-F, or water only as a control for 2 days. Transverse sections and the leaves were removed and examined under blue light fluorescence stereoscope. Green/yellow color indicates *R9-F* and the red color indicates chlorophyll auto-fluorescence A) Visualization of the seedlings in culture tubes immersed in the CPP solution. B) Transverse section of epicotyl under *R9-F* treatment C) Transverse section of epicotyl under FITC-Dextran treatment D) Leaf from *R9-F* treatment E) FITC-Dextran Leaf. Each tracking experiment was conducted three separate times using eight different seedlings, four of the control and four of the experimental.

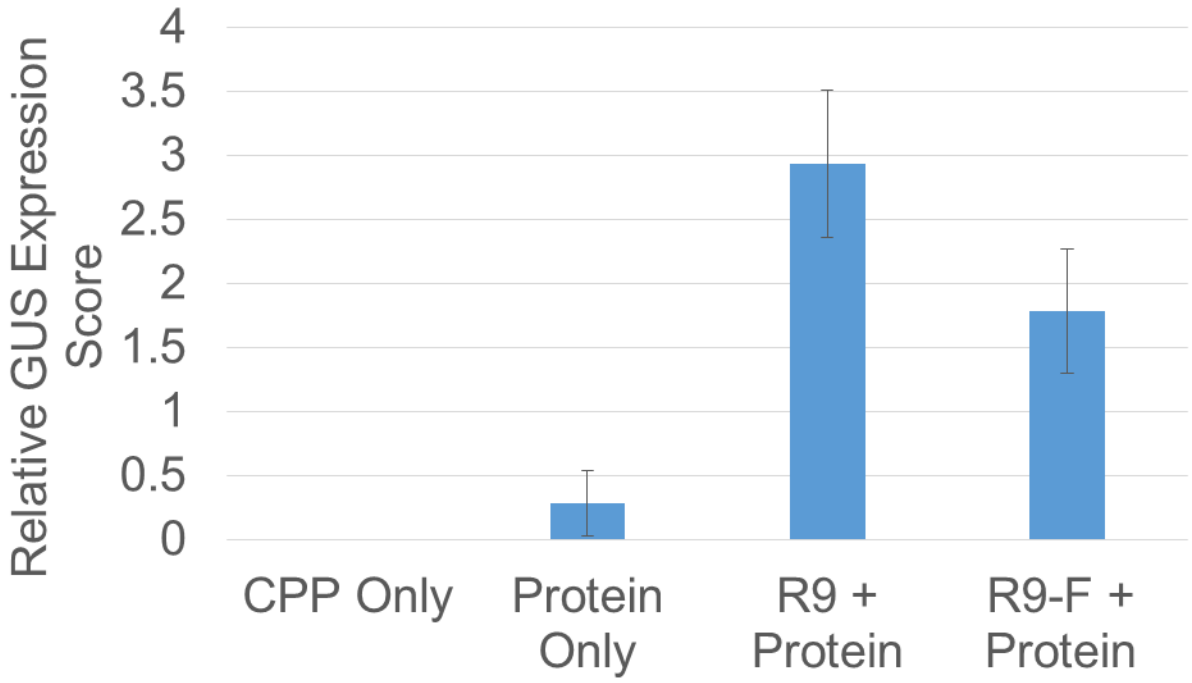

Figure 2-7. Average relative GUS scores when trafficking protein cargo in citrus epicotyl segments. Using the protein delivery in citrus protocol described in methods, the CPPs R9 and R9-F were compared in their efficacy in delivering GUS protein cargo. The resulting GUS score was recorded. The figure represents the mean of at least 10 epicotyl segments per treatment per experiment and the experiment was repeated 4 times. Error bars represent the standard error from the mean.

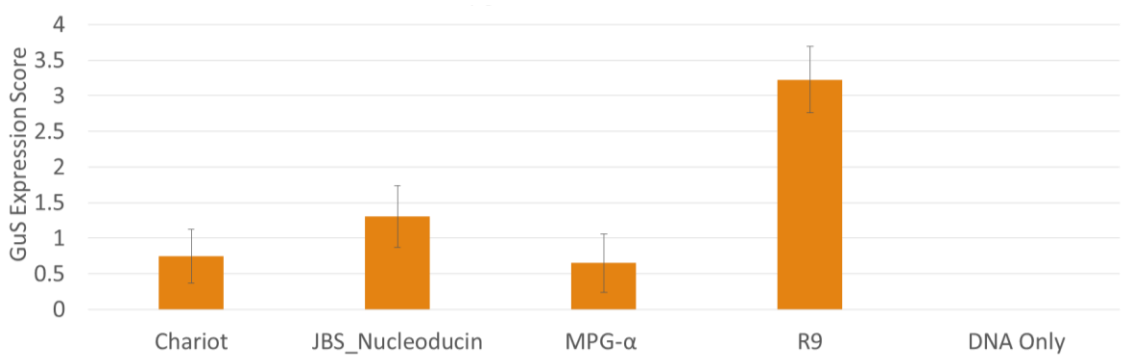

Figure 2-8. Efficacy of different CPPs in plasmid delivery of pCAMBIA 2201 in citrus. In order to choose the most efficient CPP to deliver cargo in citrus, four CPPs, Chariot, JBS Nucleoducin, MPG-α, and R9, were examined for their ability to deliver the GUS reporter plasmid, pCAMBIA 2201. Epicotyl samples were treated according to the methods, and then suspended in X-gluc overnight (16 hours) to stain and the resulting GUS score was recorded per segment. The relative GUS score was recorded. A) Visualization of the epicotyl segments post-treatment. B) Average relative GUS scores were calculated for each CPP and plotted in the chart. The experiment was repeated three times and approximately 12 segments were used per treatment per test.Error bars represent the standard error from the mean.

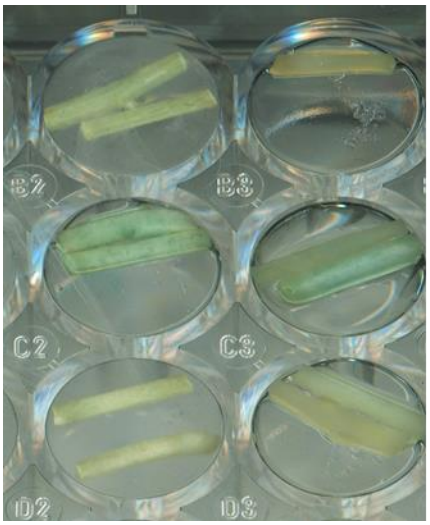

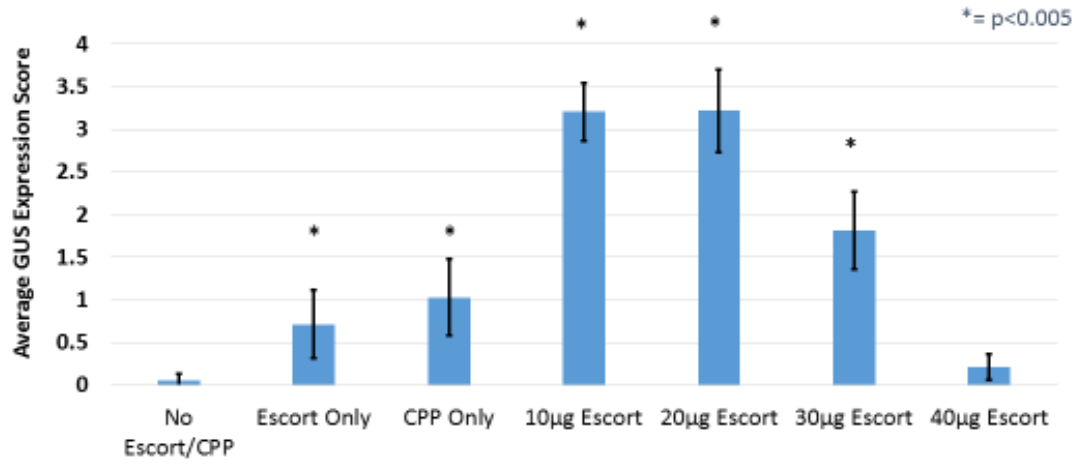

Figure 2-9. Average GUS scores from an assay testing the efficacy of Escort in assisting CPPs deliver plasmid cargo. Etiolated grapefruit epicotyl segments were subjected to the CPP transient expression protocol described in methods. The epicotyl samples were suspended in X-gluc overnight (16 hours) to stain and the resulting GUS score was recorded per segment. The assay was repeated three times with a minimum of 12 samples per treatment and the results were averaged together. Multiple controls were used: only plasmid (No Escort/CPP), only Escort (Escort Only), and one without the addition of Escort (CPP Only). Error bars represent standard error from the mean. Significance was determined using a student t-test with $\alpha=0.05$ when compared to the No Escort/CPP control. Error bars represent the standard error from the mean.

Figure 2-10. Cell-penetrating peptide transformation procedure for citrus. A) Etiolated citrus segments are co-cultivated with the CPP, Arginine 9 (R9), and pCAMBIA-2201 in liquid medium overnight (16 hours) at 25 °C. B) The segments are removed from co-cultivation media and transferred to solid medium. After 4-5 weeks, surviving segments turn green and some produce several new shoots. C) Shoots are excised and placed on auxin-containing (indole-acetic acid) rooting medium. D) Once the roots are established, about 4 weeks later, the regenerated plants are placed in soil and placed in a growth chamber with 12 hours of light per day. The plants pictured are 2 months old. When the plants have enough leaf material to survive harvesting, a reporter screen for either GUS or GFP was performed, followed with PCR confirmation.

A 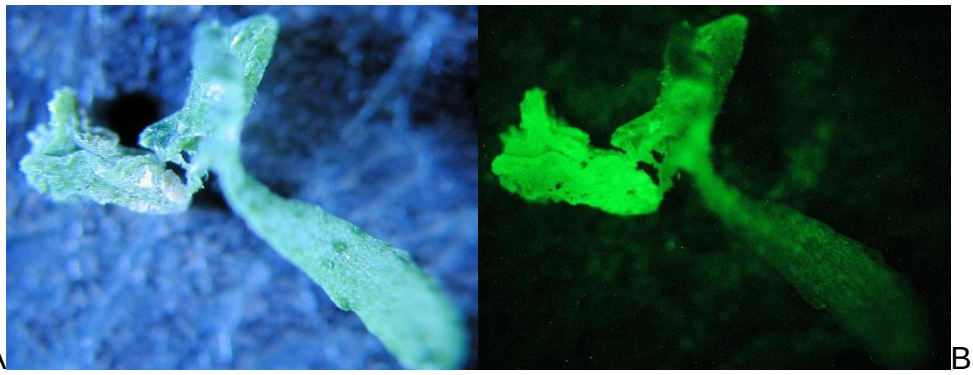 B

C 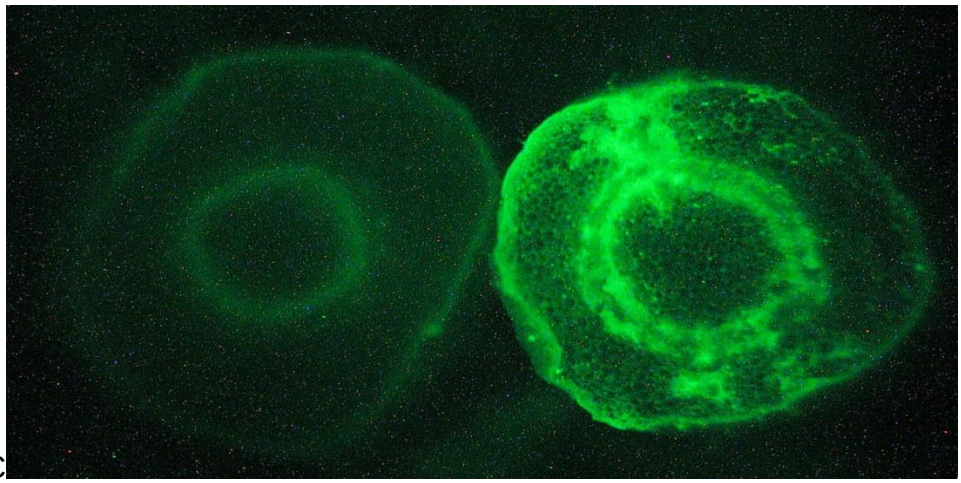

Figure 2-11. Visualization of GFP in citrus epicotyl segments from plasmid. Epicotyl segments were subjected to CPP transformation protocol described in methods and diagramed in Figure 2-9. Regenerated shoots were examined for the green fluorescent protein (GFP) from pCAMBIA-2202-SGFPS65T. A) Shoots under bright light. B) The same shoots under blue light with Abs/Em = 494/521 nm. C) The epicotyl segments from which the shoots were removed were cross sectioned and examined under blue light. The left segment indicates a control treatment, whereas the right segment indicates a segment treated with pCAMBIA-2202-GFPS65T.See Table 2-2 for number of replicates.

CHAPTER 3
NANOPARTICLES IN CITRUS: A TARGETED DELIVERY SYSTEM

Nanoparticle Literature Review

Although pH-responsive materials have been extensively studied in the realm of medicine, less attention has been given to the application of these adaptive materials in agriculture(Gao et al., 2010; Trivedi and Kompella, 2010; Puoci et al., 2008). Despite the relative lack of attention in agricultural sciences, responsive polymeric nanoparticles have significant potential to enhance the delivery efficacy of pesticides, nutrients, and drugs, which can in turn provide valuable benefits to help cure deadly plant diseases (Bhattacharyya et al., 2010; Chinnamuthu and Boopathi, 2009; Perez-de-Luque and Rubiales, 2009; Yang et al., 2014; Zhang et al., 2013). Specifically direct delivery of nanoparticles into the phloem, the vascular tissue in plants that aids in the transport of nutrients and photosynthates, is desirable not only because of its critical role in carrying nutrients but also because many plant pathogens reside in the phloem, such as citrus huanglongbing (HLB) (Bove and Garnier, 2003). While most plant tissue exists in a slightly acidic environment, the phloem exhibits a higher, slightly alkaline pH (Mendoza-Cozatl, 2008). Thus, much like pH-responsive nanoparticles designed to exploit the low pH of cancer cells, a nanodelivery system designed to respond to the higher pH of the phloem may be useful for site-specific delivery in plants, thereby potentially enhancing the efficiency of delivered component.

Reprinted with permission from: Chen, M., Jensen, S.P., Hill, M.R., Moore, G., He, Z., and Sumerlin, B.S. (2015). Synthesis of amphiphilic polysuccinimide star copolymers for responsive delivery in plants. Chemical Communications. 51: 9694-9697.

Reprinted with permission from: Hill, M.R., MacKrell, E.J., Forsthoefel, C.P., Jensen, S.P., Chen, M., Moore, G.A., He, Z.L. and Sumerlin, B.S. (2015). Biodegradable and pH-responsive nanoparticles designed for site-specific delivery in agriculture. Biomacromolecules. 16: 1276-1282.

Many fundamental questions arise when applying stimulus-responsive (Theato et al., 2013) polymers for delivery in plants. For instance, additional consideration must be given to how the nanoparticles enter plant cells and are subsequently transported to targeted sites. As opposed to a cell membrane, which takes in materials of various sizes by endocytosis, plants possess a cell wall, which is more ordered and exhibits specific pore diameters of ~30 nm (Fleischer et al., 1999). Therefore, it is important to carefully control the size of polymer nanoparticles so they can readily pass through the cell wall and reach the plasma membrane. Once in the plasma membrane, the loaded nanoparticles can be further transported to the targeted sites along apoplastic and symplastic pathways by diffusion or electrochemical gradients.

Given the lack of an excretory system in plants, the fate of materials used for such applications is another important concern. While the most well-known and studied pH-responsive polymers {e.g., poly[(meth)acrylic acid] and poly[N,N-dimethylaminoethyl(meth)acrylate]} have proven to be effective in a number of physiological applications, they typically contain nondegradable all-carbon backbones, which limits their use in plants. Because biodegradability is of utmost importance for the delivery to plants to reduce concerns about environmental fate and sustainability, new types of stimulus-responsive biodegradable materials are needed (Gao et al., 2010; Alarcon et al., 2005; Murthy et al., 2003).

The construction of nanoparticles suitable for delivery to plant phloem thus becomes more complicated. The nanoparticles must be (i) responsive to the basic pH found in the phloem, (ii) small enough to enter the plant cell through cell wall junctions, and (iii) biodegradable to reduce the extent of accumulation over time.

Additionally, these nanoparticles would ideally be equipped with moieties to facilitate transport along electrochemical gradients and, most importantly, be capable of encapsulating guest compounds, including hydrophobic and hydrophilic small molecules or drugs.

To this end, Polysuccinimide (PSI) has attracted attention for many years because of the biodegradable and hydrophilic nature of its derivatives, namely, poly(aspartic acid) (PASP) and poly(hydroxyethylaspartimide) (PHEA) (Kumar 2012; Moon et al., 2006; Tombre and Sarwade, 2005; Gu et al., 2013; Jeong et al., 2012; Lai et al., 2014; Ma et al., 2013). PSI is derived from the ring-closing condensation polymerization of l-aspartic acid. Subsequent hydrolysis of the polymeric repeat units under mildly basic conditions results in the hydrophilic derivative, PASP, with both α and β ring-opened units (Figure 3-1) (Wang et al., 2003). The biodegradability of PASP derived from the hydrolysis of PSI has been previously documented, although longer degradation periods compared to those of other poly(amino acids) were necessary, which is likely due to the presence of a mix of l- and d-aspartic acid units as well as the β-hydroxyl structures in the backbone (Tombre and Sarwade, 2005; Alford et al., 1994; Roweton et al., 1997; Nakato et al., 1998). Nevertheless, the degradation is still expected to progress as opposed to that of polymers prepared radically with polymethylene backbones. Because of the reactivity of PSI toward primary amines, previous reports have involved various moieties being readily incorporated onto the PSI backbone to give fully functionalized PASP derivatives. Alternatively, PSI has been partially functionalized, with the remaining succinimidyl units being hydrolyzed to give PASP copolymers (Xu et al., 2012; Wang et al.,

2012b). Additionally, many groups have incorporated stimulus-responsive moieties onto the PSI backbone (i.e., hydrazone bonds (Wang et al., 2012a; Lu et al., 2014a; Lu et al., 2014b; Lee et al., 2015), amines (Gu et al., 2013; Moon et al., 2010; Nemethy et al., 2013), thiols and disulfides (Gyarnati et al., 2013; Zhang et al., 2012; Cui et al., 2013), carboxyls (Xu et al., 2012), imidazole (Seo and Kim, 2006), etc.) to impart responsiveness onto the biodegradable PASP backbone.

For this project, exploring the inherent pH-responsive nature of PSI is the focus. Because PSI is hydrolyzed at elevated pH to form water-soluble and biodegradable PASP, we envisioned employing PSI as a potential platform for the development of a site-specific delivery system for agricultural applications. Thus, utilizing PSI as a pH-responsive and hydrophobic scaffold, we aimed to prepare a nanosized delivery system to capitalize on the higher pH of the phloem (Figure 3-2). The approach includes partially functionalizing the backbone of PSI to form self-assembled nanoparticles and relying on the hydrolytic lability of the remaining succinimidyl groups for stimulus responsiveness. While PSI is not water-soluble at neutral pH, its succinimidyl groups are hydrolyzed at elevated pH to yield derivatives of water-soluble PASP (Nakato et al., 2000). This pH-driven solubility transition may provide a convenient mechanism for inducing supramolecular dissociation of PSI-based polymeric assemblies. We reasoned that this transition in solubility could be exploited to allow PSI-based polymers to serve as a platform for site-specific, pH-responsive guest molecule release. Moreover, because the resulting PASP-based copolymers are known to be biodegradable, the change in water solubility may simultaneously increase the rate of degradation of the polymeric byproduct. Although

previous reports have utilized PSI as a precursor for the development of stimulus-responsive (co)polymer materials, to the best of our knowledge, the inherent pH-responsiveness of PSI itself has yet to be investigated.

In this chapter, the effect of nanoparticles were studied with respect to their toxicity in citrus. Additonally, nanoparticles can be readily controlled by precipitation conditions and that particles small enough for delivery to plant phloem are possible. Furthermore, the PSI-based copolymers showed limited toxicity to plant tissue at biologically relevant concentrations, suggesting these materials are a viable option for agricultural drug delivery systems.

Materials and Methods

Materials

l-Aspartic acid (98%), o-phosphoric acid (85%), hexylamine (99%), and 2-(2-aminoethoxy)ethanol (98%), were purchased from Sigma-Aldrich. Potassium phosphate monobasic (Fisher) was used to prepare 0.1 M phosphate buffers with adjusted pH values for release studies. Murashige and Skoog basal salt mixture (MS salts) was purchased from Phytotechnology Laboratories. Benzyl adenine (BA), myoinositol, Claforan (cefotaxime), and a plant cell viability assay kit were obtained from Sigma-Aldrich. All organic solvents were used as received.

Synthesis of Polysuccinimide (PSI)

The synthesis of polysuccinimide was prepared by M. Hill. PSI was prepared as previously reported (Moon, et al., 2006; Wang et al., 2012). Briefly, l-aspartic acid (20 g, 0.15 mol) and phosphoric acid (10 g, 0.10 mol) were added to a 500 mL round-bottom flask. The reaction vessel was placed under nitrogen and heated to 180 °C while its contents were being stirred for 2 h. The product was dissolved in

N,N-dimethylformamide (DMF, 100 mL) and precipitated into cold methanol. The product was then collected via vacuum filtration and washed with additional methanol and water to remove any remaining DMF.

Preparation of Functionalized Nanoparticles

This portion of the work was completed by M. Hill. The nucleophile (HA, 2-AEE, or NaOH) was added to a solution of PSI dissolved in DMF and stirred at room temperature overnight. The functionalized copolymer was then added dropwise to a beaker of stirring deionized water. For example, for a copolymer functionalized with 20% HA (20% PSI-HA), PSI (498 mg, 5.15 mmol) was dissolved in DMF (5 mL), and HA (0.13 mL, 1.0 mmol) was added dropwise to the solution. The solution was stirred at room temperature overnight and precipitated into deionized water (200 mL). The aqueous nanoparticle solution was transferred to dialysis tubing (Spectra/Por, molecular weight cutoff of 3500) and placed in deionized water, which was replenished daily for 1 week.

Preparation of Germination Medium for the Plant Toxicity Assay

This work was completed by the author of this document, S. Jensen. MS salts (2.15 g), myoinsoitol (50 mg), FM stock (1.865 g of Na2EDTA and FeSO4·7H2O (1.390 g) into 500 mL; 5 mL), and sucrose (15 g) were added to an autoclaved beaker. The solution pH was adjusted to 5.7, and the volume was brought to 1 L. Agar (7 g) was added to the medium and heated for 30 min to obtain the final germination medium.

Preparation of Citrus Seeds

This work was completed by the author of this document, S. Jensen. Germination medium (12 mL) was dispensed into autoclaved culture tubes. Healthy

and viable citrus seeds from grapefruit (*Citrus x paradisi*) and sweet orange (*Citrus x sinensis*) were selected, and the outer seed coats were removed. Seed kernels were kept moist at all times. Each seed was placed in a sterile autoclaved beaker with a stir bar and stirred in 300 mL of the following solutions for the indicated time intervals: 70% alcohol (2 min), 10% sodium hypochlorite (10 min), and three sterile DI water rinses (2 min).

Culture of Citrus Seeds

This work was completed by the author of this document, S. Jensen. One seed was inserted into each germination medium-filled culture tube. The test tube racks were wrapped with plastic wrap and doubly wrapped with aluminum foil to minimize light exposure. Finally, the test tube racks with seeds were placed on the bottom of a growth chamber for 5 weeks, when the etiolated seedlings were used for toxicity screening.

Preparation of MSBC Medium

This work was completed by the author of this document, S. Jensen. MS salts (4.3 g), myoinositol (100 mg), GM stock [10 mL of a solution of glycine (20 mg), nicotinic acid (50 mg), pyridoxine HCl (100 mg), and thiamine HCl (100 mg) in DI water (500 mL)], sucrose (30 g), and BA (2 mg) were dissolved in DI water. The pH of the solution was adjusted to 5.7, and additional DI water was added to bring the volume to 1 L. Agar (8 g) was added and the solution autoclaved for 25 min. After the solution had cooled, 1 mL of filtered and sterilized (500 mg/mL) Claforan stock was added to obtain 500 µg/mL MSBC medium. The medium was dispensed into sterilized culture dishes, and different concentrations of polymers were added before solidification when the MSBC medium was in liquid phase near room temperature.

Toxicity Assessment by Tissue Culture

This work was completed by the author of this document, S. Jensen. Citrus plants were cut into 1–2 cm segments and placed on an appropriate MSBC medium-filled culture dish. The dishes were then put into a growth chamber with alternating 12 h light and dark periods for 21 days. Alive and dead segments were counted after 8 and 21 days.

Results and Discussion

pH Responsiveness of Nanoparticles

To study the pH-responsiveness and the drug release of the PSI-based nanoparticles, the loaded nanoparticles were exposed to buffered solutions, and the change in fluorescence intensity was monitored over 72 h. Because Nile red is hydrophobic in water and fluoresces only within the hydrophobic interior of the nanoparticle, fluorescence is expected to decrease as the succinimidyl units are hydrolyzed and the nanoparticles disassemble to release the dye. While the hydrolysis of PSI under basic conditions is well-known, we expected some hydrolysis would still occur under neutral conditions, albeit at a reduced rate. We thus first explored the hydrolysis kinetics at various pH values with 1% PSI-2AEE. As expected, the release rate was rapid at pH 8.5 and 8 because of the hydrolysis of the succinimidyl backbone of the PSI units, with approximately 80 and 60%, respectively, of the dye being released at 30 h. On the other hand, PSI is more stable under neutral and acidic conditions; therefore, at pH 7 and 6, less than 40 and 20%, respectively, of the dye was released over 72 h (Figure 3-5A).

Release studies also showed that the functionalizing moiety (2AEE, HA, and NaOH) did not significantly affect the release rate, but incorporating high degrees of

functionality, in the e of PSI-HA, slowed the release or prevented nanoparticle disassembly, with minimal release being observed in alkaline environments (Figure 3-5B). We hypothesize that the hydrophobicity of the hexyl chains kept the copolymer sufficiently amphiphilic to maintain nanoparticle stability, even after complete hydrolysis. Greater than 15% functionalization with HA appeared to render the material sufficiently hydrophobic to prevent disassembly and any dye release. Lastly, a copolymer of 10% PSI-HA was precipitated at different concentrations to produce nanoparticles of varying sizes (13, 28, and 83 nm). The release at pH 8.5 suggested hydrolysis was slightly faster with smaller nanoparticles (Figure 3-5C), which is potentially due to the increased surface area. Although a small amount of hydrolysis occurs at neutral pH, almost no hydrolysis occurs in acidic environments. Because plant tissue is slightly acidic (pH ~5–6) except in the phloem (pH ~8), the nanoparticles offer considerable promise for site-specific delivery in agricultural applications.

Naphthaleneacetic acid (NAA) is a synthetic plant hormone in the auxin family (Flasinski and Wydro, 2014), and is involved in many processes of live plant activity, such as cell elongation, division, and response to external environmental variety (Gomez and Carpena, 2014). NAA has limited solubility in water and excellent fluorescence and UV absorption properties (Moye and Wheaton, 1979; Guo et al., 2011), making it useful as a model pesticide to provide insight into the potential utility of PASP-*co*-PSI copolymers for controlled release in plants. As shown in Figure 3-9A, only minimal NAA release was observed for the PASP-*co*-PSI copolymer nanoparticles at neutral pH, suggesting the hydrophobic succinimide units are relatively stable under these conditions. On the other hand, when the pH was increased to 8.5 (*i.e.*, near the

pH of the phloem), NAA release was significantly accelerated. These results are consistent with the pH-dependent hydrolysis of the hydrophobic PSI units to yield hydrophilic PASP units and subsequent nanoparticle disassembly. To confirm this, $(PASP_{26}\text{-}co\text{-}PSI_{17})_3$ was dissolved at pH = 8.5 and allowed to age for 48 h. Afterwards, the resulting polymer was isolated by dialysis and lyophilization and subsequently characterized by NMR and FTIR spectroscopy. The results (Figure 3-9B and C) were consistent with hydrolysis of the succinimide units, as evidenced by these spectra being nearly identical to those of polyaspartate homopolymer.

Plant Toxicity

This portion of work was designed by the author of this document, S. Jensen.To evaluate any possible toxicity of the polymers toward plant tissue, a method was developed using living plant tissue. Citrus seeds were planted on germination medium and cultured in the dark at 25 °C for 5 weeks, until the seedling reached the length of the culture tube. Each seedling was then cut into fragments and seeded on plates filled with MSBC medium with varying concentrations of the polymers (PASP, PSI, and PSI-HA). The plates were then put into a growth chamber with alternating 12 h lighting cycles and analyzed after 8 and 21 days to determine the percent of living tissue (Figure 3-6). As shown in Figure 3-6, PASP, PSI, and PSI-HA showed limited toxicity up to concentrations of 196 μg/mL. While extremely high concentrations of PSI and PSI-HA showed toxicity (0% tissue viability at 385 μg/mL PSI-HA), PASP at 385 μg/mL showed no toxicity. It should be noted that although PASP dissolved easily in the MSBC medium, the more hydrophobic PSI homopolymer and PSI-HA copolymer required DMSO to fully dissolve into the medium, which may have influenced the results of the toxicity assays for these (co)polymers at high concentrations. Nevertheless, the

relatively low toxicity of the PSI-based polymers to plant tissue provides further evidence of their promising potential for future applications in agriculture.

While there are many established methods to evaluate the safety of polymeric materials in medicine, methods for toxicity evaluation in plant cells and tissues are much less developed. We developed a method based on plant tissue culture to evaluate the toxicity of polymers in plants (Hill et al., 2015). Citrus seeds were planted on germination medium and were cultured in the dark at 25 ^{o}C for five weeks, causing the seedlings to become partially etiolated, or white, to reduce the potential interference of chlorophyll during subsequent fluorescence microscopy. The seedlings were cut into 1-2 cm fragments and placed on MSBC plates, which included specific concentrations of dissolved $(PASP_{26}$-*co*-$PSI_{17})_3$. The seedlings were placed into a growth chamber with alternating light and dark (12 h each) for two weeks. The dead and living tissue segments were counted. As shown in Figure 3-4A, almost all citrus segments survived, even at high concentrations (*i.e.,* 240 µg/mL) of polymer, indicating $(PASP_{26}$-*co*-$PSI_{17})_3$ is relatively non-toxic to citrus plant tissue.

Plant Cell Viability Assay

This portion of the work was designed by S. Jensen. To further investigate the toxicity of $(PASP_{26}$-*co*-$PSI_{17})_3$, we utilized a dual color fluorescent staining system designed for simultaneous visualization of viable and non-viable plant cells (Koyoma et al., 2001; Regan and Moffatt, 1990). Viable cells have intact plasma membranes and intracellular esterases with the ability to enzymatically hydrolyze a fluorescein diacetate probe. The resulting fluorescent hydrolyates are polar compounds that cannot cross the plasma membrane, which leads to green fluorescence within the cytoplasm. On the other hand, propidium iodide can enter non-viable cells due to their damaged

membranes, which leads to bright red fluorescence upon intercalation with DNA within the nucleus. As shown in Figure 3-4B, citrus leaves treated with $(PASP_{26}\text{-}co\text{-}PSI_{17})_3$ demonstrated the green color of fluorescein diacetate under blue light at 490nm/525nm Ex/Em (FITC), while showing no fluorescence under blue light at 570nm/590nm Ex/Em (Rho). Conversely, when dead citrus leaves were used as a positive control, very little green fluorescence from FITC was observed, while significant red fluorescence from the propidium iodide was clearly visible. These results offer further evidence that $(PASP_{26}\text{-}co\text{-}PSI_{17})_3$ is non-toxic at the concentrations considered.

Nanoparticle Conclusions

Responsive nanoparticles were developed to capitalize on the higher pH of plant phloem for the design of a site-specific delivery system to plants. Amphiphilic copolymers based on PSI were synthesized by functionalization with various amines that provided a convenient means of tuning the hydrophilic–hydrophobic balance needed for nanoparticle formation. Controlling the degree of functionalization and nanoprecipitation conditions proved to be viable methods of programming nanoparticle size, and could prove useful when developing new systems for delivery applications. The nanoparticles were loaded with a model hydrophobic compound and showed controlled release at alkaline pH, with increased rates at higher solution pH and lower degrees of functionalization. Lastly, the toxicity of the polymers was tested on plant tissue, with only minimal toxicity being observed at reasonable concentrations of the polymers.

In addition, compared to traditional methods involving the thermal condensation polymerization of aspartic acid to PSI and its subsequent partial hydrolysis to PASPA to produce amphiphilic polysuccinimide copolymers, a novel

method using NCA ring-opening polymerization was employed. The star polymer product, PBLA, was produced with a controllable molecular weight and a narrow molecular weight distribution. After deprotection, the resulting polypeptides were converted to PSI-containing copolymers by partial ring closing of the aspartic acid units. The resulting amphiphilic star copolymers self-assembled into aggregates with the ability to incapsulate NAA, a common plant hormone, and showed rapid release at an increased pH, similar to conditions present in the phloem of plants. Furthermore, a novel method to assess the toxicity of polymers in plant cells and tissues was established. Because plant cells can not be reliably cultured, plant tissue culture and a dual color fluorescent staining system were utilized to evaluate the toxicity of amphiphilic polypeptide. The results showed limited toxicity of the synthesized polymers to plant tissue. Although the utility of controlled delivery systems has been widely proposed for the treatment of human disease with the goal of reducing side effects and improving availability of the delivered drugs, similar delivery systems for pesticides and nutrients to plants have received much less attention. However, given the current low use efficiency of fertilizers and pesticides, modern agriculture could greatly benefit from a site-specific delivery system to reach targeted sites and reduce potential pollution caused by undelivered components. We believe this work has significant potential for phloem-limited release, and given the biodegradability and minimal toxicity of these polymers to plant tissue and cells, other potential applications in agriculture can be envisioned.

Figures

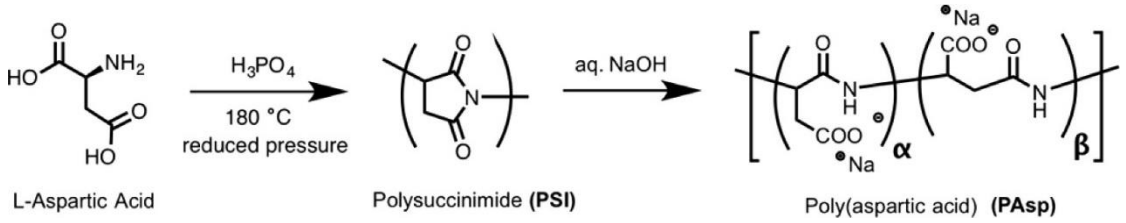

Figure 3-1. Preparation of PSI. Construction of PSI from Acid-Catalyzed Condensation of L-Aspartic Acid and Hydrolysis to PASP. Scheme created by M. Hill.

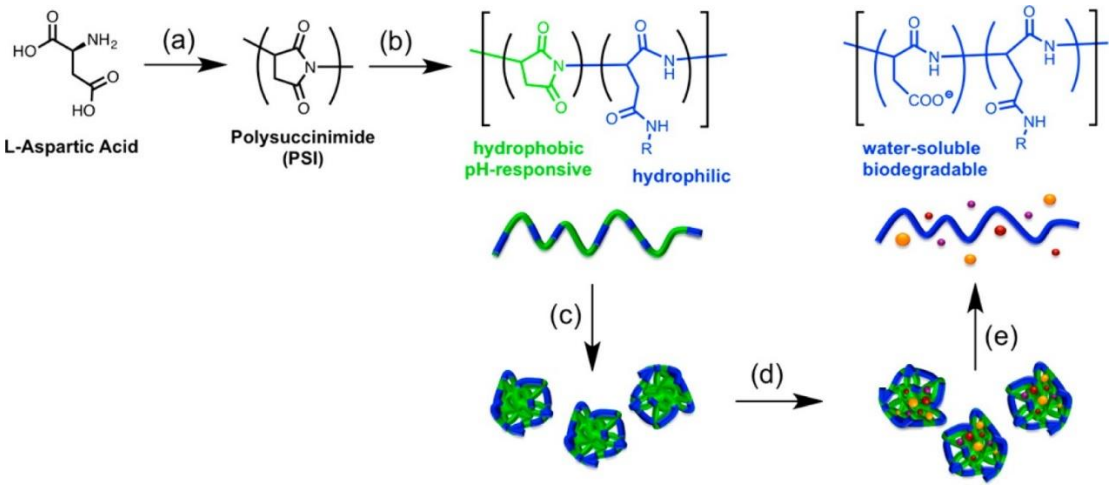

Figure 3-2. Proposed PSI-based nanoparticle delivery and release. (A) PSI is synthesized through the step growth condensation reaction of L-aspartic acid and (B) functionalized with hydrophilic primary amines to prepare amphiphilic and pH-responsive PSI copolymers. (C) Amphiphilic PSI copolymers are assembled into nanoparticles and (D) loaded with hydrophobic molecules, (E) which may disassemble and release loaded components at elevated pH, leaving behind the water-soluble and biodegradable poly(aspartic acid) derivative polymer. Scheme was created by M. Hill.

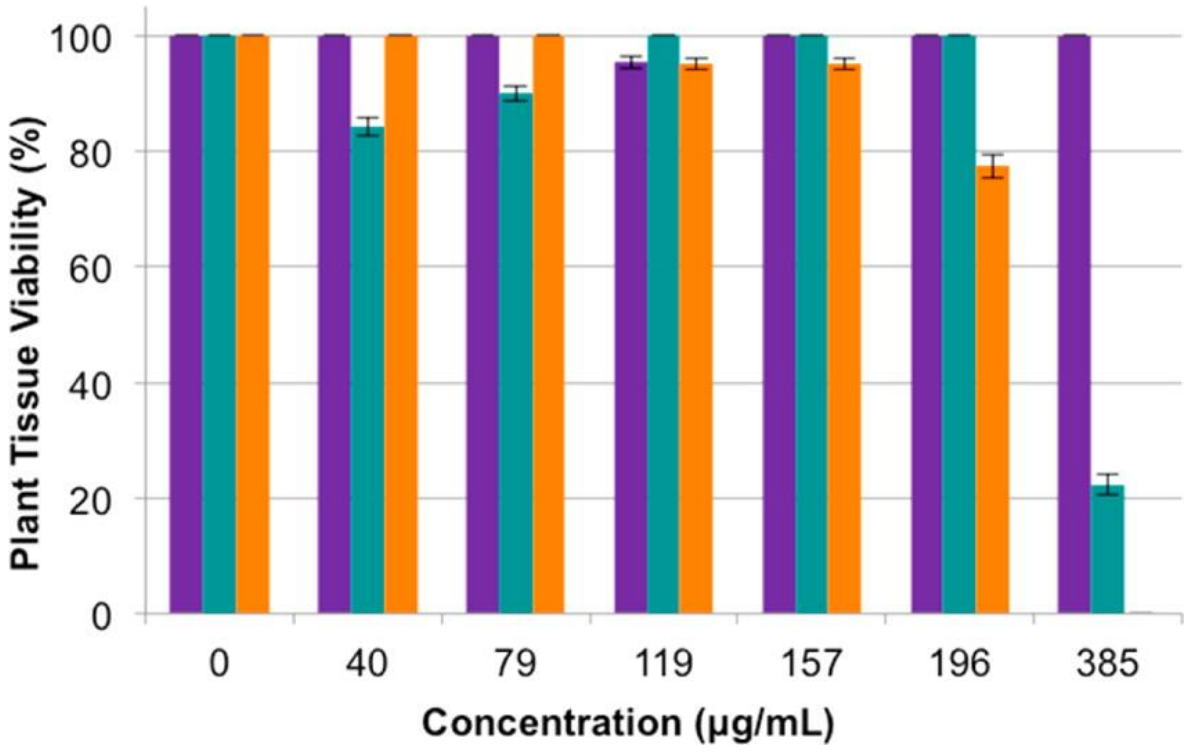

Figure 3-3. Nanoparticle toxicity in citrus. Plant tissue (citrus seed sapling) viability at various concentrations of PASP (purple), PSI (green), and PSI-HA (orange).Plant toxicity assay was designed by the author of this document, S. Jensen.

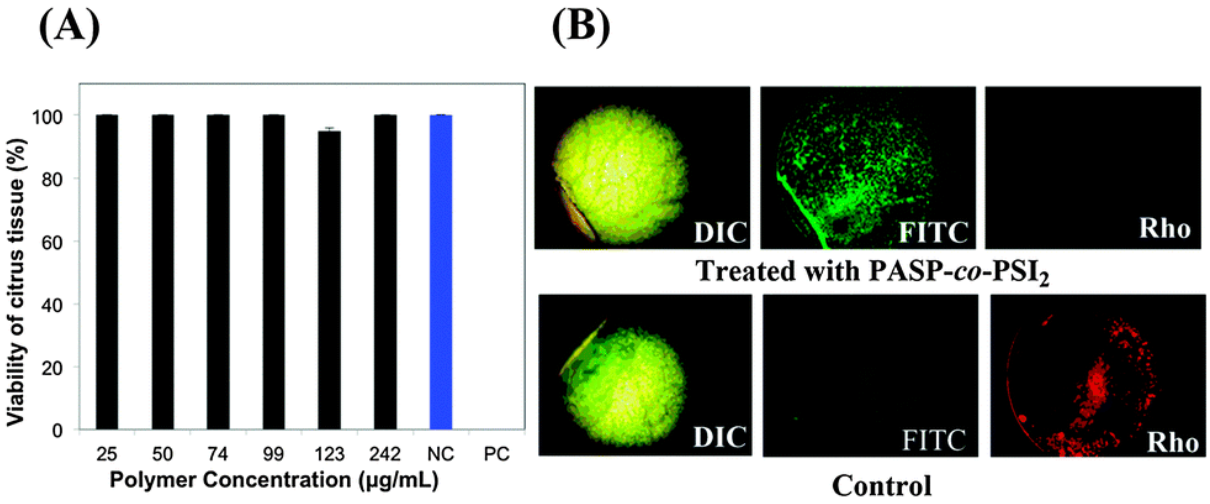

Figure 3-4. Citrus plant toxicity of $(PASP_{26}\text{-}co\text{-}PSI_{17})_3$. Toxicity evaluation of $(PASP_{26}\text{-}co\text{-}PSI_{17})_3$ by (A) plant tissue culture (where NC = negative control (no polymer) and PC = positive control) (complete tissue death induced by high concentrations of a toxicant) and (B) dual color fluorescent staining system. Top image shows the results of a live citrus leaf treated with $(PASP_{26}\text{-}co\text{-}PSI_{17})_3$ and the bottom image shows the results from analysis of a dead citrus leaf (Red areas indicate dead citrus cells and green areas indicate living citrus cells); DIC = Differential interference contrast; FITC = fluorescein isothiocyanate fluorescence setting; Rho = Rhodamine fluorescence setting. Plant toxicity assay was designed by the author of this document, S. Jensen.

CHAPTER 4
CRISPR/CAS9 TRANSCRIPTIONAL REGULATION IN CITRUS: A MOLECULAR SWITCH FOR EARLY FLOWERING

CRISPR/Cas9 Literature Review

The goal of this chapter is to enhance a modern citrus breeding program to improve yield and decrease production costs, create better quality fruit and to infer disease resistance by decreasing the rate at which citrus flowers, ultimately increasing the rate at which new generations can be produced. In this manner, targeted genome engineering technology can be used to contribute to future varietal improvement in citrus.

Genome Targeting Technologies

Current targeted genome technology primarily use zinc finger nucleases (ZFNs), transcription activator-like effector nucleases (TALENs), or clustered regularly interspaced short palindromic repeat (CRISPR) and CRISPR-associated protein-9 (Cas9) (herein called CRISPR/Cas9) systems. Each system has been successfully used to genetically modify plants, including citrus (Jia and Wang, 2014).

ZFNs can be used to cleave a target DNA site, by combining a FokI nuclease domain to a cluster of zinc finger proteins, modified transcription factors, which act as DNA targeting mechanisms. The design of the ZFNs include a linear block of tandem sequences that target a specific DNA sequence. In this way, ZFNs are extremely versatile due to the modular nature of their design (Klug, 2010). Once the DNA is cleaved at the targeted site, the DNA is subsequently repaired through nonhomologous end joining (NHEJ) that leads to mutated sequence. ZFNs have used successfully for

genome modification in plants such as soybean (*Glycine max*) (Curtin et al., 2013), *Arabidopsis* (Lloyd et al., 2005), maize (*Zea mays*) (Shukla et al., 2009).

More recently, TALEN technology has come into use as another genome targeting approach for genome engineering. TALENs can target any genome site based on a pattern that results from the repeat-variable di-residue (RVD) sequences found within a conserved TALEN repeat, with each RVD specifically binding to a corresponding nucleotide (Boch et al., 2009). This makes their design to be rather simple in the laboratory. Recently, researchers have shown TALENs can edit genomes in a variety of plant species, including *Arabidopsis* (Cermak, et al. 2011), rice (*Oryza sativa*) (Li et al., 2012), and tobacco (*Nicotiana tabacum*) (Zhang et al., 2013c).

Currently, the Cas9/sgRNA system has rapidly developed as another very promising method for genome engineering. CRISPR/Cas9 has commenced a targeted genome editing revolution and is seen as a primary method to eliminating genetic diseases in both plants and animals, including humans (Jia and Wang, 2014; Ma et al., 2017). Indeed, in 2017 Ma et al., proved that in human embryos, correction of a pathogenic gene mutation was cured, though they are skeptical to begin trials in a clinical setting.

In nature, the CRISPR/Cas9 system serves as a bacterial immune system of prokaryotes. The CRISPR locus contains the characteristic cluster of repeat sequences interspersed by spacer sequences. These sequences arise as new genetic elements emanating from previous virus or plasmid DNA infections the bacteria population encountered. During future infections, when DNA from a virus or plasmid matches the

previously encountered version in the CRISPR, a defense response is mounted and the foreign DNA is excised from the bacterial genome (Wiedenheft et al., 2012).

Overview of the CRISPR/Cas9 System

The most widely used CRISPR/Cas9 system derives from the actual bacterial defense mechanisms in *Streptococcus pyogenes* SF370, which has since been adapted for targeted genome engineering (Cong et al., 2013). This bacterial system is comprised of proteins, such as Cas9, Cas1, Cas2, and the related coat protein-9 (COP9) signalosome-1 (Csn1), as well as RNA molecules named, CRISPR RNA (crRNA) and trans-activating CRISPR RNA (tracrRNA). In response to foreign nucleic acid which mirrors a sequence in the bacterial genome's clustered repeats, the bacteria activates its nuclease activity by transcribing tracrRNA to hybridize with a crRNA and subsequently complex with the Cas9 protein. The functional crRNA:tracrRNA:Cas9 complex then targets a protospacer or spacer region, upstream of a 5'-protospacer-adjacent motif (PAM). The PAM sequence is necessary for target binding and the exact sequence is dependent upon the species of Cas9 (5′ NGG 3′ for *Streptococcus pyogenes* Cas9). The crRNA consists of a 20-25 nucleotide sequence which is complementary to the protospacer sequence, whereby in the functional complex, which then binds to the targeted region to facilitate Cas9-mediated DNA cleavage. The CRISPR/Cas system has been subsequently simplified from a three-molecule complex to a much easier two-component system, using the same Cas9 but with only one single guide RNA (sgRNA). The sgRNA is a fusion of the crRNA and tracrRNA elements and can bind to both the Cas9 and the spacer region (Hsu et al., 2013; Jia and Wang, 2014). Once the Cas9-sgRNA complex binds the target, the tracrRNA sequence of the sgRNA at the 3′ end of the gRNA targeting sequence begins to anneal to the target

DNA. If the seed and target DNA sequences match, the gRNA will continue to anneal to the target DNA in a 3′ to 5′ direction at the proper location.

Cas9 will only cleave the target if sufficient homology exists between the gRNA spacer and target sequences, though off-site targeting is of great concern (Cradick et al., 2013; Fu et al., 2013). The function of the Cas9 is to serve as a nuclease by cutting the foreign DNA. The cell's own natural genome editing pathways will repair DNA itself, leaving its genome intact, but hopefully by damaging the target so it can no longer create a functional product for the invading pathogen. To do this, Cas9 has two different endonuclease domains: RuvC and HNH. Once bound, Cas9 undergoes a second conformational change upon target binding that positions these nuclease domains to cleave on either strand of the target DNA. The end result of Cas9-mediated DNA cleavage is a known as a double strand break (DSB) within the target DNA approximately 3-4 nucleotides 5'- of the PAM sequence. The resulting DSB is then repaired by one of two repair pathways: the efficient, error-prone NHEJ pathway, mentioned previously, and the less efficient, but more accurate Homology Directed Repair (HDR) pathway (Belhaj, et al., 2015).

The NHEJ repair pathway is capable of rapidly repairing DSBs, but usually produces insertions or deletions (InDels) at the DSB. Though, it is likely produces negative results in nature, in research settings, this activity of NHEJ-mediated DSB repair has important practical implications, because one CRISPR/Cas9 treatment on a population, can result in a diverse array of mutations. In most cases, NHEJ gives rise to small InDels in the target DNA which result in in-frame amino acid deletions, insertions, or frameshift mutations leading to premature stop codons. HDR repair is rarer, but it

uses a template upon which the cell can make a more perfect repair (Belhaj et al., 2015). Ideally, the end result of the CRISPR nuclease activity is a loss-of-function mutation within the targeted gene; however, the effectiveness for this mutation does not always produce consistent phenotypes, as the repair is highly differential between cells in the same treatment.

One method to improve target mutagenesis, multiplexing, using CRISPR involves using multiple sgRNAs each targeting a different sequence on the same gene, provided there are multiple PAM locations 3' to a suitable spacer sequence. Expressing several sgRNAs present on the same plasmid ensures that a cell will express all of the desired sgRNAs and increases the likelihood that all desired genomic edits will be carried out by the CRISPR/Cas9 system (Belhaj, et al. 2015).

Current multiplex CRISPR systems enable researchers to target anywhere from 2 to10 genetic loci by cloning multiple gRNAs into a single plasmid. These multiplex gRNA vectors can conceivably be combined with any of the aforementioned Cas9-derivatives to not only knock-out target genes, but activate or repress target genes as well, discussed below.

The Cas9/sgRNA system (herein referred to as the aforementioned CRISPR/Cas9 system) is very simple and affordable. Whereas both ZFNs and TALENs require significant amounts of design for each DNA target, the Cas9/sgRNA system requires changes only in the sgRNA sequence for target specificity rather than manipulating the Cas9 protein. Cas9/sgRNA technology has been successfully used for genome editing in rice (Mia et al., 2013), tomato (Brooks, et al. 2014), and *Arabidopsis* (Feng et al., 2014).

Recently, Jia and Wang (2014), used the CRISPR/Cas9 system to induce genetic modification into sweet orange (*C. sinensis*). As previously discussed, citrus is the most economically important and extensively grown fruit tree crop in the world and the genetic improvement of citrus is limited by the slow growth and long maturation cycles. Thus, it is important to build upon their research of the CRISPR/Cas9 system in citrus in order to create other new technologies using CRISPR/Cas9, especially with regard to breeding in traits in a significantly short amount of time, due to the costly and devastating effect of HLB. In this chapter, a modified CRISPR/Cas9 system is introduced in citrus as a method to shortening citrus maturation times by inducing citrus to flower on demand. In order to convey the importance of this new method, an alternative use of CRISPR/Cas9 is discussed, citrus flowering mechanisms are described in detail, the cloning and design of the CRISPR/Cas9 system will be explained, and the results will show that reduction in flowering times is possible.

Transcriptional Regulation of Target Genes Using CRISPR/Cas9

The CRISPR/Cas system is a potent and flexible tool for genome editing. Since the Cas9 protein has the ability to bind target DNA and cleave the DNA, it is possible to mutate the Cas9 protein and allow researchers to study the effects of differential gene expression. By mutating both RuvC and HNH nuclease domains, Cas9 can be rendered inactive by four point mutations D10A, D839A, H840A, and N863A, resulting in a Cas9m4 molecule that is functionally unable to cleave target DNA, yet retains the ability to bind to target DNA based on the gRNA targeting sequence (Mali et al., 2013).

By using the nuclease-free Cas9m4 and targeting the Cas9m4-sgRNA complex to transcriptional start sites, the genes targeted could be repressed or activated, much like a light switch (Mali et al., 2013). Furthermore, this system can be enhanced with

transcriptional repressors or activators, and targeted to promoter region results providing a clear transcriptional repression or activation of downstream target genes. It is this simple activation or repression has the most importance in the regulation of citrus genes, especially with regard to citrus flowering.

In general, in the subtropical climate of Florida, flowering occurs when the plant reaches maturity and the days get cooler. Flowering is induced by a set of genes, described at length in the following section, most notably the Flowering Locus T (FT) genes in citrus. However, simply transforming citrus with a constitutive promoter (i.e. always “on”), results in citrus plants that flower while still in tissue culture (Moore et al., 2016). Therefore, using a molecular switch of activating or repressing flowering genes in order to induce early flowering in whole plants would be an extreme boon to the citrus industry and could eliminate the need for regulation and extensive tissue culture protocols, just by producing hardier and disease resistant plants much faster..

Physiology of Flowering in Citrus

In order to investigate this potential method, the overall floral induction process should first examined. Upon exiting juvenility, when the weather is cooler (usually), citrus FT-3 is induced. This is in contrast to the low basal levels of this gene in citrus. In *Arabidopsis*, FT genes have functions that promote flowering, the typical meristem structure regulators from the Terminal Flower (TFL) gene family, has delays flowering and keeps the plant meristem prolific. In many other plant species, FT homologues have been demonstrated to play a role in flowering as well (Pin and Nilsson, 2012) (Liljegren et al., 1999). The citrus TFL is nearly 65% identical to and a homolog of in *Arabidopsis* TFL, and like its counterpart is also a repressor of flowering and inhibits

flowering when overexpressed and increases flowering when down-regulated or knocked out in *Arabidopsis thaliana*(Pilliteri et al., 2004).

This chapter presents a method to modify the expression of, Terminal Flower-1 (TFL), in order to reduce juvenility. Using Cas9m4, fused to a repressor domain, we intended to directly target specific sequences in the TFL promoter and 5' UTR regions in order to decrease juvenility times without the use of a transgene insertion that is deemed unfavorable. To this end, we cloned multiple Cas9m4 fusion constructs, with activators and repressors, adaptable to any gene system in citrus with the right sgRNA sequences. We also designed several TFL sgRNA constructs designed specifically to target TFL promoter regions with a high density of transcriptional regulators. Finally, we designed a quantitative real-time PCR assay in which we can actually measure the change in transcript levels of TFL and other related flowering genes.

Materials and Methods

Plant Materials

In this study, four different cultivars were examined, 'Pineapple' sweet orange (*C. x sinensis* Osb.), 'Duncan' grapefruit (*C. x paradisi*Macf.), sour orange (*C. x aurantium*), 'Carrizo' citrange (L.) Raf) and a trifoliate relative early flowering phenotype, (*Eremocitrus glauca x Poncirus trifoliata*). Specific trees and ages are given when presented in the results.

Plasmid Construction

pCAMBIA-2201-Cas9m4 and derivatives

The plasmid pCAMBIA-2201 was obtained through CAMBIA labs (Canberra, Australia) (Figure 2-1). To insert the Cas9m4 gene sequences, the promoter and

terminator sequences, and the activator (VP16) or repressor (KRAB), the plasmid's MCS site was exploited using restriction digestion.

To generate the most important plasmid,pCAMBIA-2201-FMV::Cas9m4-NLS:KRAB::35ST and the other Cas9m4 plasmids, we next obtained a plasmid containing Cas9m4 with NLS from Addgene (Mali et al., 2013) (Figure 4-1) and the pUC118-FMV-Poly-2-1 generously given by V. Febres(Figure 4-2). Next was the design of each of primers. DNA sequences for all primers used in this study are provided in Table 4-1.

The first step toward the completed plasmid was to put the Fig Mosaic Virus (FMV) promoter, the 35S (constitutive) terminator from Cauliflower Mosaic Virus, along with an additional MCS in between, with different restriction sites. The sequence was amplified by PCR using the primers, SJ15 and SJ16 (Table 4-1). These primers contained sequences for restriction sites for KpnI and XbaI resprectively to be present in the PCR product. Once the product was purified, pCAMBIA-2201 and the PCR product were double digested withKpnI and XbaI (New England BioLabs, Ipswich, Massachussetts, USA). Once the restriction digestion was purified, DNA ligase was added to create the new plasmid.

The MCS in pUC118-Poly-2-1 allowed another double restriction digestion. First, the Cas9m4 plasmid was PCR amplified using primers SJ17 and SJ18 which would produce products with both ApaI and SpeI restriction sites (Table 4-1). A restriction digestion was performed using ApaI and SpeI on both the PCR profuct and the new plasmid containing the FMV promoter and 35S terminator. Then a ligase reaction was performed and pCAMBIA-2201-FMV::Cas9m4::35St (Figure 4-3A) was created.

Finally to add the KRAB repressor and the VP16 activator, PCR amplification using SJ22-SJ23 and SJ25-SJ26 (respectively) using followed by double restriction digestion using NotI and SpeI produced the final plasmid products pCAMBIA-2201-FMV::Cas9m4:KRAB::35St and pCAMBIA-2201-FMV::Cas9m4:VP16 were created. ::35St (Figure 4-3B, C).

Construction of pIDT:SMART::AtU6p:sgRNA::Sp_term and insertion of sgRNAs

For designing the plasmid containing the sgRNA, pIDT:SMART::AtU6p:sgRNA::Sp_term was designed by V. Febres with the sole intent of cloning sgRNAs easily into a plasmid backbone that is highly modular. Once obtained, the rest of the procedure was aided by V. Febres but performed entirely by the author.

To aid in construction of the sgRNAs, sequence data was obtained from Addgene, and then placed into Vector NTI, a sequence reading program. With these tools, sgRNA sites were found using web software “CRISPR-direct” (Naito et al., 2015) and analyzed for optimal sites in the promoter region of TFL. The TFL promoter region presented several options where sgRNAs could be used, so selected primers were compared to special promoter regions where protein binding of transcription factors occur. Five different sgRNA sites were selected and labeled by their location of the promoter sequence (Table 4-2).

To put the sgRNA sequences into the pIDT-SMART plasmid, a double restriction digestion was performed using the pIDT-SMART plasmid and the small designed oligonucleotides with restriction sites. The digestions were ligated together and then the resulting plasmids were sent for sequencing to check for size (Figure 4-4A). The sequencing was performed instead of a gel, for accuracy and for convenience, because

on a gel with a 5,000 kb product, adding only 20-25 base pairs, would not be readily visible.

Once the pIDT-sgRNA plasmids were completed. We then cloned them into pCAMBIA-2202 (Figure 2-1) since the Cas9m4 would be on pCAMBIA-2201 (Figure 2-1). This was completed using the same cloning method as before, PCR amplification with restriction sites, followed by double restriction digestion and then ligation. In this case, sgEX-F1 (Sph) and sgEX-R2 (XbaI) were used as the primers, and Sph and XbaI were the restriction enzymes. Once the plasmid was completed, the genetic material was amplified using 2201-sgRNA-F and 2201-sgRNA-R and then sequenced to confirm (Figure 4-4B)

Agroinfiltration of Citrus

Three different recombinant *Agrobacterium* (Agl1) cells containing the pCAMBIA-2201-FMV-Cas9m4-35ST, the pIDT:SMART::AtU6p:sgRNA-968::Sp_term, or pIDT:SMART::AtU6p:sgRNA-1129::Sp_term were cultured in 10 ml YEP medium with appropriate antibiotics at 28°C for 24-48 hours until the cultures reached an OD_{600}=1.0. The bacterial cultures werecentrifuged, and the pellet was washed once with a liquid media optimized for *Agrobacterium*-mediated transient expression, known as AgroBest (Wu et al., 2014)). The susepesion was centrifuged once more and then suspended in approximately 10 mL AgroBest, to an $OD._{600}$= 0.8.

Each of the cell lines were mixed and then collected in a syringe and infiltrated into the abaxial side of the citrus leaves, either grapefruit (*C. x paradisi*) or (*C.x aurantium)*. The extent of total infiltration was marked with a permanent marker. Upon sample collection, once every 24 hours (unless otherwise noted), whole or partial leaves were removed and immediately wrapped into aluminum foil and preserved in liquid

nitrogen. ceAs a control, citrus leaves were subjected to agroinfiltration in the absence of a Cas9m4 plasmid.

RNA Extraction

Samples were collected as described below (see Plant Materials) and kept in liquid nitrogen during the experiment and stored in a -80 °C freezer for no more than one week before purification of RNA. At least three different collection sites were combined to make about 100-200 mg of plant tissue and then ground to a fine powder using a mortar and pestle and liquid nitrogen. The powder was added to an approximate volume of 500 µL.

Next, 1.5mL off Trizol (Life Technologies, Carlsbad, California, USA) was added and shaken vigorously for about 30 seconds. Samples were centrifuged at 12,000 g for 10 minutes at 4 °C and the upper phase was collected and placed into a fresh tube and incubated at room temperature (RT, 23-24 °C) for 5 minutes. 0.3 mL of chloroform was added, and tubes shaken vigorously for 15 seconds, and then incubated at RT for 5 minutes.

To precipitate the RNA, the upper phase was collected and then 0.75mL of Isopropyl alcohol was added to the solution and shaken vigorously for 30 seconds. Samples were incubated for 10 minutes at RT then centrigued for 10 minutes at 12,000 g at 4°C. Following centrifugation, the supernatant was poured away and the RNA pellet was washed with 1. mL of 75% ethanol and by vortexing. To pellet the RNA, the mixture was centrifuged at only 7,500 g for 5 minutes at 4°C. The supernatant was poured away and then the pellet was dissolved into 30 µL of RNase-Free sterile water.

RNA Purification

The crude RNA extraction was then further purified to laboratory relevance. RNA purification was performed following the “RNA Cleanup” Protocol from QIAGEN (Hilden, Germany). In brief, RNeasy Mini spin columns (QIAGEN, Hilden Germany), were used to bind the RNA, where it could be washed by various buffers, and treated with DNase to remove any other foreign debris from contaminating the RNA sample. The sample was then eluted into 30 µL of RNase-Free sterile water.

Generation of cDNA

After RNA purifaction, cDNA was generated using a simple two-step process. First the concentration of the RNA was read using a nanop-spectrophotometer, and 1 µg of each RNA sample was added to a solution of 5 µM random decamers(Invitrogen, Thermo Fisher, Vilinius, Lithuania) and 2 mM dNTPs (0.5mM each) (Promega, Madison, Wisconsin) and water to a toal volume of 16 µL. The mixtures were then incubates at 85 °C for 2 minutes and quickly transferred to ice. Next, 1X 1st Strand Buffer, 100 U MMLV reverse transcriptase, (each from Invitrogen, Thermo Fisher, Vilinius, Lithuania), 40 U Rnase Inhibitor (Ambion, Foster City, California, USA) was added. The resulting solution was mixed by pipet for 30 seconds and then incubated at 42 °C for 1 hour followed by 95 °C for 10 minutes to create the cDNA. Before use and storage, cDNA was diluted to 0.0025 µg/ µL for use in qRT-PCR analyses.

Quantitative Real-Time PCR (qRT-PCR)

Using the StepOne Software (Fisher Scientific, Waltham, MA) an experimental and plate design was created. The qRT-PCR reaction mixtures used were Taqman Master Mix (2X) and Assay Mix (20X), and werekept on ice (or in the refrigerator when not immediately in use). In addition the Assay Mix, which contains the probe, should be

protected from light as much as possible. Using an electronic repetitive pipette, 18 µl of Reaction Mixed was applied to the bottom of each corresponding well. Using an electronic repetitive pipette 2 µl of diluted cDNA (2 µl of cDNA + 38 µl of sterile ddH2O) was then applied to the corresponding wells. Next, the optical adhesive film was afixed to the surface of the plate and mixed. Centrifuge for 2 minutes at 2500 RPM. Place plate in the Real Time PCR machine and start assay.

This assay will run like normal PCR, except there is an additional probe with a fluorophore. When this probe is amplified as a template, the fluorophore releases and the concentration of excited fluorophore is measured. This should be directly related to how many RNA transcripts of the gene were present at the time of liquid nitrogen preservation.

The output for the assay actually measures an RQ value, and this is calculated by comparing it to the control gene, 18S, a protein that is constitutive and has high transcript levels. By comparing the target gene with 18S, the algorithm sets the control gene to 1.0 and then calculates the fold change difference of that gene relative to the this gene.

Results and Discussion

Establishment of Flowering Gene Baseline Levels

In order to examine how much repression of TFL could actually help a citrus plant come out of juvenility and start to flower, a baseline level of TFL was first examined.

To find the basal TFL expression experiments all four cultivars were used. Grapefruit, sweet orange, and sour orange trees were 1.5 years old. For the early flowering trifoliate, plants were only 6 months old. All plants were grown in a

greenhouse from germination on campus at the University of Florida, Gainesville, Florida, and though the trifoliate was grown in a psyllid-proof facility. Three leaves were taken from three different plants and approximately 60 mg from each of leaf were combined together to make one sample.

Once the samples were prepared and the cDNA was generated, qRT-PCR was performed. The calculated RQ values are an aggregate of three different samples per species from 9 different plants per cultivar totaling 27 plants. This experiment was conducted twice, once in August and once in October, using the same plants. While each sample was compared to 18S in the qRT-PCR assay, the data presented show values relative to “Carrizo” citrange (Figure 4-5). This was due to the fact that TFL levels were generally low in the leaves compared to 18S and presenting it this way allows the differences between each cultivar to be visualized better.

The results in Figure 4-5 show that each cultivar has different levels of TFL and all are much higher than levels present in the citrus relative Carrizo. The results were also surprising due to the fact that the early flowering trifoliate had extremely high levels of TFL, even though these plants typically flower within the first 2-3 months after germination. Although it is initially surprising, the result can probably be explained by the amount of meristem activity needed to keep the plant growing past its early months into the second year of its life. If it flowered too early and couldn’t maintain its meristem identity afterward, the plant would likely die, immediately after fruiting.

Comparison of Mature vs Juvenile Flowering Gene Levels

In this experiment, we wanted to see if TFL was actually complicit in the transition from juvenility into adulthood.

For comparison of mature meristems to juvenile stems, sour orange alone was used. In this experiment, three different branch meristems were collected from mature trees grown for 10 years in the orange grove on campus at the University of Florida, Gainesville, Florida and three different apical meristems were selected from juvenile trees at 1.5 years old. Approximately 40 mg of tissue from each leaf was used to make one sample. Each RQ value is an aggregate mean from four different samples, totaling 12 leaves from 24 different plants. The experiment was conducted twice in one week in the month of November.

The results presented from the experiments are presented in Figure 4-6. The results indicate that TFL anf FT genes are approximately expressed at the same levels in mature plants, around 3-4 fold higher than the control 18S. In contrast, juvenile plants had roughly the same expression of FT genes as the mature plant, but the TFL expression levels averaged to be nearly 20-fold higher than that of the 18S gene. The difference in the RQ value from leaves to meristems of TFL expression, is not that surprising, since TFL is supposed to be expressed in the meristems, however it was shocking that TFL expression levels in juvenile tissue were approximately 4-fold higher than the levels present in mature tissue (Figure 4-6). This result further confirmed that TFL could be an acting agent in citrus juvenility and that its expression, as in *Arabdiopsis*, could limit the ability of FT3 to determine a floral identity in the meristem.

Targeted Gene Expression of TFL mediated by Cas9m4 to Induce Early Flowering

To test the potential of the Cas9/sgRNA system to induce TFL gene expression in citrus, agroinfiltration was employed to deliver the Cas9m4 and sgRNA.

For the *Agroinfiltration* experiments eighteen different grapefruit plants and eighteen different sour orange plants were grown in the greenhouse on campus at the

University of Florida, Gainesville, Florida The plants were first pruned to produce uniform shoots and young, pliable leaves. Next they were first transferred to a 12 hour day/night cycle growth chamber set to 15 °C until after the completion of the experiment. Each plant was treated with the plasmid containing *Agrobacterium* (as described above), in all of their leaves. Samples were compiled from three different treatment sites from approximately 60 mg each. Three different samples were used in each run. At the end of the experiment, leaves would still be on the plant that had been treated but not collected. For the controls, plants were inoculated with a mock treatment which contained a mixture of two different full length plasmids in *Agrobacterium*, pCAMBIA-2201 and pCAMBIA-2202 without Cas9m4, to make sure that any expression changes were not happening due to the stress of the leaf under attack from multiple bacteria, and were only happening in response to the Cas9m4 and sgRNA genes being present.. The experiment was run four different times from October to February.

Specifically, pCAMBIA-2201-FMV::Cas9m4:KRAB::35St and two TFL-targeting sgRNAs were transformed into *Agrobacterium* (See Agroinfiltration of Citrus), and directly infiltrated into grapefruit leaf tissue on the abaxial side. Up to five days after agroinfiltration, total RNA was extracted from the treated leaf areas. The amount of RNA transcripts at the time of collection of TFL gene was compared to the FT3 at 5 different time points, across five days.

The results from the experiment are presented in Figure 4-7. As expected, the TFL expression decreased by 2 fold, in the first day and Cas9m4 levels, not previously endogenous in citrus, rose to levels 4-5 fold higher than the endogenous control, 18S. This result confirmed that both the sgRNA and Cas9m4 worked, since the results were

then compared to levels in the mock trial. After the first day though, on days 2 and 43, Cas9m4 levels were reduced, but still present, and TFL levels increased as expected. Following this, at Day 4 and 5, with Cas9m4 transcript levels all but gone, TFL levels again went back down. This was unexpected, but the fact was clear, that most of the work done by the CRISPR/Cas9m4 system, would be completed by Day 3 at the latest (Figure 4-7).

The experiment with multiple cultivars and multiple days got quickly overloaded, and the test was simplified to just two different cultivars over 48 hours. The same infiltration and collection method were kept the same. Additionally, the plants were still kept in the growth chamber at 15°C. In this run, the data show that this procedure has unexpected results than previously intended (Figure 4-8).

Before infiltration, samples were collected, and the control values were all similar to one another gene for gene. After just 24 hours however, TFL in the experimental plants were reduced and Cas9m4 levels were present in abundance, as expected. However, FT3 levels were not static, by infiltrating into the leaves where FT3 is made, and TFL levels are minimal, the Cas9m4 system was actually able to increase the levels of FT3 nearly 60 fold. After two days, TFL increased well beyond its initial basal levels, Cas9m4 was still present and FT3 levels went even higher to nearly 100-fold. This finding made us wonder if a plant would actually flower early. While the effects were not visible, at least one plant was able to be phenotypically changed.

Using this method, we were successfully able to obtain an early flowering phenotype (Figure 4-9). Five weeks post-agroinfiltration, a flower bud was spotted (Figure 4-9A) and the flower was examined as it blossomed over the course of almost 6

weeks (Figure 4-9B, C). Once the flower opened (Figure 4-9C), the pollen was evaluated for its viability, the flower was pollinated with its own pollen manually, and the flower set a fruit (Figure 4-9D). The fruit did not mature or ripen and soon died, but nonetheless, this design shows that it is possible to enhance early flowering in varieties that usually have a long juvenility period such as sour orange.

The findings suggest that the method of transiently expressing *Agrobacterium* plasmids loaded with a repressor and Cas9m4 and sgRNAs of a target gene can in fact induce a change in the gene expression of both the target gene and the target genes competitors, possibly removing a feedback mechanism. These changes could be significant enough to the plant to produce a visual phenotypic effect, but since it only occurred once in multiple trials across 36 different plants, the method likely requires more optimization. With respect to this body of work, the CRISPR/Cas9m4 transcriptional regulation method has proven successful, since it will not always be so evident that one gene could have such a significant effect on the whole plant.

Tables

Table 4-1. Primers used in this chapter.

Primer #	Name	Location	Sequence
SJ15	SJ15-FwdFMV-P KpnI	FMV Promoter	aaaaaaggatcccccctggcttgtggggaccagacaa
SJ16	SJ16-Rev 35S-T XbaI	35S Terminator	ttttttttctagaactggattttggttttaggaattagaaattt
SJ17	SJ17-Fwd Cas9m4 ApaI	Cas9m4 Start Codon	aaaaaagggcccaccatggacaagaagtactccattg
SJ18	SJ18-Rev Cas9m4-NLS SpeI	Cas9m4-NLS Stop Codon	aaaaaaactagttcacaccttcctcttcttcttggggtc
SJ19	SJ19-Rev Cas9m4 SpeI	Cas9m4-end	aaaaaaactagtgtctccaccgagctgagagaggtcg
SJ20	SJ20-Fwd Cas9m4-VP64-NLS ApaI	Cas9m4-VP64-Start Codon	aaaaaagggcccaccatgcccaagaagaagaggaaggtg
SJ21	SJ21-Rev Cas9m4-VP64 SpeI	Cas9m4-VP64-Stop Codon	aaaaaaactagttcacctagagttaatcagcatgtccagg
SJ22	SJ22-Fwd-VP16 SpeI	VP16 activator start	ttttttactagtcctcccaccgatgttagcttgggcg
SJ23	SJ23-Rev-VP16/EcR NotI	EcR Stop codon	gatttcagcgcaagcggccgcttac
SJ24	SJ24-Fwd-EcR SpeI	EcR Start Codon	ttttttactagtatgcgtcccgaatgcgtcgtgcctg
SJ25	SJ25-Fwd-KRAB SpeI	KRAB domain start	ttttttactagtgtgaccttcaaggatgtatttgtggac
SJ26	SJ26-Rev-KRAB NotI	KRAB domain end	ttttttgcggccgcctagggctcttctcccttctccaac
SJ27	SJ27-Fwd FMV-P KpnI	FMV Promoter	ggtacccccctggcttgtggggaccagacaa
SJ28	SJ28-Rev 35S-T XbaI	35S Terminator	tctagaactggattttggttttaggaattagaaattt

4-1. Continued

Primer #	Name	Location	Primer Sequence
SJ30	SJ30-BsaI/HindIII	MCS	agcttgagaccaaggtctct
SJ31	SJ31-FMV-P-KpnI	FMV Promoter	ggtacccccctgggcttgtggggac
SJ32	SJ32-RV-Cas9m4-5'	bp 144 - bp 168	gtcgaacaggagggcgccaatgagg
SJ33	SJ33-FW-Cas9m4-500	bp bp 3345- bp 3370	aaggaacagcgacaagctgatcgcac
SJ34	SJ34-RV-Cas9m4-500	bp 3827 - bp 3853	cgaggatcactcttttggagaattcgc
SJ35	SJ35-FW-Cas9m4-3'	bp 3858- bp 3884	cgctaacctcgataaggtgctttctgc
SJ36	SJ36-35S-T-XbaI	35S Terminator	aaaaaaacgcgtccaccatgcccaagaagaagaggaag
SJ37	SJ37-Fwd-Cas9m4-VP64 MluI	bp 2 - bp 27	aaaaaaactagtcctagagttaatcagcatgtccaggtc
SJ38	SJ38-Rev-Cas9m4-VP64-No Stop SpeI	bp 4336- bp 4355	aaaaaaactagtaccgctggcctccaccttcct
SJ39	SJ39-Rev-Cas9m4-3'NLS SpeI	bp 4168- bp 4188	taataaagtgttgacaagatccgataaagc
	sgEX-F1 (Sph)	bp 302	ggtctcccatgggagtgatcaaaagtcccacatcg
	sgEX-R2 (XbaI)	bp 563	ggtctcactagaatgcatcggtaatacggttatccac
	2201-sgRNA-F		cgctcatgtgttgagcatataagaaacc
	2201-sgRNA-R		acgacgttgtaaaacgacggccagtg

Table 4-2. SgRNA oligonucleotides and constructed plasmids

Name	Sequence	Constructed Plasmid Name
CsTFL_602-F	GATTGTACTTGGGTCCCTTAGAAT	AtU6p::CsTFL_602_sgRNA::Sp_t
CsTFL_602-R	AAACATTCTAAGGGACCCAAGTAC	
CsTFL_786-F	GATTTACTAAGATTTAAAAGAGTA	AtU6p::CsTFL_786_sgRNA::Sp_t
CsTFL_786-R	AAACTACTCTTTTAAATCTTAGTA	
CsTFL_896-F	GATTTATACTTGGGAGTTTACTAA	AtU6p::CsTFL_896_sgRNA::Sp_t
CsTFL_896-R	AAACTTAGTAAACTCCCAAGTATA	
CsTFL_968-F	GATTTGAGATGTATGTATAGAGGG	AtU6p::CsTFL_968_sgRNA::Sp_t
CsTFL_968-R	AAACCCCTCTATACATACATCTCA	
CsTFL_1129-F	GATTCACAGTTGTTTCAAAACCTA	AtU6p::CsTFL_1129_sgRNA::Sp_t
CsTFL_1129-R	AAACTAGGTTTTGAAACAACTGTG	

Figures

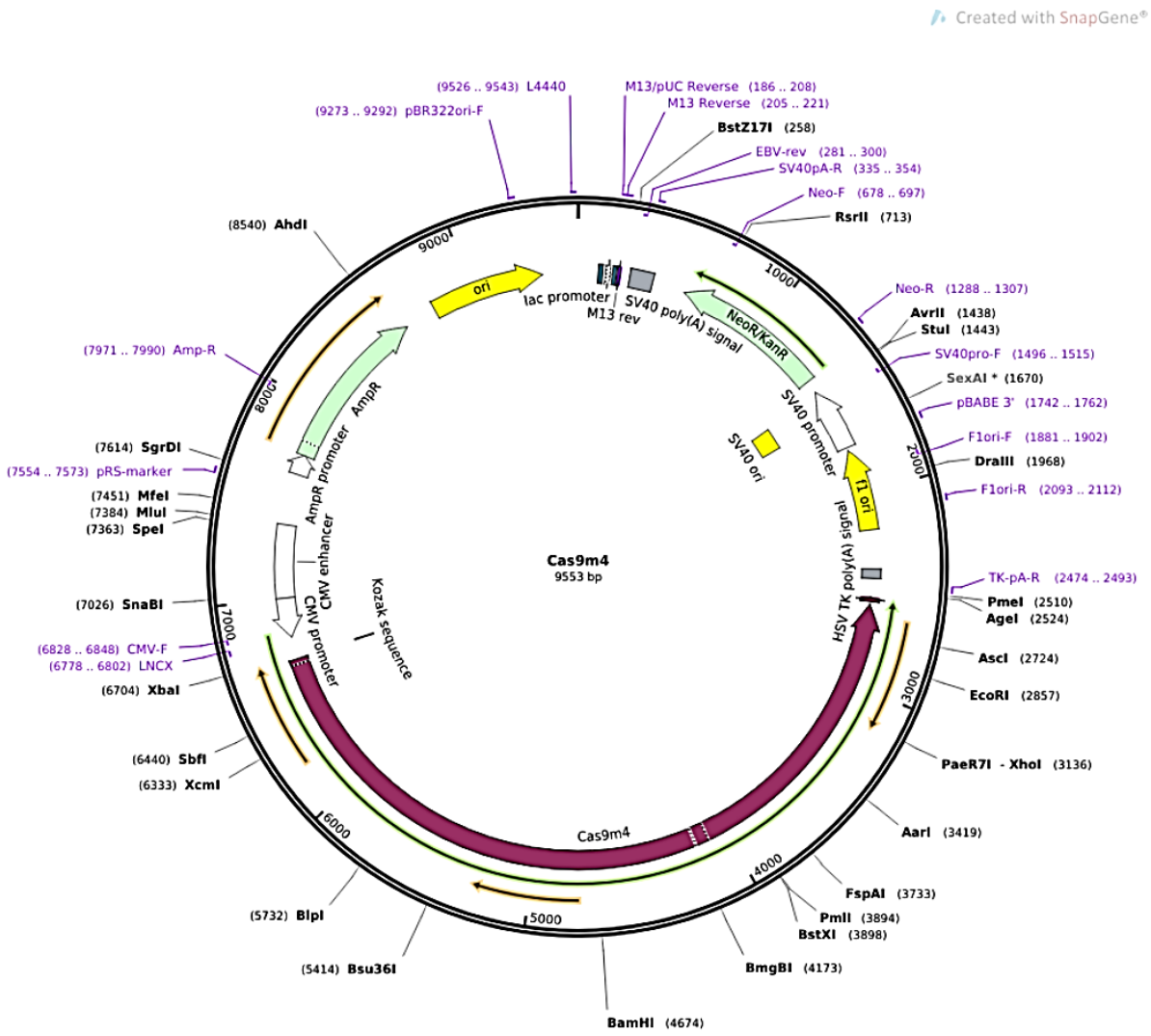

Figure 4-1. Plasmid Cas9m4. The plasmid Cas9m4 was purchased off Addgene (Mali, et al., 2013). It contains the coding sequence for Cas9m4. A mutated Cas9 at four different point to reduce fully hinder its nuclease activity. This gene is important for transcriptional regulation of genes.

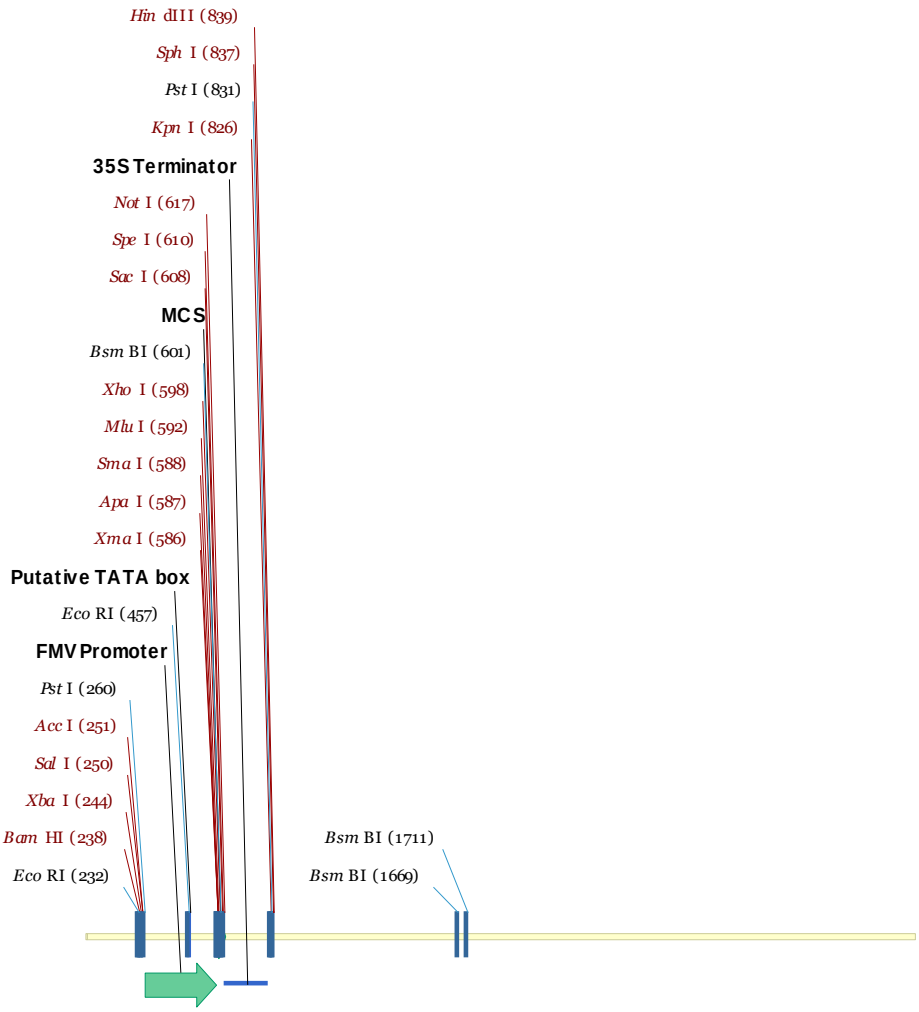

Figure 4-2. Plasmid pUC118-FMV-Poly-2-1. This plasmid is used to insert the FMV promoter and the 35S terminator into the plant-optimized reporter plasmid pCAMBIA-2201, while also containg a MCS for additional cloning.

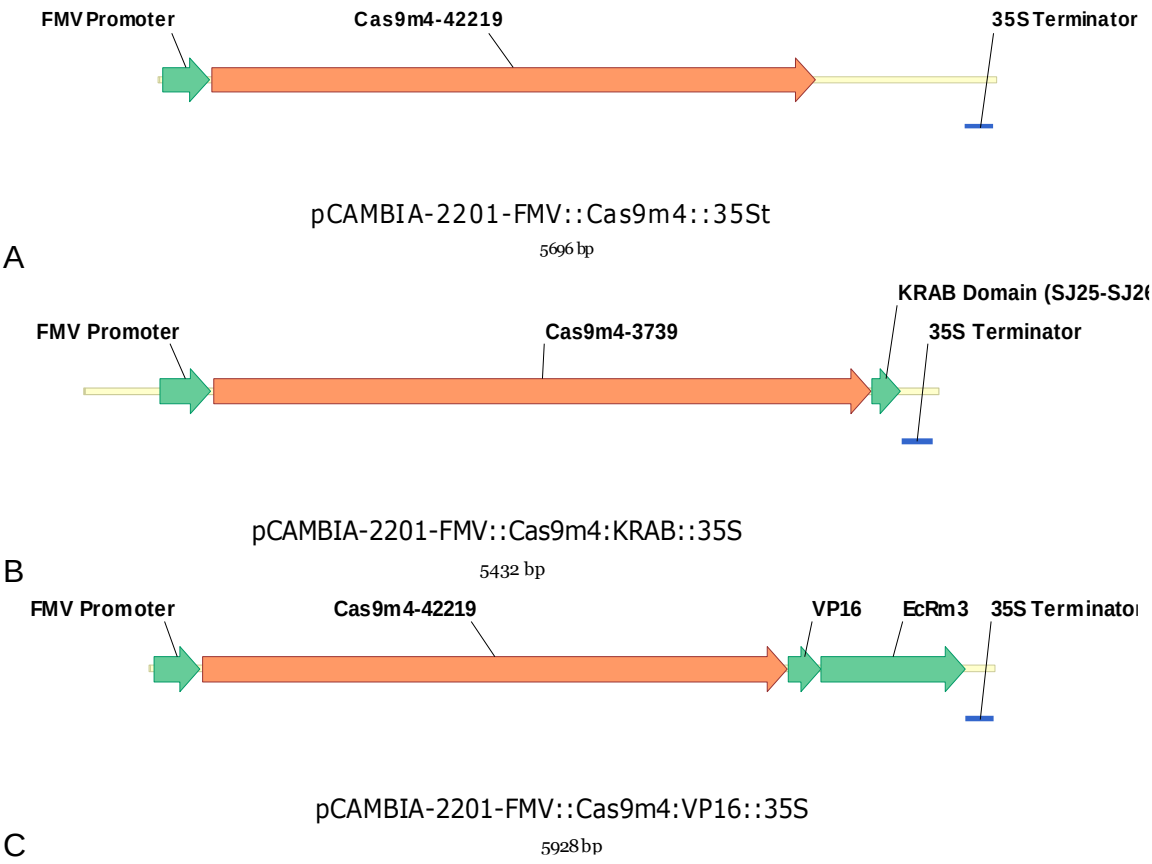

Figure 4-3. Cas9m4 plasmids. Graphical representations of sequenced cloned products of Cas9m4. Each sequence was obtained from the ICBR at the University of Florida using pCAMBIA-2201 specific primers and Cas9m4 internal primers. A). pCAMBIA-2201-FMV::Cas9m4::35St. This is used to repress target genes, though not meant to be as effective as Cas9m4:KRAb fusion pictured in B. B). pCAMBIA-2201-FMV::Cas9m4:KRAB::35St, a much more efficient repressor than just Cas9m4. C) An activator version, pCAMBIA-2201-FMV::Cas9m4:VP16::35St.

A

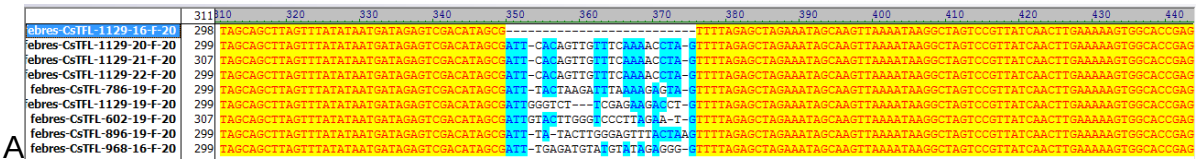

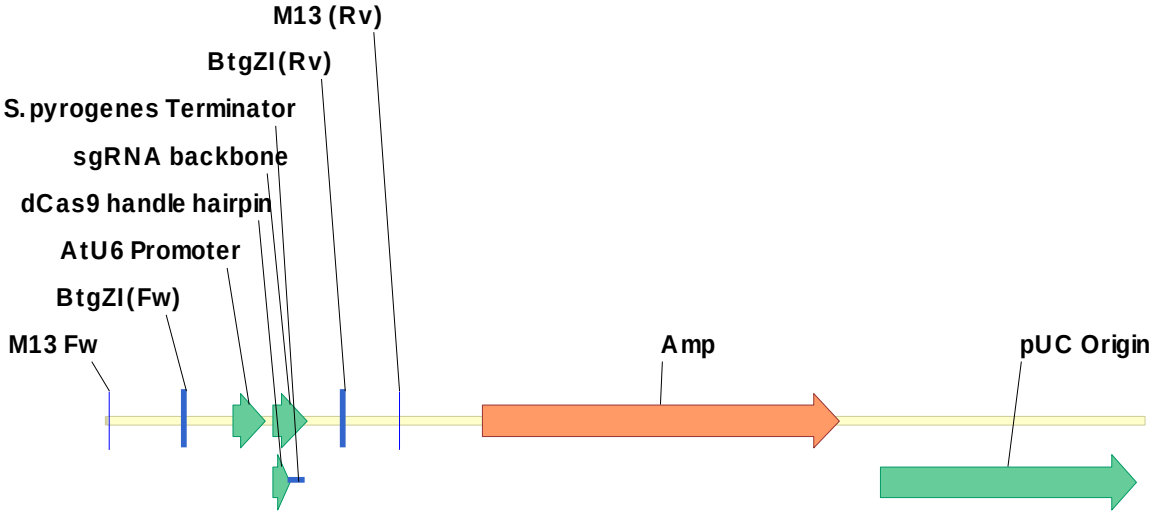

B

pIDT SMART-Amp: AtU6p::sgRNA::Sp Term

2495 bp

Figure 4-4. Cloning and confirmation of sgRNA insertions. A) Sequenced data aligned to confirm the insertion of the proper sgRNAs, since the insertions would be too small to evaluate on a gel, and no further restriction sites were inserted. B) Schematic diagram of pIDT:SMART::AtU6p:sgRNA::Sp_term indicating the promoter, terminator, and ampicillin resistance locations.

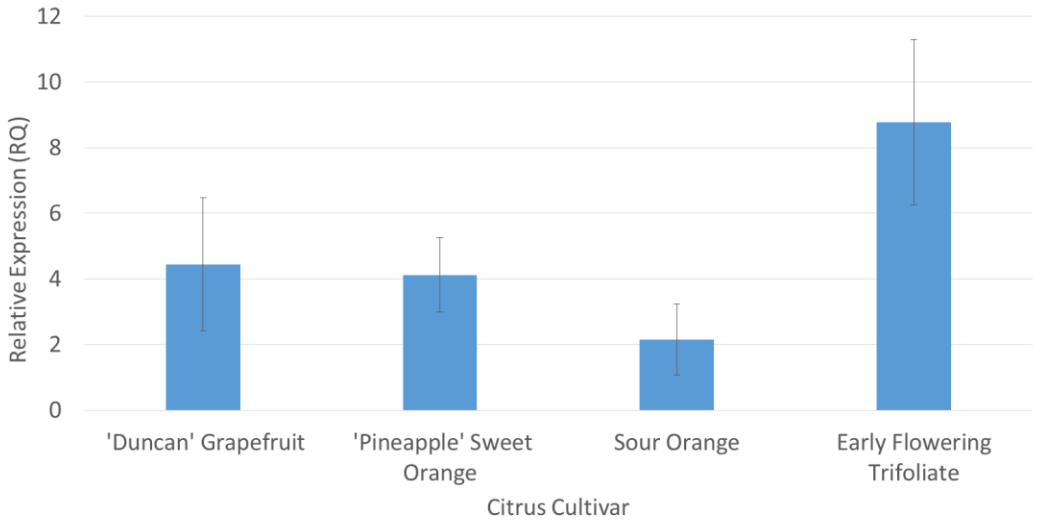

Figure 4-5. Basal expression of TFL in juvenile citrus leaves. Citrus leaves from 1 year old juvenile plants were collected and harvested for RNA. RNA was used to generate cDNA, and the resulting cDNA was used in qRT-PCR experiments. Here the basal levels of expression are presented relative to ‘Carrizo’ citrange (Citrus sinensis x Citrus trifoliata). Samples are aggregates from three different sites. Numerical data are averaged together across three different runs. Error bars represent the standard error of the mean.

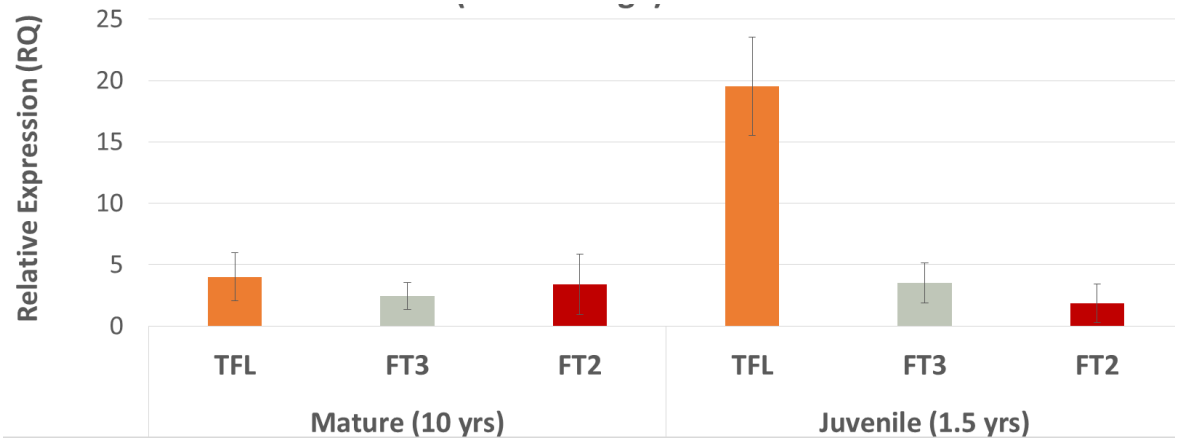

Figure 4-6. Comparison of flowering genes in mature plants vs juvenile plants. Mature meristems (10 y/o) and juvenile meristems (1.5 y/o) were collected and RNA were extracted. cDNA preparation was conducted. Then the qRT-PCR was run. TFL (Terminal Flower), FT (Flowering Locus T).

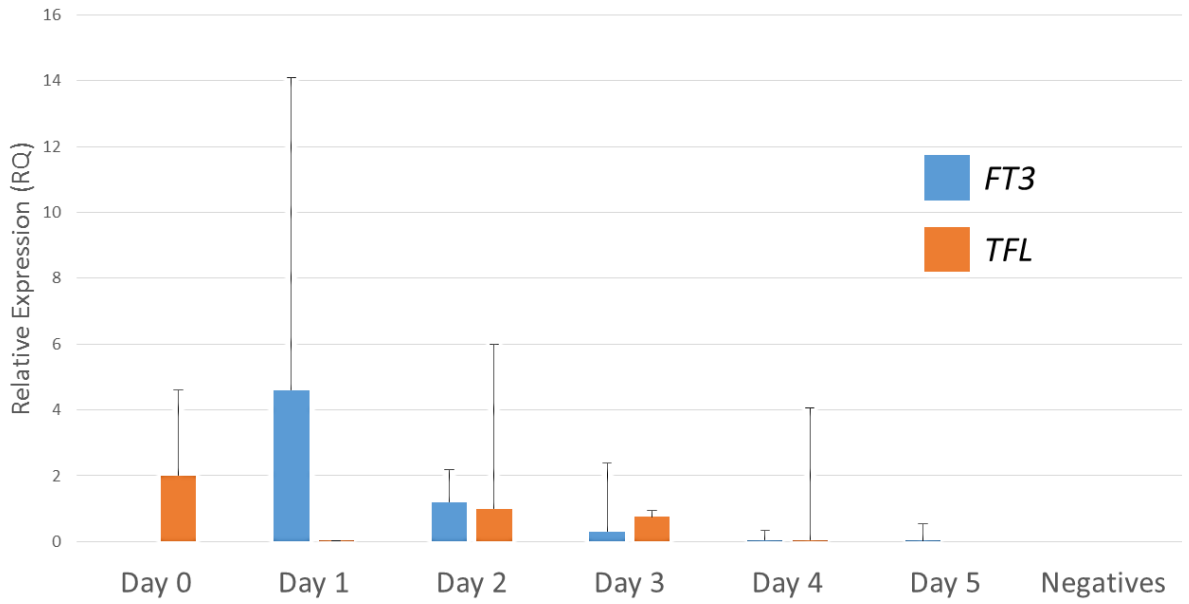

Figure 4-7. Transient expression of a Cas9 repressor and two flowering target genes. Leaf tissue of grapefruit (*C. x paradisi*) was inoculated with the plasmids, pCAMBIA-2201-Cas9m4:KRAB and AtU6p::CsTFL_968_sgRNA::Sp_term together with AtU6p::CsTFL_1129_sgRNA::Sp_term, according to the protocol presented in the metgods. Samples were collected once each day over 5 days. RNA was extracted and purified from infiltrated sections and subsequently generated into cDNA. Each sample ran was compiled from 3 different infiltrated sites. The graph presents the data from two aggregate qRT-PCR runs averaged to the mean. Error bars represent standard error of the mean.

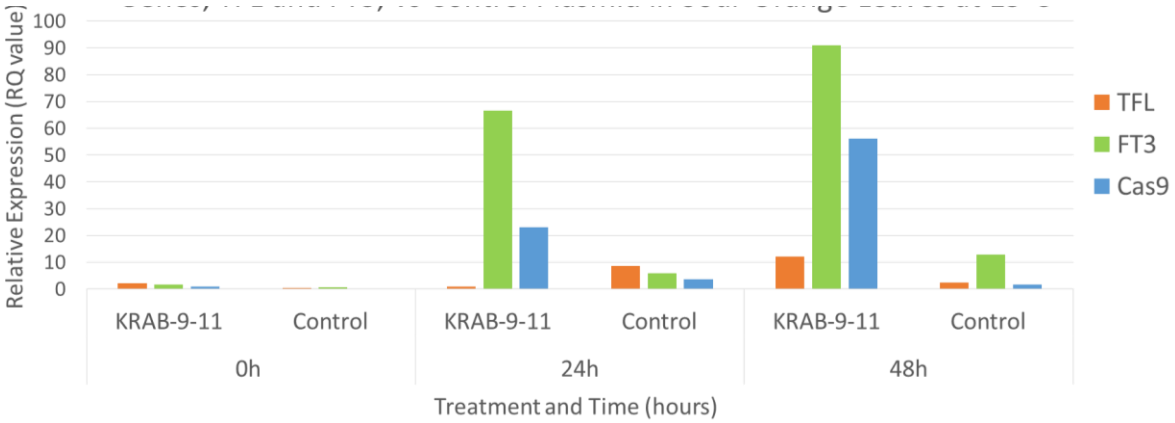

Figure 4-8. Relative expression of Cas9m4, FT3 and TFl after repression. A time course trial showing the relative expression of flowerinf genes in response to Cas9m4 and two sgRNAs designed to repress TFL. KRAB-9-11 is the experimental group and used pCAMBIA-2201-FMV::Cas9m4:**KRAB**::35St, pCAMBIA-2202-AtU6p::CsTFL_**9**68_sgRNA::Sp_term and pCAMBIA-2202-AtU6p::CsTFL_**11**29_sgRNA::Sp_term. Where the control is the mock treatment of pCAMBIA-2201 and pCAMBIA-2202.

Figure 4-9. Flower development from a young (18 months) sour orange (Citrus × aurantium). The leaves of the plant were agroinfiltrated with Cas9m4 and TFL sgRNAs 968 and 1129 as described in the methods and incubated at 15 °C. Leaf samples were taken at 1-5 days post-infiltration and the plants were placed back into the greenhouse. One plant flowered early and produced viable pollen and even set fruit before dying. A) 4 weeks post-infiltration. B) Puffy white flower; 5 weeks after infiltration C) Open flower; five weeks and two days post-infiltration. D) Fruit set; 7 weeks post-infiltration

CHAPTER 5
CONCLUSIONS

The work presented in the previous chapters represents the attempts to bring citrus breeding into the 21st century, in order to help the citrus industry survive an onslaught of pathogen vectors, most notably HLB. In doing so, we have shown that CPPs, nanoparticles, and a modified CRISPR/Cas9 wereshown to be highly effective.

Citrus faces an immediate challenge from the pathogen HLB. Genetic resistance is thought to be the solution the problem, yet even if genetic disease resistance was conferred into a GM plant line, it would be extremely costly to market and require legal proceedings. In lieu of these problems, we propose that cell-penetrating peptides could have a profound change in the perceptions of GM plants. CPPs have a variety of applications and proposed functional mechanisms. Regardless of the actual translocation method, the central role of the original CPP, Tat, is to penetrate the cell membrane and allow proteins and nucleic acids to be administered into a host cell, in order to promote the transcription of foreign DNA (Faingold *et al.*, 2012). This unique function has been reproduced using synthetic peptides and subsequently can deliver many types of cargo in all types of cells. Each proposed mechanism for the action of CPPs is likely to occur in all cells simultaneously but in varying amounts depending on the CPP, cargo and environmental conditions. It is our hope that the novel function of CPPs can be applied to many applications, and we will specifically examine their use in developing a more efficient transformation protocol in citrus that will be more readily available to the public

It is our belief that woody specialty crops, like citrus, will require the development of an innovative method to investigate their genetics of disease resistance and determine how to improve them is necessary. As citrus researchers from the University of Florida, the Moore lab is dedicated to leading the new wave of citrus biotechnology for genetic disease resistance. Our preliminary research is promising that our primary objective of achieving stable disease resistant plants could be successful. If we develop a CPP transformation method for citrus, the payoffs will be substantial and far reaching. The first individuals to benefit would be plant biologists, who already work on genetic improvement of citrus, but improved varieties of citrus would further benefit citrus producers, processors and ultimately, the consumers.

LIST OF REFERENCES

Adler, A.J., Fasman, G.D. and Blout, E.R. (1963). Base-catalyzed Formation of Cyclic Compounds from Poly-β;-benzyl-L-aspartate and Poly-γ-benzyl-L-glutamate. J. Am. Chem. Soc. **85:** 90-97.

Alarcón, C.H., Pennadam, S., and Alexander, C. (2005). Stimuli responsive polymers for biomedical applications. Chemical Society Reviews. **34:** 276-285.

Alford, D.D., Wheeler, A., and Pettigrew, C.A. (1994). Biodegradation of thermally synthesized polyaspartate. Journal of Polymers and the Environment. **2:** 225-236.

Alvarez, S., Rohrig, E., Solís, D., and Thomas, M.H. (2016). Citrus greening disease (Huanglongbing) in Florida: economic impact, management and the potential for biological control. Agricultural Research. **5:** 109-118.

APHIS. 2016. Citrus Diseases. Animal and Plant Health Inspection Service. Retrieved from: https://www.aphis.usda.gov/aphis/resources/pests-diseases/save-our-citrus/soc-citrus-diseases

Atwell, B.J., Kriedemann, P.E., and Turnbull C.G.N. (1999). Plants in action: adaptation in nature, performance in cultivation. Macmillan Education Australia, South Yarra, Victoria. Search.

Bain, J.M. (1958). Morphological, anatomical, and physiological changes in the developing fruit of the Valencia orange, Citrus sinensis (L) Osbeck. Australian Journal of Botany. **6:** 1-23.

Baligar, V.C., Fageria, N.K., and He, Z.L. (2001). Nutrient efficiency in plants. Commun. Soil Sci. Plant Anal. **32:** 921-950.

Batool, A., Iftikhar, Y., Mughal, S., Khan, M., Jaskani, M., Abbas, M., and Khan, I. (2007). Citrus greening disease–a major cause of citrus decline in the world–a review. Hort. Sci.(Prague). **34:** 159-166.

Bartz, R., Fan, H., Zhang, J., Innocent, N., Cherrin C., and Beck S.C. (2011). Effective siRNA delivery and target mRNA degradation using an amphipathic peptide to facilitate pH-dependent endosomal escape. Biochem J. **435:** 475-487

Belhaj, K., Chaparro-Garcia, A., Kamoun, S., Patron, N.J., and Nekrasov, V. (2015). Editing plant genomes with CRISPR/Cas9. Current opinion in biotechnology. **32:** 76-84.

Bent, A. (2006). Arabidopsis thaliana floral dip transformation method. Methods Mol Biol. **343:** 87-103.

Bhattacharyya, A., Bhaumik, A., Rani, P.U., Mandal, S., and Epidi, T.T. (2010). Nano-particles-A recent approach to insect pest control. African Journal of Biotechnology. **9:** 3489-3493.

Blencowe, A., Tan, J.F., Goh, T.K., and Qiao, G.G. (2009). Core cross-linked star polymers via controlled radical polymerisation. Polymer. **50:** 5-32.

Boch, J., Scholze, H., Schornack, S., Landgraf, A., Hahn, S., Kay, S., Lahaye, T., Nickstadt, A., and Bonas, U. (2009). Breaking the code of DNA binding specificity of TAL-type III effectors. Science. **326:** 1509-1512.

Bond, J.E. and Roose, M.L. (1998). Agrobacterium-Mediated Transformation of the Commercially Important Citrus Cultivar Washington Navel Orange. Plant Cell Reports.**18:** 229-234

Bove, J.M., and Garnier, M. (2003). Phloem-and xylem-restricted plant pathogenic bacteria. Plant Science. **164:** 423-438.

Bove, J.M. (2006). Huanglongbing: a destructive, newly-emerging, century-old disease of citrus. J Plant Pathol. **88:** 7-37.

Bové, J.M. (2014). Huanglongbing or yellow shoot, a disease of Gondwanan origin: Will it destroy citrus worldwide? Phytoparasitica. **42:** 579-583.

Brooks, C., Nekrasov, V., Lippman, Z.B., and Van Eck, J. (2014). Efficient gene editing in tomato in the first generation using the clustered regularly interspaced short palindromic repeats/CRISPR-associated9 system. Plant physiology. **166:** 1292-1297.

Cao, H., Glazebrook, J., Clarke, J.D., Volko, S., and Dong, X. (1997). The Arabidopsis NPR1 gene that controls systemic acquired resistance encodes a novel protein containing ankyrin repeats. Cell. **88:**57-63.

Casadei, M.A., Pitarresi, G., Calabrese, R., Paolicelli, P., and Giammona, G. (2008). Biodegradable and pH-sensitive hydrogels for potential colon-specific drug delivery: characterization and in vitro release studies. Biomacromolecules. **9:** 43-49.

Cermak, T., Doyle, E.L., Christian, M., Wang, L., Zhang, Y., Schmidt, C., Baller, J.A., Somia, N.V., Bogdanove, A.J., and Voytas, D.F. (2011). Efficient design and assembly of custom TALEN and other TAL effector-based constructs for DNA targeting. Nucleic acids research. **39:** e82-e82.

Chen, C.P., Chou, J.C., Liu, B.R., Chang, M., and Lee, H.J. (2007). Transfection and expression of plasmid DNA in plant cells by an arginine-rich intracellular delivery peptide without protoplast preparation. FEBS Lett. **581:**1891-1897.

Chen, H., Xu, W., Chen, T., Yang, W., Hu, J., and Wang, C. (2005). Aggregation of biodegradable amphiphilic poly (succinimide-co-N-propyl aspartamide) and poly (N-dodecyl aspartamide-co-N-propyl aspartamide) in aqueous medium and its preliminary drug-released properties. Polymer. **46:** 1821-1827.

Chen, H.T., Neerman, M.F., Parrish, A.R., and Simanek, E.E. (2004). Cytotoxicity, hemolysis, and acute in vivo toxicity of dendrimers based on melamine, candidate vehicles for drug delivery. J Am Chem Soc. **126:** 10044-10048.

Cheng, J., and Deming, T.J. (2012). Synthesis of Polypeptides by Ring-Opening Polymerization of α-Amino Acid N-Carboxyanhydrides. In Peptide-Based Materials, T. Deming, ed. Berlin, Heidelberg: Springer Berlin Heidelberg. 1-26.

Chinnamuthu, C., and Boopathi, P.M. (2009). Nanotechnology and agroecosystem. Madras Agric. J. **96:** 17-31.

Cho, H.Y., Averick, S.E., Paredes, E., Wegner, K., Averick, A., Jurga, S., Das, S.R., and Matyjaszewski, K. (2013). Star Polymers with a Cationic Core Prepared by ATRP for Cellular Nucleic Acids Delivery. Biomacromolecules. **14:** 1262-1267.J. Liu, H. Duong, M. R. Whittaker, T. P. Davis and C. Boyer, Macromol. Rapid Commun., 2012, 33, 760–766.

Chugh, A., and Eudes, F. (2007). Translocation and nuclear accumulation of monomer and dimer of HIV-1 Tat basic domain in triticale mesophyll protoplasts. BBA-Biomembranes. **1768:** 419-426.

Chugh, A., and Eudes, F. (2008a). Studies of uptake of Cell-penetrating peptides and their cargoes in wheat immature embryos. FEBS Journal. **275:** 2403-2414.

Chugh, A., and Eudes, F. (2008b). Cellular uptake of cell-penetrating peptides, pVEC and transportan in plants. Journal of Peptide Science. **14:** 477-481.

Chugh, A., and Eudes, F., and Shim, Y. (2010). Cell- penetrating peptides as nanocarriers for the delivery of macromolecules. IUBMB Life. **62:** 183-193.

Chugh, A., Amundsen, E., and Eudes, F. (2009). Translocation of cell-penetrating peptides and delivery of their cargoes in triticale microspores. Plant Cell Reports. **28:** 801-810.

Chung, K.-R. (2011). Elsinoë fawcettii and Elsinoë australis: the fungal pathogens causing citrus scab. Molecular Plant Pathology. **12:** 123-135.

Clough, S.J., and Bent, A.F. (1998). Floral dip: a simplified method for Agrobacterium-mediated transformation of Arabidopsis thaliana. Plant J. **16:** 735-743.

Cong, L., Ran, F.A., Cox, D., Lin, S., Barretto, R., Habib, N., Hsu, P.D., Wu, X., Jiang, W., and Marraffini, L.A. (2013). Multiplex genome engineering using CRISPR/Cas systems. Science. **339:** 819-823.

Cradick, T.J., Fine, E.J., Antico, C.J., and Bao, G. (2013). CRISPR/Cas9 systems targeting β-globin and CCR5 genes have substantial off-target activity. Nucleic acids research. **41:** 9584-9592.

Cuenca, J., Aleza, P., Garcia-Lor, A., Ollitrault, P., and Navarro, L. (2016). Fine mapping for identification of Citrus Alternaria Brown Spot candidate resistance genes and development of new SNP markers for marker-assisted selection. Frontiers in Plant Science. **7**: 01948

Cui, C., Xue, Y.N., Wu, M., Zhang, Y., Yu, P., Liu, L., Zhuo, R.X., and Huang, S.W. (2013). Poly(L-aspartamide)-based reduction-sensitive micelles as nanocarriers to improve doxorubicin content in cell nuclei and to enhance antitumor activity. Macromol Biosci. **13:** 1036-1047.

Curtin, S.J., Anderson, J.E., Starker, C.G., Baltes, N.J., Mani, D., Voytas, D.F., and Stupar, R.M. (2013). Targeted mutagenesis for functional analysis of gene duplication in legumes. Legume Genomics: Methods and Protocols**:** 25-42.

Curtolo, M., Cristofani-Yaly, M., Gazaffi, R., Takita, M.A., Figueira, A., and Machado, M.A. (2017). QTL mapping for fruit quality in Citrus using DArTseq markers. BMC genomics. **18:** 289.

Darad, R., De, A.K., and Aiyar, A.S. (1983). Toxicity of nitrite and dimethylamine in rats. Toxicol. Lett. **17:** 125-130.

Deming, T.J. (1997). Facile synthesis of block copolypeptides of defined architecture. Nature. **390:** 386-389.

Deming, T.J. (2007). Synthetic polypeptides for biomedical applications. Progress in Polymer Science. **32:** 858-875.

Dewdney, M., Schubert, T., Estes, M., and Peres, N. (2010). Citrus black spot. Citrus Ind. **91:** 19-20.

Dewdney, M.M. (2017). Citrus Scab. 2017-2018 Florida Citrus Production Guide. UF/IFAS Citrus Extension. 127-128

Dewdney, M.M., Schubert, T.S., Estes, M.R., Roberts, P.D., and Peres, N.A. (2017). Citrus Black Spot. 2017-2018 Florida Citrus Production Guide. UF/IFAS Citrus Extension. 121-125

Dom, G., Shaw-Jackson, C., Matis, C., Bouffioux, O., Picard, J.J., Prochiantz, A., Brasseur, R., Mingeot-Leclercq, M., and Rezsohazy, R. (2003). Cellular uptake of Antennapedia Penetratin peptides is a two-step process in which phase transfer precedes a tryptophan-dependent translocation. Nucleic Acids Research. **31:** 556–561.

EC-HFS. (2016). Plant Health: Emergency measures for the import of citrus fruit from several non-EU countries. European Commission- Health and Food Safety.

Eiriksdottir, E., Konate, K., Langel, U., Divita, G., and Deshayes, S. (2010). Secondary structure of cell-penetrating peptides controls membrane interaction and insertion. BBA Biomembranes. **1798:** 1119-1128.

El-Sayed, A., Futaki S., Harashima, H. (2009). Delivery of macromolecules using arginine-rich cell-penetrating peptides: ways to overcome endosomal entrapment. AAPS J. **11**:13-22.

FAO. (2016). Citrus Fruit Statistics 2015. Food and Agriculture Organization of the United Nations. Rome, Italy.

Febres, V.F., Fisher, L., Khalaf, A., Moore, G.A. (2011). Citrus transformation: Challenges and prospects. Genetic Transformation. DOI: 10.5772/24526.

Febres, V.F., Lee, R.F., and Moore, G.A. (2007). 14 Genetic Transformation of citrus for pathogen resistance. Citrus Genetics, Breeding and Biotechnology. 287-305.

Feng, Z., Mao, Y., Xu, N., Zhang, B., Wei, P., Yang, D.-L., Wang, Z., Zhang, Z., Zheng, R., and Yang, L. (2014). Multigeneration analysis reveals the inheritance, specificity, and patterns of CRISPR/Cas-induced gene modifications in Arabidopsis. Proceedings of the National Academy of Sciences. **111:** 4632-4637.

Flasinski, M., and Hąc-Wydro, K. (2014). Natural vs synthetic auxin: Studies on the interactions between plant hormones and biological membrane lipids. Environmental research. **133:** 123-134.

Fleischer, A., O'Neill, M.A., and Ehwald, R. (1999). The pore size of non-graminaceous plant cell walls is rapidly decreased by borate ester cross-linking of the pectic polysaccharide rhamnogalacturonan II. Plant Physiology. **121:** 829-838.

Fox, J.E., Gulledge, J., Engelhaupt, E., Burow, M.E., and McLachlan, J.A. (2007). Pesticides reduce symbiotic efficiency of nitrogen-fixing rhizobia and host plants. Proc Natl Acad Sci U S A. **104:** 10282-10287.

Frankel, A.D. and Pabo, C.O. (1988). Cellular uptake of the tat protein from human immunodeficiency virus. Cell. **55:**1189-1193.

Fretz, M., Jin, J., Conibere, R., Penning, N.A., Al-Taei, S., Storm, G., Futaki, S., Takeuchi, T., Nakase, I., Jones, A.T. (2006). Effects of Na+/H+ exchanger inhibitors on subcellular localisation of endocytic organelles and intracellular dynamics of protein transduction domains HIV-TAT peptide and octaarginine. J Control Release. **116:** 247-254.

Fu, Y., Foden, J.A., Khayter, C., Maeder, M.L., Reyon, D., Joung, J.K., and Sander, J.D. (2013). High-frequency off-target mutagenesis induced by CRISPR-Cas nucleases in human cells. Nature biotechnology. **31:** 822-826.

Fu, Z.Q., Yan, S., Saleh, A., Wang, W., Ruble, J., Oka, N., Mohan, R., Spoel, S.H., Tada, Y., Zheng, N., Dong, X. (2012). NPR3 and NPR4 are receptors for the immune signal salicylic acid in plants. Nature. **486:**228-232.

Futaki, S., Nakase, I., Tadokoro, A., Takeuchi, T., Jones, A.T. (2007). Arginine-rich peptides and their internalization mechanisms. Biochem Soc Trans. **35:**784-787.

Gabrielson, N.P., Lu, H., Yin, L., Li, D., Wang, F. and Cheng, J. (2012). Reactive and Bioactive Cationic α-Helical Polypeptide Template for Nonviral Gene Delivery. Angew. Chem., Int. Ed. **51:** 1143-1147.

Gao, W., Chan, J.M., and Farokhzad, O.C. (2010). pH-responsive nanoparticles for drug delivery. Molecular pharmaceutics. **7:** 1913-1920.

Gmitter, F.G., Deng, Z., and Chen, C. (2007a). 13 Cloning and characterization of disease resistance genes. Citrus Genetics, Breeding and Biotechnology. 287-305.

Gmitter, F.G., Grosser, J.W., Castle, W.S., and Moore, G.A. (2007b). 2 A Comprehensive citrus genetic improvement programme. Citrus Genetics, Breeding and Biotechnology. 9-18.

Gomez, D.A., and Carpena, R.O. (2014). Effect of 1-naphthaleneacetic acid on organic acid exudation by the roots of white lupin plants grown under phosphorus-deficient conditions. Journal of plant physiology. **171:** 1354-1361.

Gonzalez, C.A., Sala, N., and Rokkas, T. (2013). Gastric cancer: epidemiologic aspects. Helicobacter. **18:** 34–38.

Gonzalez-Melendi, P., Fernandez-Pacheco, R., Coronado, M., Corredor, E., Testillano, P., Risueno, M., Marquina, C., Ibarra, M., Rubiales, D., and Perez-de-Luque, A. (2007). Nanoparticles as smart treatment-delivery systems in plants: assessment of different techniques of microscopy for their visualization in plant tissues. Annals of botany. **101:** 187-195.

Gottwald, T.R., Graham, J.H., and Schubert, J.S. (2002). Citrus canker: The pathogen and its impact. Plant Health Progress.

Gottwald, T.R., and Irey, M. (2007). Post-hurricane analysis of citrus canker II: Predictive model estimation of disease spread and area potentially impacted by various eradication protocols following catastrophic weather events. Plant Health Progress. **10**.

Green, M. and Loewenstein, P.M. (1988). Autonomous functional domains of chemically synthesized human immunodeficiency virus TAT trans-activator protein. Cell. **55:**1179-1188.

Greenspan, P., and Fowler, S.D. (1985). Spectrofluorometric studies of the lipid probe, Nile red. J Lipid Res. **26:** 781-789.

Gu, X., Wang, J., Liu, X., Zhao, D., Wang, Y., Gao, H., and Wu, G. (2013). Temperature-responsive drug delivery systems based on polyaspartamides with isopropylamine pendant groups. Soft Matter. **9:** 7267-7273.

Guo, W. and Grosser, J.W. (2005). Somatic hybrid vigor in Citrus: Direct evidence from protoplast fusion of an embryogenic callus line with a transgenic mesophyll parent expressing the GFP gene. Plant Science. **168:** 1541–1545.

Guo, W., Duan, Y., Olivares-Fuster, O., Wu, Z., Arias, C.R., Burns, J.K., Grosser, J.W. (2005). Protoplast transformation and regeneration of transgenic Valencia sweet orange plants containing a juice quality-related pectin methylesterase gene. Plant Cell Rep. **24:** 482–486

Guo, X.F., Zhou, Y., Tu, F.Q., Xiong, X.J., Wang, H., and Zhang, H.S. (2011). Determination of phytohormones in plant samples based on the precolumn fluorescent derivatization with 1, 3, 5, 7-tetramethyl-8-aminozide-difluoroboradiaza-s-indacene by HPLC for routine use. Journal of separation science. **34:** 789-795.

Gyarmati, B., Vajna, B., Nemethy, A., Laszlo, K., and Szilagyi, A. (2013). Redox- and pH-responsive cysteamine-modified poly(aspartic acid) showing a reversible sol-gel transition. Macromol Biosci. **13:** 633-640.

Han, S.-Y., and Kim, Y.-A. (2004). Recent development of peptide coupling reagents in organic synthesis. Tetrahedron. **60:** 2447-2467.

Hill, M.R., MacKrell, E.J., Forsthoefel, C.P., Jensen, S.P., Chen, M., Moore, G.A., He, Z.L. and Sumerlin, B.S. (2015). Biodegradable and pH-responsive nanoparticles designed for site-specific delivery in agriculture. Biomacromolecules. **16:** 1276-1282.

Hodges, A., and Spreen, T. (2012). Economic impacts of citrus greening (HLB) in Florida, 2006/07–2010/11. Electronic Data Information Source (EDIS) FE903 (Gainseville, FL: University of Florida).

Hoshino, Y., Koide, H., Furuya, K., Haberaecker, W.W., 3rd, Lee, S.H., Kodama, T., Kanazawa, H., Oku, N., and Shea, K.J. (2012). The rational design of a synthetic polymer nanoparticle that neutralizes a toxic peptide in vivo. Proc Natl Acad Sci U S A. **109:** 33-38.

Huang, Y., Tang, Z., Zhang, X., Yu, H., Sun, H., Pang, X., and Chen, X. (2013). pH-triggered charge-reversal polypeptide nanoparticles for cisplatin delivery: preparation and in vitro evaluation. Biomacromolecules. **14:** 2023-2032.

Iglesias, D.J., Cercós, M., Colmenero-Flores, J.M., Naranjo, M.A., Ríos, G., Carrera, E., Ruiz-Rivero, O., Lliso, I., Morillon, R., and Tadeo, F.R. (2007). Physiology of citrus fruiting. Brazilian Journal of Plant Physiology. **19:** 333-362.

Jeong, J.H., Cha, C., Kaczmarowski, A., Haan, J., Oh, S., and Kong, H. (2012). Polyaspartamide vesicle induced by metallic nanoparticles. Soft matter. **8:** 2237-2242.

Kang, H.S., Kim, S.R.Y.J., Han, S. and Chang, I. (2001) Effects of grafted alkyl groups on aggregation behavior of amphiphilic poly(aspartic acid). Langmuir. **17:** 7501-7506.

Kausik, R., Srivastava, A., Korevaar, P.A., Stucky, G., Waite, J.H., and Han, S. (2009). Local Water Dynamics in Coacervated Polyelectrolytes Monitored through Dynamic Nuclear Polarization-Enhanced 1H NMR. Macromolecules. **42:** 7404-7412.

Klug, A. (2010). "The discovery of zinc fingers and their applications in gene regulation and genome manipulation". Annual Review of Biochemistry. **79:** 213–31.

Koyama, H., Toda, T., and Hara, T. (2001). Brief exposure to low-pH stress causes irreversible damage to the growing root in Arabidopsis thaliana: pectin–Ca interaction may play an important role in proton rhizotoxicity. Journal of Experimental Botany. **52:** 361-368.

Kricheldorf, H.R., Lossow, C.V., Lomadze, N., and Schwarz, G. (2008). Cyclic polypeptides by thermal polymerization of α-amino acid N-carboxyanhydrides. Journal of Polymer Science Part A: Polymer Chemistry. **46:** 4012-4020.

Koltunow, A.M., Soltys, K., Nito, N., and McClure, S. (1995). Anther, ovule, seed, and nucellar embryo development in Citrus sinensis cv. Valencia. Canadian Journal of Botany. **73:** 1567-1582.

Kumar, A. (2012). Polyaspartic acid-a versatile green chemical. Chem Sci Rev Lett. **1:** 162-167.

Ladanyia, M. (2010). Citrus fruit: biology, technology and evaluation. Academic press.

Lai, M.H., Jeong, J.H., DeVolder, R.J., Brockman, C., Schroeder, C., and Kong, H. (2012). Ellipsoidal Polyaspartamide Polymersomes with Enhanced Cell-Targeting Ability. Advanced functional materials. **22:** 3239-3246.

Lai, M.-H., Lee, S., Smith, C.E., Kim, K., and Kong, H. (2014). Tailoring polymersome bilayer permeability improves enhanced permeability and retention effect for bioimaging. ACS applied materials & interfaces. **6:** 10821-10829.

Lakshmanan, M., Kodama, Y., Yoshizumi, T., Sudesh, K., and Numata, K. (2013). Rapid and Efficient Gene Delivery into Plant Cells Using Designed Peptide Carriers. Biomacromolecules. **14:** 10-16.

Langel, U. (2007). Handbook of Cell-Penetrating Peptides, Second Edition. Boca Raton London New York CRC ISBN: 0849350905

Lapienis, G. (2009). Star-shaped polymers having PEO arms. Progress in Polymer Science. **34:** 852-892.

Lee, M., Jeong, J., and Kim, D. (2015). Intracellular Uptake and pH-Dependent Release of Doxorubicin from the Self-Assembled Micelles Based on Amphiphilic Polyaspartamide Graft Copolymers. Biomacromolecules. **16:** 136-144.

Lenman, M.M., Lewis, A., and Gani, D. (1997). Synthesis of fused 1, 2, 5-triazepine-1, 5-diones and some N 2-and N 3-substituted derivatives: potential conformational mimetics for cis-peptidyl prolinamides1. Journal of the Chemical Society, Perkin Transactions **1:** 2297-2312.

Li, T., Liu, B., Spalding, M.H., Weeks, D.P., and Yang, B. (2012). High-efficiency TALEN-based gene editing produces disease-resistant rice. Nature biotechnology. **30:** 390-392.

Liljegren, S.J., Gustafson-Brown, C., Pinyopich, A., Ditta, G.S., and Yanofsky, M.F. (1999). Interactions among APETALA1, LEAFY, and TERMINAL FLOWER1 specify meristem fate. The Plant Cell. **11:** 1007-1018.

Liu, Y., Heying, E., Tanumihardjo, S.A. (2012). History, global distribution, and nutritional importance of citrus fruits. Comprehensive Reviews in Food Science and Food Safety. **11:** 530–545.

Lu, C., Li, B., Liu, N., Wu, G., Gao, H., and Ma, J. (2014a). A hydrazone crosslinked zwitterionic polypeptide nanogel as a platform for controlled drug delivery. RSC Advances. **4:** 50301-50311.

Lu, C., Wang, X., Wu, G., Wang, J., Wang, Y., Gao, H., and Ma, J. (2014b). An injectable and biodegradable hydrogel based on poly(α,β-aspartic acid) derivatives for localized drug delivery. Journal of Biomedical Materials Research Part A. **102:** 628-638.

Lu, H., Wang, J., Song, Z., Yin, L., Zhang, Y., Tang, H., Tu, C., Lin, Y., and Cheng, J. (2014c). Recent advances in amino acid N-carboxyanhydrides and synthetic polypeptides: chemistry, self-assembly and biological applications. Chem. Comm. **50:** 139-155.

Lux, C.G., Joshi-Barr, S., Nguyen, T., Mahmoud, E., Schopf, E., Fomina, N., and Almutairi, A. (2012). Biocompatible Polymeric Nanoparticles Degrade and Release Cargo in Response to Biologically Relevant Levels of Hydrogen Peroxide. Journal of the American Chemical Society **134:** 15758-15764.

Ma, D.X., Shi, N.Q., and Qi, X.R. (2011). Distinct transduction modes of arginine-rich cell-penetrating peptides for cargo delivery into tumor cells. Int J Pharm. **419:** 200-208.

Ma, Y., Jiang, X., and Zhuo, R. (2013). Biodegradable and thermosensitive micelles of amphiphilic polyaspartamide derivatives containing aromatic groups for drug delivery. Journal of Polymer Science Part A: Polymer Chemistry. **51:** 3917-3924.

Ma, H., Marti-Gutierrez, N., Park, S.-W., Wu, J., Lee, Y., Suzuki, K., Koski, A., Ji, D., Hayama, T., Ahmed, R., et al. (2017). Correction of a pathogenic gene mutation in human embryos. Nature. **548:** 413-419.

Main, D., Jung, S., et al. (2017). Citrus Genome Database. Mainlab Bioinformatics at Washington State University. www.citrusgenomedb.org

Mali, P., Aach, J., Stranges, P.B., Esvelt, K.M., Moosburner, M., Kosuri, S., Yang, L., and Church, G.M. (2013). CAS9 transcriptional activators for target specificity screening and paired nickases for cooperative genome engineering. Nature biotechnology. **31:** 833-838.

Manthe, R.L., Foy, S.P., Krishnamurthy, N., Sharma, B., and Labhasetwar, V. (2010). Tumor Ablation and Nanotechnology. Molecular Pharmaceutics **7:** 1880-1898.

McClean, A.P.D., and Oberholzer, P.C.J. (1965). Greening disease of sweet orange: evidence that it is caused by a transmissible virus. South African Journal of Agricultural Science. **8:** 253–276.

McDaniel, J.R., Callahan D.J., and Chilkoti A. (2010). Drug delivery to solid tumors by elastin-like polypeptides. Adv. Drug Delivery Rev. **62:** 1456-1467.

Mendoza-Cozatl, D.G., Butko, E., Springer, F., Torpey, J.W., Komives, E.A., Kehr, J., and Schroeder, J.I. (2008). Identification of high levels of phytochelatins, glutathione and cadmium in the phloem sap of Brassica napus. A role for thiol-peptides in the long-distance transport of cadmium and the effect of cadmium on iron translocation. The Plant Journal. **54:** 249-259.

Miao, J., Guo, D., Zhang, J., Huang, Q., Qin, G., Zhang, X., Wan, J., Gu, H., and Qu, L.-J. (2013). Targeted mutagenesis in rice using CRISPR-Cas system. Cell research. **23:** 1233.

Mishra, A., Lai, G.H., Schmidt, N.W., et al. (2011). Translocation of HIV TAT peptide and analogues induced by multiplexed membrane and cytoskeletal interactions. Proc Natl Acad Sci. **108:**16883-16888.

Moon, J.R., Kim, B.S., and Kim, J. (2006). Preparation and properties of novel biodegradable hydrogel based on cationic polyaspartamide derivative. Bulletin-Korean Chemical Society. **27:** 981.

Moon, J.R., Kim, M.W., Kim, D., Jeong, J.H., and Kim, J.-H. (2011). Synthesis and self-assembly behavior of novel polyaspartamide derivatives for anti-tumor drug delivery. Colloid and Polymer Science. **289:** 63-71.

Moore, G.A., Jacono, C.C., Neidigh, J.L., Lawrence, S.D., and Cline, K. (1992). Agrobacterium-Mediated Transformation of Citrus Stem Segments and Regeneration of Transgenic Plants. Plant Cell Reports. **115:** 238-242

Moore, G.A., Rogers, K., Kamps, T., Pajon, M., Stover, J., J Febres, V., and Stover, E. (2016). Rapid cycling plant breeding in citrus.

Moreau, M., Tian, M., and Klessig, D.F. (2012). Salicylic acid binds NPR3 and NPR4 to regulate NPR1-dependent defense responses. Cell Res. **22:** 1631 – 1633

Morris, M.C., Vidal, P., Chaloin, L., Heitz, F., and Divita, G. (1997). A new peptide vector for efficient delivery of oligonucleotides into mammalian cells. Nucleic Acids Res. **25:** 2730-2736

Moye, H.A., and Wheaton, T.A. (1979). Determination of naphthaleneacetic acid (NAA) in oranges, tangerines, and processed products: high-performance liquid chromatography with fluorometric detection. Journal of agricultural and food chemistry. **27:** 291-294.

Murthy, N., Campbell, J., Fausto, N., Hoffman, A.S., and Stayton, P.S. (2003). Design and synthesis of pH-responsive polymeric carriers that target uptake and enhance the intracellular delivery of oligonucleotides. Journal of Controlled Release. **89:** 365-374.

Naito, Y., Hino, K., Bono, H., and Ui-Tei, K. (2015). CRISPRdirect: software for designing CRISPR/Cas guide RNA with reduced off-target sites. Bioinformatics. **31:** 1120-1123.

Nakase, I., Tadokoro, A., Kawabata, N., Takeuchi, T., Katoh, H., Hiramoto, K., Negishi, M., Nomizu, M., Sugiura, Y., and Futaki, S. (2007). Interaction of arginine-rich peptides with membrane-associated proteoglycans is crucial for induction of actin organization and macropinocytosis. Biochemistry **46:** 492-501.

Nakase, I., Takeuchi, T., Tanaka, G., and Futaki, S. (2008). Methodological and cellular aspects that govern the internalization mechanisms of arginine-rich cell-penetrating peptides. Adv Drug Deliv Rev **60:** 598-607.

Nakato, T., Kusuno, A., and Kakuchi, T. (2000). Synthesis of poly (succinimide) by bulk polycondensation of L-aspartic acid with an acid catalyst. Journal of Polymer Science Part A: Polymer Chemistry. **38:** 117-122.

Nakato, T., Yoshitake, M., Matsubara, K. and Tomida, M. (1998). Relationships between Structure and Properties of Poly(aspartic acid)s. Macromolecules. **31:** 2107-2113.

Nemethy, A., Solti, K., Kiss, L., Gyarmati, B., Deli, M.A., Csanyi, E., and Szilagyi, A. (2013). pH-and temperature-responsive poly (aspartic acid)-l-poly (N-isopropylacrylamide) conetwork hydrogel. European Polymer Journal. **49:** 2392-2403.

Nicolosi, E. (2007). 3 Origin and Taxonomy. Citrus Genetics, Breeding and Biotechnology. 19-43.

Nishikawa, F. (2013). Regulation of Floral Induction in Citrus. Journal of the Japanese Society for Horticultural Science. **82:** 283-292.

NRC. (2010). Strategic planning for the Florida citrus industry: addressing citrus greening disease. National Research Council. The National Academies Press.

Oliveira, M.L.P., Febres, V.J., Costa, M.G.C., Moore, G.A. and Otoni, W.C. (2008). "High-efficiency Agrobacterium-mediated transformation of citrus via sonication and vacuum infiltration." Plant Cell Reports **28:** 387.

Oliveira, M.L.P., Moore, G.A., Thomson, J.G., and Stover, E. (2015). Agrobacterium-mediated transformation of Mexican lime (Citrus aurantifolia Swingle) using optimized systems for epicotyls and cotyledons. Advances in Bioscience and Biotechnology. **6:** 12.

Pal, S., Roy, S.G., and De, P. (2014). Synthesis via RAFT polymerization of thermo- and pH-responsive random copolymers containing cholic acid moieties and their self-assembly in water. Polymer Chemistry. **5:** 1275-1284.

Penjor, T., Yamamoto, M., Uehara, M., Ide, M., Matsumoto, N., Matsumoto, R., et al. (2013). Phylogenetic relationships of citrus and its relatives based on matK gene sequences. PLoS ONE **8:** e62574.

Perez-de-Luque, A., and Rubiales, D. (2009). Nanotechnology for parasitic plant control. Pest management science. **65:** 540-545.

Pillitteri, L.J., Lovatt, C.J., and Walling, L.L. (2004). Isolation and Characterization of a TERMINAL FLOWER Homolog and Its Correlation with Juvenility in Citrus. Plant Physiology. **135:** 1540-1551.

Pin, P., and Nilsson, O. (2012). The multifaceted roles of FLOWERING LOCUS T in plant development. Plant, cell & environment. **35:** 1742-1755.

Puoci, F., Iemma, F., Spizzirri, U.G., Cirillo, G., Curcio, M., Picci, N. (2008). Polymer in agriculture: a review. Am. J. Agric. Biol. Sci. 2008, **3:** 299– 314.

Raun, W.R., and Johnson, G.V. (1999). Improving nitrogen use efficiency for cereal production. Agron. J. **91:** 357-363

Regan, S.M., and Moffatt, B.A. (1990). Cytochemical analysis of pollen development in wild-type Arabidopsis and a male-sterile mutant. The Plant Cell. **2:** 877-889.

Roweton, S., Huang, S., and Swift, G. (1997). Poly (aspartic acid): synthesis, biodegradation, and current applications. Journal of Polymers and the Environment. **5:** 175-181.

Schwarze, S.R., Ho, A., Vocero-Akbani, A., and Dowdy, S.F. (1999). In vivo protein transduction: delivery of a biologically active protein into the mouse. Science **285:** 1569-1572.

Seo, K., and Kim, D. (2006). Phase transition behavior of novel pH-sensitive polyaspartamide derivatives grafted with 1-(3-aminopropyl)imidazole. Macromol Biosci. **6:** 758-766.

Shu, S., Zhang, X., Teng, D., Wang, Z., and Li, C. (2009). Polyelectrolyte nanoparticles based on water-soluble chitosan-poly(L-aspartic acid)-polyethylene glycol for controlled protein release. Carbohydr Res. **344:** 1197-1204.

Shukla, V.K., Doyon, Y., Miller, J.C., DeKelver, R.C., Moehle, E.A., Worden, S.E., Mitchell, J.C., Arnold, N.L., Gopalan, S., and Meng, X. (2009). Precise genome modification in the crop species Zea mays using zinc-finger nucleases. Nature. **459:** 437.

Song, J. and Bae, J. (2013). "Citrus fruit intake and breast cancer risk: a quantitative systematic review". Journal of Breast Cancer. **16:** 72–76.

Southwick, S.M., and Davenport, T.L. (1986). Characterization of water stress and low temperature effects on flower induction in Citrus. Plant Physiol. **81:** 26-29

Stover, E., Stange, R.R., McCollum, T.G., Jaynes, J., Irey, M., and Mirkov, E. (2013). Screening antimicrobial peptides in vitro for use in developing transgenic citrus resistant to Huanglongbing and citrus canker. Journal of the American Society for Horticultural Science. **138:** 142-148.

Sun, B., Li, W., and Wu, P. (2008). Innovative spectral investigations on the thermal-induced poly (aspartic acid). Polymer. **49:** 2704-2708.

Syers, J., Johnston, A., and Curtin, D. (2008). Efficiency of soil and fertilizer phosphorus use. FAO fertilizer and plant nutrition bulletin. **18**.

Tabatt, K., Kneuer, C., Sameti, M., Olbrich, C., Müller, R.H., Lehr, C.-M., and Bakowsky, U. (2004). Transfection with different colloidal systems: comparison of solid lipid nanoparticles and liposomes. Journal of Controlled Release. **97:** 321-332.

Tarn, D., Ashley, C.E., Xue, M., Carnes, E.C., Zink, J.I., and Brinker, C.J. (2013). Mesoporous silica nanoparticle nanocarriers: biofunctionality and biocompatibility. Acc Chem Res. **46:** 792-801.

Theato, P., Sumerlin, B.S., O'Reilly, R.K., and Epps III, T.H. (2013). Stimuli responsive materials. Chemical Society Reviews. **42:** 7055-7056.

Thombre, S., and Sarwade, B. (2005). Macromol Sci Part A. Pure Appl Chem. **42:** 1299.

Thoren, P.E., Persson, D., Karlsson, M., and Norden, B. (2000). The antennapedia peptide penetratin translocates across lipid bilayers - the first direct observation. FEBS Lett. **482:** 265-268.

Kanes, K., Tisserat, B., Berhow, M., and Vandercook, C. (1992). Phenolic composition of various tissues of rutaceae species. Phytochemistry **32:** 967-974.

Tomida M., Nakato, T. and Kuramochi, M. (1996). Novel method of synthesizing poly(succinimide) and its copolymeric derivatives by acid-catalysed polycondensation of l-aspartic acidPolymer. **37:** 4435-4437.

Trivedi, R., and Kompella, U.B. (2010). Nanomicellar formulations for sustained drug delivery: strategies and underlying principles. Nanomedicine. **5:** 485-505.

USDA. (2011). Citrus ID morphology: habit, twigs, leaves, flowers, fruits. Citrus ID Edition 2. United States Department of Agriculture. Retrieved from: http://idtools.org/id/citrus/citrusid/morphology.php

USDA. (2016). Florida Citrus Statistics 2014-2015. United States Department of Agriculture. National Agricultural Statistics Service, Southern Region, Florida Field Office.

van Bel, A.J.E., and Hess, P.H. (2008). Hexoses as phloem transport sugars: the end of a dogma? Journal of Experimental Botany **59:** 261-272.

Velázquez, K., Agüero, J., Vives, M. C., Aleza, P., Pina, J. A., Moreno, P., Navarro, L. and Guerri, J. (2016), Precocious flowering of juvenile citrus induced by a viral vector based on Citrus leaf blotch virus: a new tool for genetics and breeding. Plant Biotechnol J.**14:** 1976–1985.

Vives, E., Richard, J.P., Rispal, C., and Lebleu, B. (2003). TAT peptide internalization: seeking the mechanism of entry. Curr Protein Pept Sci. **4:** 125-132.

Vreugdenhil, D., and Koot-Gronsveld, E.A.M. (1989). Measurements of pH, sucrose and potassium ions in the phloem sap of castor bean (Ricinus communis) plants. Physiologia Plantarum **77:** 385-388.

Wadia, J.S. and Dowdy, S.F. (2005). Transmembrane delivery of protein and peptide drugs by TAT-mediated transduction in the treatment of cancer. Adv Drug Deliv Rev. **57:** 579-596.

Walrant, A., Vogel, A., Correia, I., Lequin, O., Olausson, B.E., Desbat, B., Sagan, S., and Alves, I.D. (2012). Membrane interactions of two arginine-rich peptides with different cell internalization capacities. Biochim Biophys Acta. **1818:** 1755-1763.

Wang, J., Lu, H., Kamat, R., Pingali, S.V., Urban, V.S., Cheng, J., and Lin, Y. (2011). Supramolecular polymerization from polypeptide-grafted comb polymers. Journal of the American Chemical Society. **133:** 12906-12909.

Wang, T., Xu, Q., Wu, Y., Zeng, A., Li, M., and Gao, H. (2009). Quaternized chitosan (QCS)/poly (aspartic acid) nanoparticles as a protein drug-delivery system. Carbohydr Res. **344:** 908-914.

Wang, X., Wu, G., Lu, C., Zhao, W., Wang, Y., Fan, Y., Gao, H., and Ma, J. (2012a). A novel delivery system of doxorubicin with high load and pH-responsive release from the nanoparticles of poly (α, β-aspartic acid) derivative. European Journal of Pharmaceutical Sciences. **47:** 256-264.

Wang, Y., Hou, Y., Ruan, G., Pan, M., and Liu, T. (2003). Study on the polymerization of aspartic acid catalyzed by phosphoric acid. Journal of Macromolecular Science, Part A. **40:** 293-307.

Wang, Y., Xue, M., Wei, J., Li, C., Zhang, R., Cao, H., Yang, J., and Tan, T. (2012b). Novel solvent-free synthesis and modification of polyaspartic acid hydrogel. RSC advances. **2:** 11592-11600.

Weaver, C.L., LaRosa, J.M., Luo, X., and Cui, X.T. (2014). Electrically Controlled Drug Delivery from Graphene Oxide Nanocomposite Films. ACS Nano **8:** 1834-1843.

Wender, P.A., Mitchell, D.J., Pattabiraman, K., Pelkey, E., Steinman L., and Rothbard, J. (2000). The design, synthesis, and evaluation of molecules that enable or enhance cellular uptake: peptoid molecular transporters. PNAS USA. **97:** 13003-13008.

Wiedenheft, B., Sternberg, S.H., and Doudna, J.A. (2012). RNA-guided genetic silencing systems in bacteria and archaea. Nature. **482:** 331.

Wolk, S.K., Swift, G., Paik, Y.H., Yocom, K.M., Smith, R.L., and Simon, E.S. (1994). One-and two-dimensional nuclear magnetic resonance characterization of poly (aspartic acid) prepared by thermal polymerization of L-aspartic acid. Macromolecules. **27:** 7613-7620.

Wu, H.-Y., Liu, K.-H., Wang, Y.-C., Wu, J.-F., Chiu, W.-L., Chen, C.-Y., Wu, S.-H., Sheen, J., and Lai, E.-M. (2014). AGROBEST: an efficient Agrobacterium-mediated transient expression method for versatile gene function analyses in Arabidopsis seedlings. Plant Methods. **10:** 19.

Xiong, M.-H., Bao, Y., Du, X.-J., Tan, Z.-B., Jiang, Q., Wang, H.-X., Zhu, Y.-H., and Wang, J. (2013). Differential Anticancer Drug Delivery with a Nanogel Sensitive to Bacteria-Accumulated Tumor Artificial Environment. ACS Nano **7:** 10636-10645.

Xu, M., Zhao, Y., and Feng, M. (2012). Polyaspartamide derivative nanoparticles with tunable surface charge achieve highly efficient cellular uptake and low cytotoxicity. Langmuir. **28:** 11310-11318.

Yang, H., Park, C.W., Woo, M., Kim, M., Jo, Y.M., Park, H.G. and Kim, J.H. (2010). HER2/neu antibody conjugated poly(amino acid)-coated iron oxide Nanoparticles for breast cancer MR imaging. Biomacromolecules. **11:** 2866-2872.

Yang, J., Dong, C., Dong, Y., Liu, S., Pan, L., and Zhang, C. (2014). Logic nanoparticle beacon triggered by the binding-induced effect of multiple inputs. ACS applied materials & interfaces. **6:** 14486-14492.

Yao, J.L., Wu, J.H., Gleave, A.P., and Morris, B.A.M. (1996). Transformation of Citrus Embryogenic Cells Using Particle Bombardment and Production of Transgenic Embryos. Plant Science. **113:** 175-183.

Zhang, G., Liu, J., Yang, Q., Zhuo, R., and Jiang, X. (2012). Disulfide-containing brushed polyethylenimine derivative synthesized by click chemistry for nonviral gene delivery. Bioconjug Chem. **23:** 1290-1299.

Zhang, C., Ma, J., Yang, J., Inaki Schlaberg, H., Liu, S., and Xu, J. (2013a). Nanoparticle aggregation logic computing controlled by DNA branch migration. Applied Physics Letters. **103:** 093106.

Zhang, J., Yuan, Z.-F., Wang, Y., Chen, W.-H., Luo, G.-F., Cheng, S.-X., Zhuo, R.-X., and Zhang, X.-Z. (2013b). Multifunctional Envelope-Type Mesoporous Silica Nanoparticles for Tumor-Triggered Targeting Drug Delivery. Journal of the American Chemical Society **135:** 5068-5073.

Zhang, Y., Zhang, F., Li, X., Baller, J.A., Qi, Y., Starker, C.G., Bogdanove, A.J., and Voytas, D.F. (2013c). Transcription activator-like effector nucleases enable efficient plant genome engineering. Plant physiology. **161:** 20-27.

Zhang, Y., Cheng, Y.T., Qu, N., Zhao, Q., Bi, D., Li, X. (2006). Negative regulation of defense responses in Arabidopsis by two NPR1 paralogs. Plant J. **48:** 647-656.

Ziemienowicz, A., Shim, Y.S, Matsuoka, A., Eudes, F., Kovalchuk, I. (2012). A novel method of transgene delivery into triticale plants using the Agrobacterium transferred DNA-derived nano-complex. Plant Physiol. 2012. **154:** 1503-1513

Ziemienowicz, A., Tzfira, T., and Hohn, B. (2008). Mechanisms of T-DNA integration. Agrobacterium: From Biology to Biotechnology. **11:** 395-440

BIOGRAPHICAL SKETCH

Shaun Jensen was born in Charleston, South Carolina in July 1986 to Claude Emil Jensen III and Tammy Barry. As an infant, his family moved to Florida. He and his family lived on the Gulf Coast of Florida, chiefly Sarasota, Florida and Indian Rocks Beach, Florida. In 2004, he graduated summa cum laude from Largo High School with honors. Immediately after graduation, he attended the University of Florida. In 2008, he obtained his B.S. in Biology with a minor in anthropology. After undergraduate studies, he worked in a water testing laboratory until he began graduate school in 2011 in the Plant Molecular and Cellular Biology Program. In March 2016, he married his wife, Molly Lahiff. In 2017, he graduated with a Master of Science degree from the PMCB program and had his first child, a daughter.